

# Quantum field theory for multipolar composite bosons with mass defect and relativistic corrections

Tobias Aßmann <sup>1,\*</sup>, Enno Giese <sup>2,3,†</sup> and Fabio Di Pumpo <sup>1,‡</sup>

<sup>1</sup>*Institut für Quantenphysik and Center for Integrated Quantum Science and Technology (IQST), Universität Ulm, Albert-Einstein-Allee 11, D-89069 Ulm, Germany*

<sup>2</sup>*Technische Universität Darmstadt, Fachbereich Physik, Institut für Angewandte Physik, Schlossgartenstr. 7, D-64289 Darmstadt, Germany*

<sup>3</sup>*Institut für Quantenoptik, Leibniz Universität Hannover, Welfengarten 1, D-30167 Hannover, Germany*

Atomic high-precision measurements have become a competitive and essential technique for tests of fundamental physics, the Standard Model, and our theory of gravity. It is therefore self-evident that such measurements call for a consistent relativistic description of atoms that eventually originates from quantum field theories like quantum electrodynamics. Most quantum-metrological approaches even postulate effective field-theoretical treatments to describe a precision enhancement through techniques like squeezing. However, a consistent derivation of interacting atomic quantum gases from an elementary quantum field theory that includes both the internal structure as well as the center of mass of atoms, has not yet been addressed. We present such an effective quantum field theory for interacting, spin-carrying, and possibly charged ensembles of atoms composed of nucleus and electron that form composite bosons called cobosons, where the interaction with light is included in a multipolar description. Relativistic corrections to the energy of a single coboson, light-matter interaction, and the scattering potential between cobosons arise in a consistent and natural manner. In particular, we obtain a relativistic coupling between the coboson's center-of-mass motion and internal structure encoded by the mass defect, together with an ion spin-orbit coupling. We use these results to derive modified bound-state energies including the motion of ions, modified scattering potentials, a relativistic extension of the Gross-Pitaevskii equation, and the mass defect applicable to atomic clocks or quantum-clock interferometry. Our theory does not only combine and generalize aspects of effective field theories, quantum optics, scattering theory, and ultracold quantum gases, but it also bridges the gap between quantum electrodynamics and effective field theories for ultracold quantum gases.

## I. INTRODUCTION

Quantum field theories (QFT) [1] are powerful and successful tools with applications ranging from the field of particle physics described by the Standard Model [2], over quantum electrodynamics (QED) [3] to nonrelativistic (NR) ultracold quantum gases [4, 5]. Because these gases consist of atoms, *i. e.*, composite particles, and not of elementary particles, they have to be described by an *effective field theory* (EFT) [6–8]. Such EFTs are *the* method of choice, for instance in describing Bose-Einstein condensates (BEC) [9, 10], but are usually not derived from an elementary theory. Hence, they give no direct access to relativistic and further corrections, including radiative corrections [11–14], effects from the composite nature of the nucleus [15], or the mass defect [16, 17] relevant for quantum clocks [18]. In this work, we derive an EFT from QED to describe NR composite particles including relativistic corrections. As a result, we obtain a field-theoretical description of charged, interacting atomic ensembles including both the coupling of the center-of-mass (c.m.) motion to the internal atomic structure, as well as atom-atom and light-matter interactions with relativistic corrections.

Since in many applications atoms move at NR velocities and pair creation plays no role, the respective EFT leads to nonrelativistic QED (NRQED) [6–8, 19]. It is routinely used to describe an individual neutral, composite particle, where usually the c.m. degrees of freedom are not taken into account and the light-matter interaction is only considered to lowest

order. This approach is suited for studying atomic structures, such as in spectroscopy [20], giving rise to, *e. g.*, radiative QED corrections. On the other hand, atomic scattering experiments imply the presence of more than one particle and rely on the c.m. of atoms, so that the theory mentioned above has to be extended. Common approaches [21] usually include the c.m. and atom-atom scattering by generalizing single-atom theories to a corresponding effective QFT, so that both coincide in the single-atom limit. However, fundamental effects from QED remain inaccessible in such a treatment. By extending NRQED to an EFT for interacting atomic ensembles and taking their c.m. degrees of freedom into account, we find from first principles a description that reduces in limiting cases to common approaches, but with access to radiative corrections and scattering potentials. The coupling of the inner-atomic structure to the atom's c.m. motion is a consequence of the relativistic mass defect [16–18, 22], *e. g.*, used in quantum-clock interferometry [23–26], and which gives access to quantum tests of fundamental physics [27–34]. This coupling has been derived in single-particle quantum mechanics for spin- and chargeless particles with [17] and without [16] gravitational backgrounds.

In this work, we unify, generalize, and extend these concepts into one framework. To this end, we use NRQED to describe two different fermions (constituents of the coboson) on flat spacetime, and derive an EFT describing charged (ionized) spin-carrying atomic clouds including the mass defect, which are exposed to atom-atom and light-matter interactions.

The article follows the hierarchical steps presented in Fig. 1, summarizing transitions between different EFTs at each step, originating from QED as a fundamental starting point for the description of interactions between fermions and photons. We aim for a model of interacting composite particles consisting

\* tobias.assmann@uni-ulm.de; tobias.assmann@gmx.de

† enno.giese@tu-darmstadt.de; enno.a.giese@gmail.com

‡ fabio.di-pumpo@uni-ulm.de; fabio.di-pumpo@gmx.de

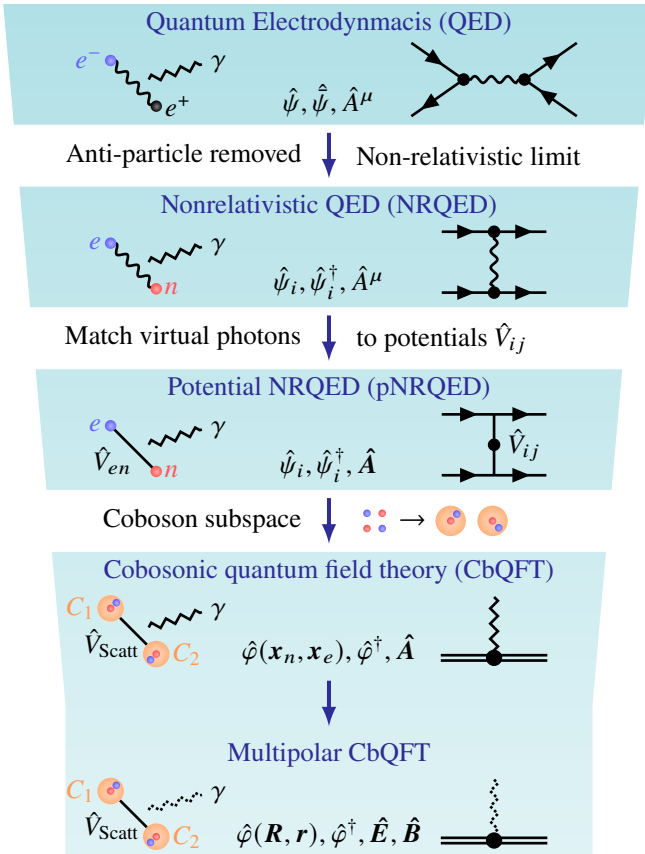


Figure 1. Hierarchy of effective field theories and methodology developed in this article: At the top level, quantum electrodynamics (QED) describes the interaction of fermions (dots), in particular electrons (blue) and positrons (black), with photons, where real (measurable) photons are represented by zigzag lines and virtual photons between two fermions by wiggly lines. The respective field operators are the four-component spinors  $\hat{\psi}$  and  $\hat{\psi}^\dagger$  and four potential  $\hat{A}^\mu$ , whose interaction is described by typical Feynman diagrams such as the vacuum polarization (solid line with arrows are fermions) shown on the right. The next refined field theory is nonrelativistic QED (NRQED), where the antiparticle can be removed from the description by the restriction to an NR limit of QED. In NRQED field operators are replaced by two-component spinors  $\hat{\psi}_i$  creating and annihilating electrons or nuclei, where the latter are assumed as elementary fermions as well. These fermions can interact with each other. For example, the Feynman diagram shows two solid lines representing now two fermions scattering via a virtual photon. In a next step potential NRQED (pNRQED) replaces virtual photons in a second-order scattering process by a nonlocal potential  $\hat{V}^{(ij)}$  for an effective first-order scattering process, where external photons are completely described by the vector potential in Coulomb gauge. Cobosonic quantum field theory (CbQFT) follows from a projection, where we restrict the Hilbert space to only electron-nucleus pairs (cobosons) and introduce a separation of scales, *i. e.*, atomic dimensions and scattering length. As a consequence, fermionic field operators are replaced by cobosonic field operators  $\hat{\phi}$  and interactions between cobosons (orange) are mediated by scattering potentials  $\hat{V}_{\text{Scatt}}$ . Here, Feynman diagrams now feature double solid lines representing a coboson. Multipolar CbQFT describes external photons by EM fields  $\hat{\mathbf{E}}$  and  $\hat{\mathbf{B}}$  (dashed zigzag line) interacting with cobosons via multipoles whose degrees of freedom are described by c.m. and relative coordinates.

of bound fermions. Since antiparticles are irrelevant in bound systems like atoms at NR energies, we use NRQED by restricting ourselves to the NR limit of QED, where the antiparticle is removed from the formalism. The resulting model is described in Sec. II and covers the interaction of nuclei and electrons on a field-theoretical level, including relativistic effects. This interaction is mediated by (virtual) photons that account for the binding potential between the constituents of the composite particle.

In a next step, such virtual photons are matched to instantaneous potentials  $\hat{V}^{(ij)}$ , resulting in potential NRQED (pNRQED) [35–37]. These potentials mediate the electromagnetic (EM) interaction in the spirit of the classical Coulomb problem, but still include relativistic corrections. However, such potentials between elementary fermions do not describe solely attractive potentials between constituents of an atom, but also repulsive interactions in a gas of fermions. To this end, we reduce pNRQED to cobosonic QFT (CbQFT) via a projection technique on a subspace of paired nuclei and electrons that is based on different length scales (Sec. III). In addition, we introduce field operators for so-called cobosons (composite bosons) [38] whose commutation relation differs from the fundamental bosonic one [39]. The resulting theory of composite particles has the desired form, but is still given in terms of the degrees of freedom of their constituents.

In Sec. IV we therefore describe the interaction of such composite particles with light via electric and magnetic fields [40, 41] instead of the vector potential. At the same time, we introduce c.m. and relative coordinates commonly used in the description of bound or composite particles. This approach clearly distinguishes between the internal structure of composite particles and their c.m. motion, so that it connects to the field-theoretical treatment of quantum gases.

We present the main results in Sec. V. Our *multipolar cobosonic QFT* gives rise to a field-theoretical description of atoms, together with their internal degrees of freedom and their c.m. motion, as well as their interactions with EM fields and scattering between different cobosons. It includes relativistic QED corrections in the spectrum of the bound system, but also in the motion of the composite particles, their scattering, as well as their interaction with EM fields. In particular, we observe a coupling between relative and c.m. coordinates as a consequence of the mass defect, but also a spin-orbit coupling for charged cobosons.

Finally, we put our results in Sec. VI into context with existing approaches in various subfields, and we use this discussion as a motivation for sample applications given in Sec. VII. We present the coupling of the atom’s energy spectrum to the c.m. motion, reduce the scattering potential to a generalized dipole-dipole potential, derive a QFT for interacting cobosonic quantum gases, and find in a mean-field description a modified Gross-Pitaevskii equation [42, 43] including the mass defect. We conclude in Sec. VIII.

For completeness, Appendix A presents a derivation of the fermion-fermion potentials from pNRQED. We discuss aspects of the coboson-subspace projection in Appendix B and derive unitary transformations of the coboson field operator in Appendix C. The full transformation from CbQFT to multipolar

CbQFT is performed in Appendix D, while Appendix E presents the eigenfunctions for the relative motion of hydrogen-like composite particles.

## II. POTENTIAL NONRELATIVISTIC QED

We assume that composite particles are built from two fermionic particle species, namely electrons ( $e$ ) and nuclei ( $n$ ) [44]. Since NR effects are primarily responsible for the bound-state dynamics between the constituents, we rely on NRQED [6–8, 19, 45, 46] for a field-theoretical description. NRQED is an EFT of QED valid in NR regimes of both nucleus and electron momenta where antiparticles are of no relevance. This assumption requires sufficiently low photon energies such that the particle-antiparticle dynamics remains negligible.

Because of the absence of antiparticles, the constituents are simply described by two-component field operators  $\hat{\psi}_i(\mathbf{x})$  and  $\hat{\psi}_i^\dagger(\mathbf{x})$ , associated with the annihilation and creation of particle  $i = e, n$  at position  $\mathbf{x}$ , rather than four-component spinors containing both particle and antiparticle field operators. Thus, the components  $u, v = 1, 2$  of field operators of the same species obey anti-commutation relations  $\{\hat{\psi}_{i,u}(\mathbf{x}), \hat{\psi}_{i,v}^\dagger(\mathbf{x}')\} = \delta_{uv}\delta(\mathbf{x} - \mathbf{x}')$  and  $\{\hat{\psi}_{i,u}(\mathbf{x}), \hat{\psi}_{i,v}(\mathbf{x}')\} = 0$ . Simultaneously, electron and nucleus field operators act on different Hilbert spaces implying vanishing commutators  $[\hat{\psi}_{i,\alpha}, \hat{\psi}_{j,\beta}^\dagger] = 0 = [\hat{\psi}_{i,\alpha}, \hat{\psi}_{j,\beta}]$  for  $i \neq j$  between different particle species.

The Lagrangian density governing the dynamics of the fermionic field operators may be constructed [19] by considering all possible operator combinations that preserve the symmetries (namely hermiticity, as well as gauge, rotational, parity, and time-reversal invariance). Each combination is then equipped with a coefficient determined by a matching of cross sections in the low-energy limit of QED [7, 45]. Alternatively, the NRQED Lagrangian follows directly from the QED Lagrangian by applying the Foldy-Wouthuysen transformation [47], where the matching coefficients have to be added manually. These so-called *Wilson coefficients* [48, 49] partly account for QED effects that are no longer accessible in NRQED, such as the anomalous magnetic moment [50–52]. In the spirit of EFTs, they also account for composite-particle aspects of the nucleus, loop corrections, or radiative effects.

After a Legendre transformation of the NRQED Lagrangian density [53] up to order  $c^{-2}$  of the speed of light  $c$ , the NRQED Hamiltonian density

$$\hat{\mathcal{H}} = \hat{\mathcal{H}}_{\text{EM}} + \sum_{i=e,n} \hat{\psi}_i^\dagger \hat{h}_i \hat{\psi}_i + \hat{\mathcal{H}}_{\text{Cont}} \quad (1)$$

contains three contributions [54]. The first one corresponds to the free energy density of the EM field  $\hat{\mathcal{H}}_{\text{EM}} = \varepsilon_0(\hat{\mathbf{E}}^2 + \hat{\mathbf{B}}^2/c^2)/2$ . The second term accounts for the energy density of

electrons and nuclei, where the single-fermion Hamiltonian

$$\begin{aligned} \hat{h}_i = & m_i c^2 + q_i \hat{\phi} + \frac{\hat{\mathbf{p}}_i^2}{2m_i} - c_{\text{F}}^{(i)} q_i \frac{\hat{\mathbf{s}}_i \cdot \hat{\mathbf{B}}}{m_i} - \frac{\hat{\mathbf{p}}_i^4}{8m_i^3 c^2} \\ & - c_{\text{D}}^{(i)} q_i \hbar^2 \frac{\nabla \cdot \hat{\mathbf{E}}}{8m_i^2 c^2} + c_{\text{S}}^{(i)} q_i \hat{\mathbf{s}}_i \cdot \frac{\hat{\mathbf{p}}_i \times \hat{\mathbf{E}} - \hat{\mathbf{E}} \times \hat{\mathbf{p}}_i}{4m_i^2 c^2} \\ & + c_{\text{W1}}^{(i)} q_i \frac{\{\hat{\mathbf{p}}_i^2, \hat{\mathbf{s}}_i \cdot \hat{\mathbf{B}}\}}{4m_i^3 c^2} - c_{\text{A1}}^{(i)} q_i^2 \hbar^2 \frac{\hat{\mathbf{B}}^2}{8m_i^3 c^2} \end{aligned} \quad (2)$$

corresponds to the energy of a single fermion of species  $i$ . The Hamiltonian constitutes the basis for the Schrödinger equation of first-quantized systems. It is sandwiched between the field operators  $\hat{\psi}_i^\dagger \dots \hat{\psi}_i$  and creates a weighted particle-number density in a field-theoretical treatment.

In leading order, the energy of particle species  $i$  is the sum of rest energy due to its rest mass  $m_i$ , energy caused by the scalar potential  $\hat{\phi}$  because of its charge  $q_i$ , kinetic energy, as well as energy due to the coupling of spin  $\hat{\mathbf{s}}_i = \hbar \hat{\sigma}_i / 2$  with Pauli-matrix vector  $\hat{\sigma}_i$  of particle  $i$  to a magnetic field  $\hat{\mathbf{B}}$ . The kinetic energy associated with the particle's minimally-coupled momentum  $\hat{\mathbf{p}}_i = \hat{\mathbf{p}} - q_i \hat{\mathbf{A}}$ , with momentum operator  $\hat{\mathbf{p}} = -i\hbar \nabla$ , is modified by the vector potential  $\hat{\mathbf{A}}$ , and obeys the commutation relation  $[x_u, \hat{p}_v] = i\hbar \delta_{\ell m}$  for  $u, v = x, y, z$ .

The first-order relativistic corrections are the kinetic ( $\hat{\mathbf{p}}_i^4$ ) and electric-field corrections, covering the Darwin term ( $\nabla \cdot \hat{\mathbf{E}}$ ) and spin-orbit term ( $\hat{\mathbf{p}}_i \times \hat{\mathbf{E}}$ ), which give rise to a corresponding hydrogen fine-structure contribution. While  $\hat{\mathbf{p}}_i$  acts on the field operator,  $\nabla \cdot \hat{\mathbf{E}}$  is only a spatial derivative of  $\hat{\mathbf{E}}$ . The last line of Eq. (2) contains relativistic corrections to light-matter interaction in form of general magnetic moment and diamagnetic corrections. All light fields are functions of position  $\mathbf{x}$  and are connected to  $\hat{\phi}$  and  $\hat{\mathbf{A}}$  via  $\hat{\mathbf{E}} = -\nabla \hat{\phi} - \partial_t \hat{\mathbf{A}}$  and  $\hat{\mathbf{B}} = \nabla \times \hat{\mathbf{A}}$ .

The Wilson coefficients  $c_k^{(i)}$  in Eq. (2) are determined from tree-level QED matching [7], and particular subscripts stand for *Fermi*, *Darwin*, and *Seagull*. In particular,  $c_{\text{F}}^{(i)} = Z_i + a_i$  is related to the anomalous magnetic moment  $a_i$  of particle  $i$  and its charge number  $Z_e = 1$  and  $Z_n = Z$ . For instance, we can relate  $c_{\text{F}}^{(e)} = g_e/2$  to the g-factor of the electron. Some Wilson coefficients are defined completely through other coefficients [53]; and specific values for electrons [7] or protons [55] have been determined.

The third term

$$\hat{\mathcal{H}}_{\text{Cont}} = \hbar^3 \sum_{i,j} \frac{d_1^{(ij)} \hat{\psi}_i^\dagger \hat{\psi}_i \hat{\psi}_j^\dagger \hat{\psi}_j - d_2^{(ij)} \hat{\psi}_i^\dagger \hat{\sigma}_i \hat{\psi}_i \cdot \hat{\psi}_j^\dagger \hat{\sigma}_j \hat{\psi}_j}{m_i m_j c} \quad (3)$$

of the Hamiltonian density from Eq. (1) describes contact interactions through which fermions couple directly (Darwin-like contact interaction) and through their spin (spin-spin contact interaction). The Wilson coefficients  $d_1^{(ij)}$  and  $d_2^{(ij)}$  are in lowest order proportional to the fine-structure constant  $\alpha = e^2/(4\pi\varepsilon_0\hbar c)$  with vacuum permittivity  $\varepsilon_0$ . These terms solely arise from loop corrections [56], such that they cannot be

obtained from a pure tree-level treatment. As a result,  $\hat{\mathcal{H}}_{\text{Cont}}$  is of order  $\alpha/c$  and by that of  $c^{-2}$  [57]. The Hamiltonian neglects loop corrections of the order  $c^{-2}$ , which are suppressed by another  $d$ -type Wilson coefficient and are in fact of order  $\alpha/c^2$ .

### A. Matching of scattering processes to potentials

The Hamiltonian from Eq. (1) allows to describe composite particles based on their fermionic constituents. However, the defining property of composite particles, *i. e.*, a bound-state potential due to EM interactions between fermions, does not appear explicitly yet. Instead, it is contained in the EM fields which give rise to all allowed NRQED Feynman diagrams involving photons. These photons may be categorized into real (external lines in Feynman diagrams) and virtual (internal lines in Feynman diagrams) photons. The former describe all photons from external fields that scatter with the composite particle, the latter are virtual mediating EM interaction between the fermionic constituents of the composite particle. Such a separation is sketched in Fig. 2a) where all possible Feynman diagrams between two constituents (solid lines) may be written as a sum of all virtual photon diagrams (dashed and wiggly lines), that scatter an increasing number of real photons (zigzag lines).

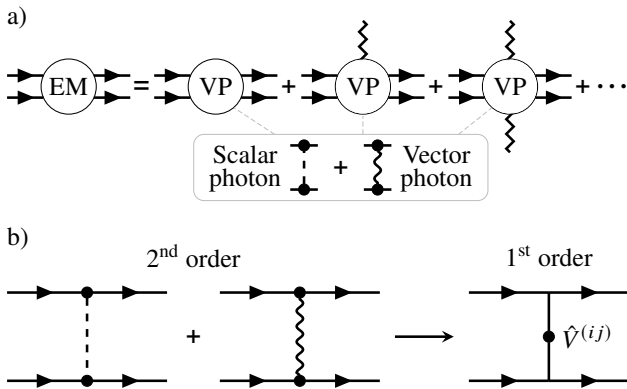


Figure 2. a) Set of all possible Feynman diagrams of two real fermions (which model in our treatment the constituents of a composite particle), interacting with EM fields. It can be described by the exchange of purely virtual photons (VP) and real photons (zigzag lines). The former can be any combination of scalar photons (dashed line), and vector photons (wiggly line) mediating the interaction between both fermions. This set of Feynman diagrams can be expanded into an increasing amount of scattering processes with real photons that account for external EM fields. b) The lowest-order nontrivial set of virtual photons includes all possible Feynman diagrams with one virtual scalar or vector photon (second-order scattering). All diagrams are reduced to an effective first-order scattering by matching to an effective potential  $\hat{V}^{(ij)}$  in the framework of pNRQED.

We integrate over all positions and perform such a separation to find the new Hamiltonian

$$\hat{H} = \hat{H}_{\text{EM}} + \sum_i \int d^3x_i \hat{\psi}_i^\dagger \hat{h}_i \hat{\psi}_i + \hat{H}_{\text{f-f}}, \quad (4)$$

where the EM interaction between two fermions now explicitly appears in a modified fermion-fermion interaction Hamiltonian  $\hat{H}_{\text{f-f}}$  absorbing also  $\hat{H}_{\text{Cont}}$ , while the EM fields in the original single-fermion Hamiltonian [first term in Eq. (4)] are now only associated with real photons scattering with fermions (light-matter interaction).

To determine  $\hat{H}_{\text{f-f}}$ , we consider the first type of Feynman diagram in Fig. 2a) involving solely virtual photons. According to Fig. 2b), the interaction or scattering between two real fermions  $i$  and  $j$  follows to lowest order from a second-order scattering process, *i. e.*, two vertices in a Feynman diagram connected by a virtual scalar (dashed line) or vector photon (wiggly line). These second-order interactions are reduced to an effective first-order scattering processes with one vertex containing an instantaneous potential  $\hat{V}^{(ij)}$ . Consequently, the resulting Hamiltonian takes the form

$$\hat{H}_{\text{f-f}} = \sum_{i,j} \int d^3x_i \int d^3x'_j \hat{\psi}_i^\dagger \hat{\psi}_j^\dagger \hat{V}^{(ij)} \hat{\psi}_j \hat{\psi}_i + O(c^{-3}) \quad (5)$$

and gives rise to the effective field theory of *potential nonrelativistic quantum electrodynamics* (pNRQED) [35–37, 55, 58, 59]. In Eq. (5) we use the abbreviations  $\hat{\psi}_i = \hat{\psi}_i(\mathbf{x}_i)$ ,  $\hat{\psi}'_j = \hat{\psi}_j(\mathbf{x}'_j)$ , and  $\hat{V}^{(ij)} = \hat{V}^{(ij)}(\mathbf{x}_i, \mathbf{x}'_j, \hat{\mathbf{p}}_i, \hat{\mathbf{p}}'_j, \hat{\mathbf{s}}_i, \hat{\mathbf{s}}'_j)$ . The potential itself is determined by considering all possible virtual photons as indicated in Fig. 2b), leading to potentials of order  $c^{-2}$ . They are summarized by Fig. 3 which shows all relevant Feynman diagrams and their corresponding terms contributing to  $\hat{V}^{(ij)}$ . A more detailed procedure is discussed in Appendix A.

The full potential presented in Fig. 3 is given with respect to single-fermion coordinates up to order  $c^{-2}$ . As expected, we find in lowest order the Coulomb interaction  $V_C^{(ij)}$ . The potential is completed by the orbit-orbit  $\hat{V}_{\text{LL}}^{(ij)}$ , spin-orbit  $\hat{V}_{\text{LS}}^{(ij)}$ , spin-spin  $\hat{V}_{\text{SS}}^{(ij)}$ , Darwin  $V_D^{(ij)}$ , and contact interaction. The last term already had the form of a fermion-fermion interaction. These potentials are also known as part of the *Breit-Pauli* Hamiltonian [60–62], however, augmented by QED corrections in our description.

Since the matching procedure requires a specified gauge to evaluate virtual photons via propagators in Feynman diagrams, Fig. 3 shows the potentials for the Coulomb gauge, *i. e.*,  $\nabla \cdot \hat{\mathbf{A}} = 0$ , and Lorenz gauge [63]. While potentials connected to a specific Feynman diagram may differ, the overall potential  $\hat{V}^{(ij)}$  and by that the total pNRQED Hamiltonian remains gauge invariant. In addition, matching in order  $c^{-2}$  can be extended to order  $\alpha/c^2$  by including relevant loop corrections [36].

In pNRQED, virtual photons mediating EM interaction between two fermions are frozen out into potentials and any Feynman diagram depicted in Fig. 3 is included in  $\hat{H}_{\text{f-f}}$ . All other Feynman diagrams up to the order  $c^{-2}$  may be determined with the new Hamiltonian, *e. g.*, the self-energy of the fermions, responsible for one contribution to the Lamb shift [64, 65], containing a virtual fermion and a virtual vector photon, since both Hamiltonians yield the same physical results. The renormalization of the theory is similar to the transition from QED to NRQED [36].

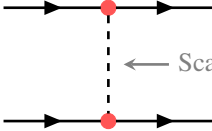
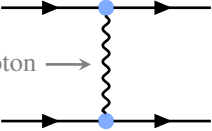
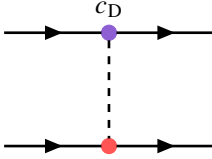
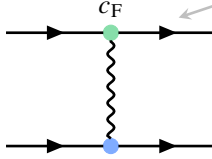
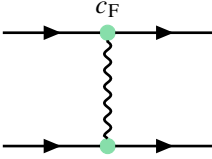
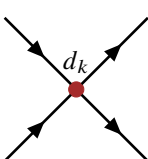
Name	Coulomb $V_C^{(ij)}$	Orbit-orbit $\hat{V}_{LL}^{(ij)}$	
Feynman diagram			
Coulomb $\hat{V}^{(ij)}$	$\frac{q_i q_j}{\kappa_{ij} 8\pi \epsilon_0  \mathbf{r} }$	$\frac{1}{2 \mathbf{r} ^3} \hat{\boldsymbol{\ell}}_i \cdot \hat{\boldsymbol{\ell}}_j + \frac{1}{ \mathbf{r} ^3} (\mathbf{r} \cdot \hat{\boldsymbol{p}}_i) (\mathbf{r} \cdot \hat{\boldsymbol{p}}_j)$	
Lorenz $\hat{V}^{(ij)}$	$\frac{q_i q_j}{\kappa_{ij} 8\pi \epsilon_0  \mathbf{r} } - \frac{1}{2 \mathbf{r} ^3} \hat{\boldsymbol{\ell}}_i \cdot \hat{\boldsymbol{\ell}}_j + \pi \hbar^2 \delta(\mathbf{r})$	$\frac{1}{ \mathbf{r} ^3} \hat{\boldsymbol{\ell}}_i \cdot \hat{\boldsymbol{\ell}}_j + \frac{1}{ \mathbf{r} ^3} (\mathbf{r} \cdot \hat{\boldsymbol{p}}_i) (\mathbf{r} \cdot \hat{\boldsymbol{p}}_j) - \pi \hbar^2 \delta(\mathbf{r})$	
Darwin $V_D^{(ij)}$	Spin-orbit $\hat{V}_{LS}^{(ij)}$	Spin-spin $\hat{V}_{SS}^{(ij)}$	Contact
			
$+\pi \hbar^2 \frac{m_j^2 c_D^{(i)} + m_i^2 c_D^{(j)}}{2m_i m_j} \delta(\mathbf{r}) + \frac{c_F^{(j)}}{ \mathbf{r} ^3} \hat{\boldsymbol{\ell}}_i \cdot \hat{\boldsymbol{s}}_j - \frac{c_F^{(i)}}{ \mathbf{r} ^3} \hat{\boldsymbol{\ell}}_j \cdot \hat{\boldsymbol{s}}_i + \frac{c_S^{(i)}}{ \mathbf{r} ^3} \frac{m_j \hat{\boldsymbol{\ell}}_i \cdot \hat{\boldsymbol{s}}_i}{2m_i} - \frac{c_S^{(j)}}{ \mathbf{r} ^3} \frac{m_i \hat{\boldsymbol{\ell}}_j \cdot \hat{\boldsymbol{s}}_j}{2m_j} + c_F^{(i)} c_F^{(j)} \left( 4\pi \delta(\mathbf{r}) \hat{\boldsymbol{s}}_i \cdot \hat{\boldsymbol{s}}_j + \frac{\hat{S}_{ij}}{ \mathbf{r} ^3} \right) + \frac{\hbar^3 d_1^{(i)} - 4\hbar d_2^{(ij)} \hat{\boldsymbol{s}}_i \cdot \hat{\boldsymbol{s}}_j}{\kappa_{ij} m_i m_j c} \delta(\mathbf{r})$			

Figure 3. Relevant Feynman diagrams up to order  $c^{-2}$ . The dashed and wiggly lines correspond to scalar photons, resulting from a contraction of the scalar potential, and vector photons arising from contracting vector potential components, respectively. The vertices are labeled according to the specific term in the Hamiltonian density being contracted: Electric energy (red), kinetic energy (blue), spin-magnetic field (green,  $c_F$ ), Darwin term (purple,  $c_D$ ), spin-orbit term (orange,  $c_S$ ), and contact interaction (brown). The potential connected to each Feynman diagram is calculated in both Coulomb (top, blue shaded) and Lorenz gauge (bottom, orange shaded). The Feynman diagrams of the first row yield different potentials that depend on the gauge, whereas the potentials of the second row are identical in both gauges. The overall effective potential is the sum of all contributions from the first and second row and is gauge invariant. The potential is given in units of  $\kappa_{ij} = -q_i q_j / (8\pi \epsilon_0 m_i m_j c^2)$  and we introduce abbreviations for individual angular momenta  $\hat{\boldsymbol{\ell}}_i = \mathbf{r} \times \hat{\boldsymbol{p}}_i$  and relative distance  $\mathbf{r} = \mathbf{x}_i - \mathbf{x}_j$ , omitting indices  $i$  and  $j$  for simplicity. In addition, we defined the spin contribution  $\hat{S}_{ij} = -\hat{\boldsymbol{s}}_i \cdot \hat{\boldsymbol{s}}_j + 3(\mathbf{r} \cdot \hat{\boldsymbol{s}}_i)(\mathbf{r} \cdot \hat{\boldsymbol{s}}_j)/|\mathbf{r}|^2$  of the magnetic dipole-dipole potential.

## B. Matching potentials with external photons

So far we derived the potential between two fermions due to EM interactions mediated by virtual photons that will eventually give rise to the binding potential of composite particles. In addition, we also aim to describe light-matter interaction between composite particles and external light fields. The scattering process of a real photon with a composite particle contains fermion-photon interactions that correspond to the EM fields appearing in the single-fermion Hamiltonian  $\hat{h}_i$  from Eq. (4). Since the constituents form a bound system, we have to include also the case of a real photon that scatters from two fermions exchanging a virtual photon. This process is not yet accounted for in  $\hat{H}_{f-f}$ , since no minimally-coupled momentum operators appear in the potential that originates in the first term of Fig. 2a). We incorporate this case in  $\hat{H}_{f-f}$  by including Feynman diagrams according to the remaining two terms in Fig. 2a). The relevant additional Feynman diagrams with external photons (depicted in red) are summarized in Fig. 4. Together with these additional diagrams, we derive potentials in which the momentum operators are replaced by

minimally-coupled momenta. Here, we use Coulomb gauge ( $\nabla \cdot \hat{\mathbf{A}} = 0$ ) to determine the matching, and consequently our remaining external photons are also fixed to this gauge from now on. In this case, the vector potential can be decomposed as

$$\hat{\mathbf{A}} = \sum_{r=1}^2 \frac{1}{(2\pi)^{3/2}} \int d^3k \mathcal{A}_{\mathbf{k}} e_r(\mathbf{k}) [\hat{a}_r(\mathbf{k}) e^{i\mathbf{k} \cdot \mathbf{x}} + \text{H.c.}] . \quad (6)$$

We introduced the vacuum amplitude  $\mathcal{A}_{\mathbf{k}} = \sqrt{\hbar/2\epsilon_0 c |\mathbf{k}|}$  and unit polarization vectors  $e_r(\mathbf{k})$  corresponding to the wave vector  $\mathbf{k}$ . The commutators of the field-operator components commute as usual. Hence, we have  $[\hat{A}_u(\mathbf{x}), \hat{A}_v(\mathbf{x}')] = 0$  for  $u, v = x, y, z$ .

The scalar potential  $\hat{\phi}$  contains both real and all virtual photons arising from contractions, such as the Coulomb potential  $\hat{V}_C^{(ij)}$ . In Coulomb gauge, there are no real scalar photons in the absence of a free charge density sourcing the external field, and up to order  $c^{-2}$  we determined all possible virtual scalar-photon contributions by collecting them in  $\hat{H}_{f-f}$ . Consequently, we set  $\hat{\phi} = 0$  [66]. The self-energy of the fermions, being the main contribution to the Lamb shift [64, 65], can still be determined

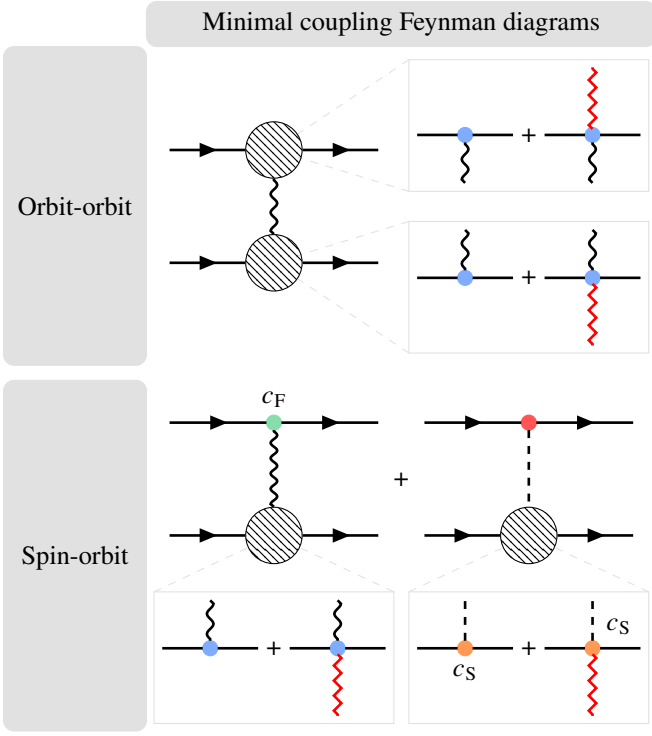


Figure 4. Canonical momenta appear in the effective potentials of the orbit-orbit (LL) coupling  $\hat{V}_{LL}^{(ij)}$  and the spin-orbit (LS) coupling  $\hat{V}_{LS}^{(ij)}$ . To replace these by minimally-coupled momentum operators, we augment the orbit-orbit Feynman diagram by three additional diagrams: two fermions  $i$  and  $j$  exchanging a virtual photon while they scatter a real photon, respectively, together with the diagram where simultaneously both fermions scatter a real photon. Both spin-orbit diagrams exchanging a virtual vector or a virtual scalar photon, respectively, each have to be augmented by one additional diagram describing the scattering of a real photon during this process.

since only the virtual vector photon contributes in Coulomb gauge to it.

We conclude this section with the full minimally-coupled Hamiltonian

$$\hat{H} = \hat{H}_{EM} + \sum_i \int d^3x_i \hat{\psi}_i^\dagger \hat{h}_i \hat{\psi}_i + \sum_{i,j} \int d^3x_i \int d^3x'_j \hat{\psi}_i^\dagger \hat{\psi}'_j \hat{V}^{(ij)} \hat{\psi}'_j \hat{\psi}_i \quad (7)$$

where the potential  $\hat{V}^{(ij)} = \hat{V}^{(ij)}(\mathbf{x}_i, \mathbf{x}'_j, \hat{\mathbf{p}}_i, \hat{\mathbf{p}}'_j, \hat{\mathbf{s}}_i, \hat{\mathbf{s}}'_j)$  is now a function of minimally-coupled momenta and all EM fields are given in Coulomb gauge.

### III. COBOSONIC QFT

We now move from the single-fermion to a composite-particle description. Moreover, we restrict ourselves to ensembles of one atomic species and we reduce the problem to the simplest case of electron-nucleus pairs, forming a composite

boson, *i. e.*, a *coboson* [37–39]. The distance between electron and nucleus that form a coboson is given by an atomic length scale, whereas the distance to other cobosons and their constituents is much larger. Thus, we consider a situation which is sufficiently dilute, such that individual cobosons do not overlap. Motivated by these different length scales, we describe atoms as *spatially restricted* cobosons resembling *hard-sphere* based models [67–69], such that two constituents within a sphere of a certain cutoff radius form a composite particle and are, by definition, free fermions outside of it. Formally, we achieve such a transition from the single-fermion theory to *cobosonic quantum field theory* (CbQFT) by means of a projection  $\hat{\pi}_{Cb}$  of the Schrödinger equation  $i\hbar d|\Psi\rangle/dt = \hat{H}|\Psi\rangle$ . Here, cobosonic states are part of the general second-quantized state  $|\Psi\rangle$ , represented in the following by upper-case symbols, in contrast to lower-case symbols that represent first-quantized states. Thus, the projection operator is chosen such that only spatially-restricted cobosonic states are selected, giving rise to intra-cobosonic and inter-cobosonic length scales. Conversely, observations like atomic decay, free fermions, multi-electron atoms, molecules, *etc.* do not lie within the subspace spanned by this projection. Figure 5a) shows one exemplary configuration that is ruled out by projection and another one that is selected by the projector. Guided by the intuitive picture in the figure, we define the intra-cobosonic scale  $a$  and the length scale  $b \gg a$  associated with the distance between different cobosons. As a result, the dominant EM interaction between fermions are the attractive binding potentials between atomic constituents. Contrarily, inter-cobosonic interactions are based both on attractive and repulsive interactions between the fermionic constituents of *different* cobosons.

In the spirit of EFTs for atoms, we expect cobosonic creation  $\hat{\phi}^\dagger = \hat{\psi}_n^\dagger \hat{\psi}_e^\dagger$  and annihilation operators  $\hat{\phi} = \hat{\psi}_n \hat{\psi}_e$  instead of single-fermion field operators such that only cobosons can be created and annihilated. To reduce the Hilbert space to the states depicted in Fig. 5a) we define a projector  $\hat{\pi}_{Cb} = \sum_{k=0}^N \hat{\pi}_k$  that projects on up to  $N$  cobosons, where  $\hat{\pi}_k$  projects onto a subspace of  $k$  cobosons. As such, the subspace projection

$$\hat{\pi}_k = \frac{1}{k!} \int_{C_1} d^6x_1 \dots \int_{C_k} d^6x_k \left( \prod_{\ell=1}^k \hat{\phi}_\ell^\dagger \right) |0\rangle \langle 0| \left( \prod_{\ell=1}^k \hat{\phi}_\ell \right) \quad (8)$$

is defined by the cobosonic operator  $\hat{\phi}_\ell^\dagger = \hat{\psi}_n^\dagger(\mathbf{x}_{\ell,n}) \hat{\psi}_e^\dagger(\mathbf{x}_{\ell,e})$ , creating a coboson at position  $(\mathbf{x}_{\ell,n}, \mathbf{x}_{\ell,e})$ , with an analogous definition for the annihilation operator. Moreover, Eq. (8) contains the abbreviation of a six-dimensional integration measure  $d^6x_k = d^3x_{k,n} d^3x_{k,e}$  and by definition the subspace projectors are orthogonal, *i. e.*,  $\hat{\pi}_k \hat{\pi}_\ell = 0$  for  $k \neq \ell$ . As explained in Fig. 5a), such a projection implies that not all fermion coordinates are independent. In fact, we have to equip the integrals with proper integration regions  $C_k = C_{k,n} \times C_{k,e}$  for the nucleus and electron of the  $k$ -th coboson. This way, we introduce the internal cobosonic (atomic) length scale  $a$  by restricting the electron coordinates  $\mathbf{x}_{k,e}$  of coboson  $k$  to  $C_{k,e} = B_a(\mathbf{x}_{k,n})$  denoting a spherical volume with radius  $a$  around the nucleus of coboson  $k$  positioned at  $\mathbf{x}_{k,n}$ . The inter-cobosonic scale  $b$  enters through regions for nuclei coordinates in an iterative manner, see also Fig. 3b). The first nucleus

may be positioned anywhere, *i. e.*, in the volume  $C_{1,n} = \mathbb{R}^3$ . However, the second nucleus must not be within a sphere of radius  $b$  around the first nucleus and is therefore located in a region  $C_{2,n} = \mathbb{R}^3 \setminus B_b(\mathbf{x}_{1,n})$ . The distance  $b$  between the cobosons has to be larger than the atomic length scale  $a$  such that the pairing of nucleus  $k$  and electron  $k$  remains unique. A generalization to the  $k$ -th coboson [70] yields

$$C_k = C_{k,n} \times C_{k,e} = \mathbb{R}^3 \setminus \bigcup_{\ell=1}^{k-1} B_b(\mathbf{x}_{\ell,n}) \times B_a(\mathbf{x}_{k,n}). \quad (9)$$

Because of these limits of integration, the projector is normalized with  $1/k!$ . In the absence of such limits, *i. e.*, spatially independent fermion pairs, the normalization factor would be  $1/k!$ . The normalization ensures idempotence, *i. e.*,  $\hat{\pi}_k^2 = \hat{\pi}_k$  and by that  $\hat{\pi}_{C_b}^2 = \hat{\pi}_{C_b}$ , see also Appendix B. This projector resembles boson-like properties: if the integration regions in Eq. (8) are dropped and  $\hat{\phi}$  is replaced by a bosonic field opera-

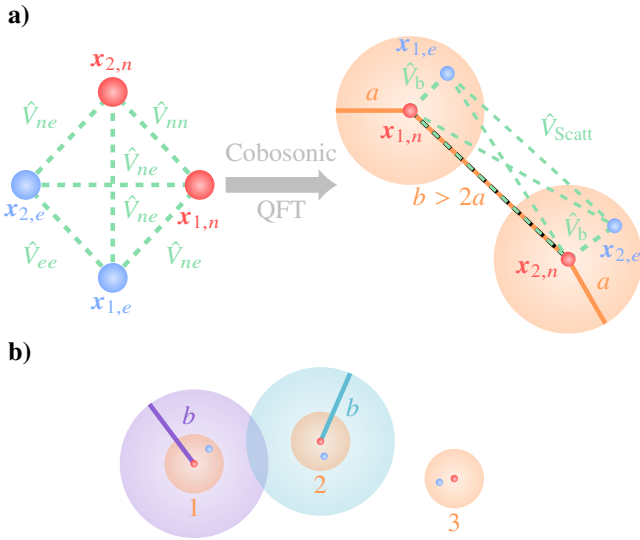


Figure 5. a) The left-hand side shows the situation in pNRQED, where all elementary fermions of the system interact with each other and no interaction is dominant compared to others. A projection to the coboson subspace introduces length scales, and by that our system is only composed of uniquely assigned electron-nucleus pairs. In particular, we find an atomic length scale  $a$  associated with the inner-atomic distance between the constituents and a scattering length scale  $b$  associated with the distance between different cobosons. The separation of scales allows for the identification of the dominant binding potential  $\hat{V}_b = \hat{V}^{(ne)} + \hat{V}^{(en)}$  between the constituents of a coboson compared to the weaker scattering potential  $\hat{V}_{\text{Scatt}} = \hat{V}^{(nn)} + \hat{V}^{(ne)} + \hat{V}^{(en)} + \hat{V}^{(ee)}$  composed of attractive and repulsive interactions among constituents of different cobosons. b) The separation of scales has also implications for the allowed position of different cobosons. The nucleus of coboson 1 can be placed anywhere, but the corresponding electron only within a vicinity of radius  $a$  around it. The nucleus of coboson 2 must not be closer than a distance  $b$  around the nucleus of coboson 1. As a consequence, the purple sphere around coboson 1 is excluded for coboson 2. Similarly, coboson 3 must not be located in the purple and green spheres around cobosons 1 and 2, respectively.

tor obeying canonical commutation relations, idempotence is obtained for  $1/k!$ .

Using this time-independent projection operator, we define the projected states via  $|\Psi\rangle_{C_b} = \hat{\pi}_{C_b} |\Psi\rangle$  and their equation of motion

$$i\hbar \frac{d}{dt} |\Psi\rangle_{C_b} = \hat{\pi}_{C_b} \hat{H} \hat{\pi}_{C_b} |\Psi\rangle_{C_b} + \hat{\pi}_{C_b} \hat{H} (\mathbb{1} - \hat{\pi}_{C_b}) |\Psi\rangle. \quad (10)$$

In the remainder of this article we focus on the contribution to the motion induced by the cobosonic Hamiltonian  $\hat{H}_{C_b} = \hat{\pi}_{C_b} \hat{H} \hat{\pi}_{C_b}$ , as well as its eigenvalues and properties. However, the coupling to states  $(\mathbb{1} - \hat{\pi}_{C_b}) |\Psi\rangle$  that lie outside of our projected Hilbert space leads to additional energy shifts and other effects of the environment in the spirit of open quantum systems [71, 72].

While we present only the results for  $\hat{H}_{C_b}$ , a more detailed derivation is carried out in Appendix B. The projected single-fermion Hamiltonian

$$\int d^3x_i \hat{\psi}_i^\dagger \hat{h}_i \hat{\psi}_i \hat{\pi}_{C_b} = \int_{C_1} d^6x_1 \hat{\phi}_1^\dagger \hat{h}_1 \hat{\phi}_1 \hat{\pi}_{C_b} \quad (11)$$

has the form of a composite-particle theory as the fermion operators are replaced by coboson operators, while the region accessible to the electron is restricted to the atomic scale around the nucleus. Similarly, the projection of the fermion-fermion Hamiltonian for the potentials  $\hat{V}^{(ij)}$  resolves to

$$\begin{aligned} \hat{H}_{f-f} \hat{\pi}_{C_b} &= \int_{C_1} d^6x_1 \hat{\phi}_1^\dagger (\hat{V}^{(ne)} + \hat{V}^{(en)}) \hat{\phi}_1 \hat{\pi}_{C_b} \\ &+ \int_{C_1} d^6x_1 \int_{C_2} d^6x_2 \hat{\phi}_1^\dagger \hat{\phi}_2^\dagger \sum_{i,j} \hat{V}^{(ij)} \hat{\phi}_2 \hat{\phi}_1 \hat{\pi}_{C_b}. \end{aligned} \quad (12)$$

As indicated in Fig. 5a), the interaction between the fermions divides into the dominant binding potential given by  $\hat{V}_b = \hat{V}^{(ne)} + \hat{V}^{(en)}$  in the single-coboson part (first line), while the inter-cobosonic scattering potential  $\sum_{i,j} \hat{V}^{(ij)}$  in the two-coboson part includes attractive and repulsive interactions. Because of the separation of scales, these interactions are weaker than the binding potential. Moreover,  $\hat{H}_{EM} \hat{\pi}_{C_b}$  is unaffected as  $\hat{H}_{EM}$  contains no fermion field operators. Hence, the projected Hamiltonian reads

$$\begin{aligned} \hat{H}_{C_b} &= \hat{H}_{EM} + \int_{C_1} d^6x_1 \hat{\phi}_1^\dagger \hat{h}_{C_b} \hat{\phi}_1 \\ &+ \int_{C_1} d^6x_1 \int_{C_2} d^6x_2 \hat{\phi}_1^\dagger \hat{\phi}_2^\dagger \hat{V}_{\text{Scatt}} \hat{\phi}_2 \hat{\phi}_1 \end{aligned} \quad (13)$$

with the internal cobosonic energy  $\hat{h}_{C_b} = \hat{h}_n + \hat{h}_e + \hat{V}^{(ne)} + \hat{V}^{(en)}$ . This contribution gives rise to the Breit-Pauli Hamiltonian for an electron and a nucleus [60–62] consisting of the sum of individual fermionic energies together with their total binding potential  $\hat{V}^{(ne)} + \hat{V}^{(en)}$  arising from EM interaction between the fermionic constituents. The scattering potential  $\hat{V}_{\text{Scatt}} = \hat{V}^{(nn)} + \hat{V}^{(ne)} + \hat{V}^{(en)} + \hat{V}^{(ee)}$  is based on both attractive ( $\hat{V}^{(ne)} +$

$\hat{V}^{(en)}$ ) and repulsive ( $\hat{V}^{(nn)} + \hat{V}^{(ee)}$ ) EM interactions among all fermions of different cobosons. In particular, these attractive terms are weaker than the single-particle binding potentials, since the coordinates  $\mathbf{x}_{1,i}$  and  $\mathbf{x}_{2,j}$  of different cobosons are separated by  $b \gg a$ . Compared to bosonic field theories for atomic ensembles [21, 73], our effective field theory is based on creation  $\hat{\phi}^\dagger$  and annihilation  $\hat{\phi}$  operators whose components  $\alpha, \beta = 1, 2$  obey a cobosonic commutation [39] relation

$$\begin{aligned} \left[ \hat{\phi}'_{\alpha'\beta'}, \hat{\phi}^\dagger_{\alpha\beta} \right] &= \delta_{\alpha'\alpha} \delta_{\beta'\beta} \delta(\mathbf{x}'_n - \mathbf{x}_n) \delta(\mathbf{x}'_e - \mathbf{x}_e) \\ &\quad - \delta_{\alpha'\alpha} \delta(\mathbf{x}'_n - \mathbf{x}_n) \hat{\psi}'_e \hat{\psi}_e^\dagger \\ &\quad - \delta_{\beta'\beta} \delta(\mathbf{x}'_e - \mathbf{x}_e) \hat{\psi}'_n \hat{\psi}_n^\dagger, \end{aligned} \quad (14)$$

whereas the first line of Eq. (14) describes the fundamental bosonic commutator. Moreover, the projection operator includes integration regions that naturally ensure a boson-like normalization of  $1/k!$  even for this type of commutation relation. In fact, the cobosonic part of the commutator in the second and third line is responsible for the scattering potential in Eq. (12). When projecting to a single-coboson subspace [36], these two aspects, the cobosonic part of the commutator and integration regions ensuring unique electron-nucleus pairs, become irrelevant. In this case, we recover conventional single-particle quantum mechanics.

So far, we constructed a cobosonic theory from second-order scattering of fermions, where the internal structure is governed by the combined single-fermion energy and where their binding potential results from attractive interactions. Furthermore, the inter-cobosonic dynamics arises from the inter-fermionic interactions between the constituents of different cobosons. We emphasize that this projection does not exclusively work for the single-fermion Hamiltonian from Eq. (2) and the potential from Fig. 3 but rather for arbitrary single-fermion Hamiltonians and potentials. However, effects of the environment given by states that do not lie within the coboson subspace have been neglected in our treatment.

#### IV. SECOND-QUANTIZED TRANSFORMATIONS

Although the Hamiltonian from Eq. (13) has already the desired form of an EFT for cobosons, it still involves the constituents' coordinates. In the spirit of composite particles, we now move to center-of-mass (c.m.) and relative coordinates, where the latter take the internal cobosonic, *i. e.*, atomic, structure into account. Also, light-matter interaction enters in lowest order via the vector potential  $\hat{\mathbf{A}}$  contained in the canonical momenta through minimal coupling. For a description of experiments, it is more convenient to express the coupling by EM fields  $\hat{\mathbf{E}}$  and  $\hat{\mathbf{B}}$ . In this section we derive a method to incorporate the multipolar form of cobosonic QFT and move to relativistically-corrected c.m. and relative coordinates of the second-quantized Hamiltonian  $\hat{H}_{\text{Cb}}$  from Eq. (13).

In first-quantized regimes (characterized by lower-case symbols), realizing these operations involves unitary transformations [40, 41, 74–76]  $\hat{u}$  that transform a state  $|\psi\rangle = \hat{u}|\tilde{\psi}\rangle$ , where  $\hat{u} = \exp\{i\hat{\lambda}/\hbar\}$  may be expressed through a (time-

independent) single-particle generator  $\hat{\lambda}$ . Consequently, the effective Schrödinger equation  $i\hbar d|\psi\rangle/dt = \hat{H}_{\text{Cb}}|\psi\rangle$  for the single-coboson Hamiltonian  $\hat{H}_{\text{Cb}}$  yields a transformed operator

$$\hat{h}_{\text{Cb}} = \hat{u}^\dagger \hat{h}_{\text{Cb}} \hat{u} \quad (15)$$

as long as  $\hat{u}$  is time independent.

Guided by this concept, we define for the second-quantized Hamiltonian  $\hat{H}_{\text{Cb}}$  from Eq. (13) an analogues transformation  $|\Psi\rangle_{\text{Cb}} = \hat{U}|\tilde{\Psi}\rangle_{\text{Cb}}$  on a second-quantized state  $|\Psi\rangle_{\text{Cb}}$  (characterized by upper-case symbols) with a unitary  $\hat{U} = \exp\{i\hat{\Lambda}/\hbar\}$  generated by  $\hat{\Lambda}$ . We choose the second-quantized generator  $\hat{\Lambda}$  in such a way that the transformation reduces to the single-particle transformation acting on the first-quantized Hamiltonian  $\hat{h}_{\text{Cb}}$ . With the choice

$$\hat{\Lambda} = \int_{C_1} d^6x_1 \hat{\phi}_1^\dagger \hat{\lambda} \hat{\phi}_1, \quad (16)$$

where  $\hat{\lambda}$  is the generator of the corresponding first-quantized transformation, we achieve the desired behavior of the transformation together with the relation  $\hat{U}^\dagger \hat{\phi}_k \hat{U} = \hat{u}_k \hat{\phi}_k$  shown in Appendix C. Here, the first-quantized unitary transformation  $\hat{u}_k = \hat{u}(\mathbf{x}_{k,n}, \mathbf{x}_{k,e})$  of coboson  $k$  acts only on coordinates and operators associated with coboson coordinates  $(\mathbf{x}_{k,n}, \mathbf{x}_{k,e})$ . As a result, we obtain the transformed second-quantized Hamiltonian

$$\begin{aligned} \hat{U}^\dagger \hat{H}_{\text{Cb}} \hat{U} &= \hat{U}^\dagger \hat{H}_{\text{EM}} \hat{U} + \int_{C_1} d^6x_1 \hat{\phi}_1^\dagger \hat{u}_1^\dagger \hat{h}_{\text{Cb}} \hat{u}_1 \hat{\phi}_1 \\ &\quad + \int_{C_1} d^6x_1 \int_{C_2} d^6x_2 \hat{\phi}_1^\dagger \hat{\phi}_2^\dagger \hat{u}_1^\dagger \hat{u}_2^\dagger \hat{V}_{\text{Scatt}} \hat{u}_2 \hat{u}_1 \hat{\phi}_2 \hat{\phi}_1 \end{aligned} \quad (17)$$

given that  $[\hat{\Lambda}, \hat{h}_{\text{Cb}}] = [\hat{\Lambda}, \hat{V}_{\text{Scatt}}] = 0$ . If  $\hat{\lambda}$  contains EM fields, we also need to transform  $\hat{H}_{\text{EM}}$ , otherwise it remains invariant.

With this procedure, we may apply any first-quantized unitary specified by  $\hat{\lambda}$  to the first-quantized Hamiltonian  $\hat{h}_{\text{Cb}}$  and the potential  $\hat{V}_{\text{Scatt}}$  within the second-quantized framework as long as the requirements above are met. In the following, we specify the transformations to obtain a multipolar CbQFT in c.m. and relative coordinates including relativistic corrections.

##### A. Nonrelativistic c.m. and relative coordinates

First, we move from the set of electron  $\{\mathbf{x}_{k,e}, \hat{\mathbf{p}}_{k,e}, \hat{\mathbf{s}}_{k,e}\}$  and nucleus  $\{\mathbf{x}_{k,n}, \hat{\mathbf{p}}_{k,n}, \hat{\mathbf{s}}_{k,n}\}$  coordinates to NR c.m.  $\{\mathbf{R}_k, \hat{\mathbf{P}}_k, \hat{\mathbf{S}}_k\}$  and relative  $\{\mathbf{r}_k, \hat{\mathbf{p}}_k, \hat{\mathbf{s}}_k\}$  coordinates describing coboson  $k$ . The connection between the different coordinates are listed in Table I and chosen such that c.m. (position  $\mathbf{R}_k$ , momentum  $\hat{\mathbf{P}}_k$ ) and relative (position  $\mathbf{r}_k$ , momentum  $\hat{\mathbf{p}}_k$ ) share nonvanishing canonical commutators  $[R_\ell^{(u)}, \hat{P}_k^{(v)}] = [r_\ell^{(u)}, \hat{p}_k^{(v)}] = i\hbar \delta_{uv} \delta_{\ell k}$  where  $u, v = x, y, z$ . These coordinates are defined through the total mass  $M = m_e + m_n$  as well as the



Table I. Single-fermion coordinates of coboson  $k$  expressed through their c.m. and relative counterparts in the NR limit. The positions, momenta, and spins  $\{\mathbf{x}_{k,j}, \hat{\mathbf{p}}_{k,j}, \hat{\mathbf{s}}_{k,j}\}$  of fermion  $j = e, n$  are expressed through their respective c.m. and relative coordinates  $\{\mathbf{R}_k, \hat{\mathbf{P}}_k, \hat{\mathbf{S}}_k\}$  and  $\{\mathbf{r}_k, \hat{\mathbf{p}}_k, \hat{\mathbf{s}}_k\}$ . Here,  $M = m_e + m_n$  and  $m_r = m_e m_n / M$  describe the total and reduced mass of the coboson, respectively, and  $m_j$  is the mass of its constituents.

	$j$	$e$	$n$
position	$\mathbf{x}_{k,j}$	$\mathbf{R}_k + m_r \mathbf{r}_k / m_e$	$\mathbf{R}_k - m_r \mathbf{r}_k / m_n$
momentum	$\hat{\mathbf{p}}_{k,j}$	$m_e \hat{\mathbf{P}}_k / M + \hat{\mathbf{p}}_k$	$m_n \hat{\mathbf{P}}_k / M - \hat{\mathbf{p}}_k$
spin	$\hat{\mathbf{s}}_{k,j}$	$m_e \hat{\mathbf{S}}_k / M + \hat{\mathbf{s}}_k$	$m_n \hat{\mathbf{S}}_k / M - \hat{\mathbf{s}}_k$

total spin  $\hat{\mathbf{S}}_k$  and the relative spin  $\hat{\mathbf{s}}_k$ . Changing the coordinates leaves the integration measure invariant and we replace  $d^6 x_k \rightarrow d^6 \mathcal{R}_k = d^3 R_k d^3 r_k$  in  $\hat{H}_{\text{Cb}}$  from Eq. (13) together with single-particle coordinates in  $\hat{h}_{\text{Cb}}$  and  $\hat{V}_{\text{Scatt}}$  according to the transformation specified in Table I. Note that the field operators  $\hat{\varphi}_k = \hat{\varphi}(\mathbf{R}_k - m_r \mathbf{r}_k / m_n, \mathbf{R}_k + m_r \mathbf{r}_k / m_e)$  have thus become a function of c.m. and relative coordinates as well.

### B. Relativistic corrections to c.m. and rel. coordinates

Our description contains relativistic corrections up to the order  $c^{-2}$ . However, the transformation to NR c.m. and relative coordinates from Table I is inconsistent to this order and has to be modified [74, 75, 77, 78]. Consequently, we take relativistic corrections to NR c.m. and relative coordinates into account, in order to remain consistent in  $c^{-2}$ . These corrections can be implemented via a first-quantized unitary transformation [74, 75], which circumvents issues regarding the integration measure and the transformation of certain terms in the scattering potential that arise with an actual coordinate transformation. Such a first-quantized unitary [74] is generated by

$$\hat{\lambda}_k^{(\text{rel})} = \frac{\mathbf{r}_k \cdot \hat{\mathbf{P}}_k}{4M^2 c^2} \left[ \hat{\mathbf{p}}_k \cdot \hat{\mathbf{p}}_k + \Delta m \left( \frac{\hat{\mathbf{p}}_k^2}{m_r} + \frac{q_e q_n}{4\pi \epsilon_0 |\mathbf{r}_k|} \right) \right] + \text{H.c.} \\ - \frac{1}{4m_r M c^2} \left( \hat{\mathbf{p}}_k \times \hat{\mathbf{P}}_k + \text{H.c.} \right) \cdot \hat{\mathbf{s}}_k. \quad (18)$$

The Coulomb-potential term proportional to the mass difference  $\Delta m = m_n - m_e$  arises due to the internal EM interactions. In addition, single-particle masses are contained in the total mass  $M = m_e + m_n$  and the reduced mass  $m_r = m_e m_n / M$ , and the Hermitian conjugate H.c. ensures hermiticity of the generator. We also account for  $c^{-2}$  corrections to light-matter interactions by using gauge-invariant minimally-coupled momenta [77]  $\hat{\mathbf{P}}_k = \hat{\mathbf{p}}_{k,e} + \hat{\mathbf{p}}_{k,n}$  and  $\hat{\mathbf{p}}_k = (m_n \hat{\mathbf{p}}_{k,e} - m_e \hat{\mathbf{p}}_{k,n}) / M$  instead of purely kinetic momentum operators. To apply this first-quantized transformation to a second-quantized theory, we need to confirm that  $[\hat{\Lambda}_{\text{rel}}, \hat{h}_{\text{Cb}}] = [\hat{\Lambda}_{\text{rel}}, \hat{V}_{\text{Scatt}}] = 0$ , where  $\hat{\Lambda}_{\text{rel}}$  and  $\hat{\lambda}_k^{(\text{rel})}$  are connected through Eq. (16). Since  $\hat{\Lambda}_{\text{rel}}$  contains an integration over coordinates that are independent of  $\hat{h}_{\text{Cb}}$  and  $\hat{V}_{\text{Scatt}}$ , the cobosonic operators trivially commute. While

the vector potential commutes in Coulomb gauge with itself, its commutator with the electric fields in  $\hat{h}_{\text{Cb}}$  (Darwin term and spin-orbit term) is nonvanishing. The resulting additional terms from this commutator, however, are yet ruled out by the limits of integration in  $\hat{H}_{\text{Cb}}$ . This fact is a consequence of the projection, ensuring that a coboson can only contain one nucleus and electron, and may be made explicit by introducing  $\hat{\varphi} = \hat{\pi}_{\text{Cb}} \hat{\varphi}$ , similar to Appendix C. Thus, the transformation reduces to Eq. (17).

### C. Power-Zienau-Woolley transformation

We now introduce the interaction of light with matter through electric and magnetic fields  $\hat{\mathbf{E}}$  and  $\hat{\mathbf{B}}$  rather than through the vector potential, *i. e.*, we move to *multipolar cobosonic quantum field theory*. This transition follows from applying the unitary *Power-Zienau-Woolley* (PZW) transformation [40, 41, 76] defined by its first-quantized generator  $\hat{\lambda}_k^{(\text{PZW})} = \int d^3 y \mathcal{P}_k(\mathbf{y}) \cdot \hat{\mathbf{A}}(\mathbf{y})$  through the polarization field [79]

$$\mathcal{P}_k(\mathbf{y}) = \sum_i q_i (\mathbf{x}_{k,i} - \mathbf{R}_k) \int_0^1 d\rho \delta[\mathbf{y} - \mathbf{R}_k - \rho(\mathbf{x}_{k,i} - \mathbf{R}_k)] \quad (19)$$

of the  $k$ -th coboson. Here, we choose the coordinate  $\mathbf{R}_k$ , which could be arbitrary in general, to coincide with the c.m. position. Based on the discussion above, it can be shown that this generator meets the requirements to reduce the second-quantized transformation to the first-quantized one as well.

### D. Transformation sequence

Finally, the total transformation sequence addresses first the generation of relativistic corrections to NR c.m. and relative coordinates, followed by the PZW transformation. This particular order of transformations is crucial to remain gauge invariant. The transformations of Eq. (13) leads to the replacements

$$\hat{h}_{\text{Cb}} \rightarrow \hat{u}_1^{(\text{PZW})\dagger} \hat{u}_1^{(\text{rel})\dagger} \hat{h}_{\text{Cb}} \hat{u}_1^{(\text{rel})} \hat{u}_1^{(\text{PZW})} \quad (20a)$$

$$\hat{V}_{\text{Scatt}} \rightarrow \hat{u}_{12}^{(\text{PZW})\dagger} \hat{u}_{12}^{(\text{rel})\dagger} \hat{V}_{\text{Scatt}} \hat{u}_{12}^{(\text{rel})} \hat{u}_{12}^{(\text{PZW})} \quad (20b)$$

$$\hat{H}_{\text{EM}} \rightarrow \hat{U}_{\text{PZW}}^\dagger \hat{U}_{\text{rel}}^\dagger \hat{H}_{\text{EM}} \hat{U}_{\text{rel}} \hat{U}_{\text{PZW}} \quad (20c)$$

where  $\hat{u}_{12} = \hat{u}_1 \hat{u}_2$  combines the transformation of both coordinate sets. For a more detailed discussion on the above transformations, we refer to Appendix D and present the major results in the next section.

## V. MULTIPOLAR COBOSONIC QFT

Together with the transformations from the previous section, our multipolar CbQFT is formulated with respect to c.m. and

relative coordinates, while every scale is corrected in  $c^{-2}$ . In particular, the theory includes corrections to internal dynamics encoded in  $\hat{h}_{\text{Cb}}$ , inter-cobosonic dynamics in  $\hat{V}_{\text{Scatt}}$ , and light-matter interactions contained in both terms. Consequently, the multipolar cobosonic Hamiltonian

$$\begin{aligned} \hat{H}_{\text{MpCb}} = & \hat{H}_{\text{EM}} + \int_C d^6\mathcal{R} \hat{\varphi}^\dagger \hat{h}_{\text{MpCb}} \hat{\varphi} + \\ & + \int_{C_1} d^6\mathcal{R}_1 \int_{C_2} d^6\mathcal{R}_2 \hat{\varphi}_1^\dagger \hat{\varphi}_2^\dagger \hat{V}_{\text{Scatt}} \hat{\varphi}_2 \hat{\varphi}_1 \end{aligned} \quad (21)$$

accounts via  $\hat{h}_{\text{MpCb}}$  for the single-coboson energy, while the scattering potential is accounted for by  $\hat{V}_{\text{Scatt}}$ . In the former, we omit the subscript ‘‘1’’ for simplicity and, therefore, whenever there are no interactions between more than one coboson in the following.

### A. Single-coboson Hamiltonian

The explicit form of the single-coboson Hamiltonian

$$\begin{aligned} \hat{h}_{\text{MpCb}} = & Mc^2 + \hat{h}_{\text{rel}}^{(0)} + \hat{h}_{\text{rel}}^{(1)} + \frac{\hat{\mathbf{P}}_Q^2}{2M} \left( \mathbb{1} - \frac{\hat{h}_{\text{rel}}^{(0)}}{Mc^2} \right) - \frac{\hat{\mathbf{P}}_Q^4}{8M^3c^2} \\ & + \hat{h}_{\mathbf{r} \times \hat{\mathbf{P}}_Q} + \hat{h}_1^{(0)} + \hat{h}_1^{(1)} \end{aligned} \quad (22)$$

consists of the internal structure  $\hat{h}_{\text{rel}}^{(0)} + \hat{h}_{\text{rel}}^{(1)}$ , c.m. kinetic terms proportional to the minimally-coupled momentum  $\hat{\mathbf{P}}_Q^2$ , as well as the light-matter interaction  $\hat{h}_1^{(0)} + \hat{h}_1^{(1)}$ . The kinetic term couples to the internal structure as a consequence of the mass defect [16–18]. The rest energy  $Mc^2$  is modified by the relative motion

$$\hat{h}_{\text{rel}}^{(0)} = \frac{\hat{\mathbf{p}}^2}{2m_r} + \frac{q_e q_n}{4\pi\epsilon_0|\mathbf{r}|} \quad (23)$$

solely given by a hydrogen-type Hamiltonian. The next-order correction is given by

$$\begin{aligned} \hat{h}_{\text{rel}}^{(1)} = & -\frac{\hat{\mathbf{p}}^4}{8m_r^3c^2} \frac{m_e^3 + m_n^3}{M^3} - \frac{\kappa}{|\mathbf{r}|^3} \left( \frac{1}{2} \hat{\ell}^2 + (\mathbf{r} \cdot \hat{\mathbf{p}})^2 \right) \\ & + \kappa \alpha_D \pi \hbar^2 \delta(\mathbf{r}) + \kappa \frac{\alpha_{\ell S}}{|\mathbf{r}|^3} \hat{\ell} \cdot \hat{\mathbf{S}} + \kappa \frac{\alpha_{\ell s}}{|\mathbf{r}|^3} \hat{\ell} \cdot \hat{\mathbf{s}} \\ & + \kappa \alpha_{ss} \pi \delta(\mathbf{r}) \hat{\mathbf{s}}_n \cdot \hat{\mathbf{s}}_e + \kappa \frac{c_F^{(n)} c_F^{(e)}}{|\mathbf{r}|^3} \hat{S}_{ne}. \end{aligned} \quad (24)$$

Similar to Sec. II A, we defined  $\kappa = 2\kappa_{ne} = -q_e q_n / (4\pi\epsilon_0 m_r M c^2)$  and the abbreviation  $\alpha_v$  summarizes all Wilson coefficients in Table II. These corrections [60–62] give rise to the fine- and hyperfine structure of hydrogen-like atoms and correspond in the same order to: the kinetic relative correction, orbit-orbit coupling, Darwin term, spin-orbit coupling of angular momentum  $\hat{\ell} = \mathbf{r} \times \hat{\mathbf{p}}$  to total and relative spin, spin-spin contact coupling, as well as the magnetic

Table II. Low-energy effective Wilson coefficients  $\alpha_v$  that contribute to the relativistic corrections of the relative motion, *i. e.*, to the internal structure. They can be connected to the high-energy Wilson coefficients  $c_D^{(j)}$ ,  $c_F^{(j)}$ , and  $c_S^{(j)}$  that correspond to the Darwin, Fermi, and Seagull coefficients of Fermion  $j = e, n$  as well as to the Wilson coefficients  $d_1^{(ij)}$  and  $d_2^{(ij)}$  for  $j \neq i$  that originate in the contact interaction.

	$v$	$\alpha_v$
Darwin	D	$\frac{m_n^2 c_D^{(e)} + m_e^2 c_D^{(n)}}{2m_r M} + \frac{d_1^{(en)} + d_1^{(ne)}}{\pi Z \alpha}$
(total spin)-orbit	$\ell S$	$\frac{m_e c_F^{(e)} + m_n c_F^{(n)}}{M} + \frac{m_e c_S^{(n)} + m_n c_S^{(e)}}{2M}$
(relative spin)-orbit	$\ell s$	$c_F^{(e)} - c_F^{(n)} + \frac{c_S^{(e)} m_n^2 - c_S^{(n)} m_e^2}{2m_r M}$
spin-spin	ss	$4c_F^{(n)} c_F^{(e)} - 4 \frac{d_2^{(en)} + d_2^{(ne)}}{\pi Z \alpha}$

dipole-dipole interaction  $\hat{S}_{ne} = -\hat{\mathbf{s}}_n \cdot \hat{\mathbf{s}}_e + 3(\hat{\mathbf{s}}_n \cdot \mathbf{r})(\hat{\mathbf{s}}_e \cdot \mathbf{r})/|\mathbf{r}|^2$ . Note that  $\hat{\mathbf{s}}_n$  and  $\hat{\mathbf{s}}_e$  refer to the spin of nucleus and electron and may be expressed through their corresponding total and relative spin. Here, we reproduce results known from the literature [37] that are augmented by particle-species dependent Wilson coefficients  $c_F^{(i)}$  and  $c_S^{(i)}$ .

In addition to the internal structure, our results include c.m. degrees of freedom. The c.m. kinetic energy appears as dominating, lowest-order contribution but is modified by a correction proportional to the relative Hamiltonian  $\hat{h}_{\text{rel}}^{(0)}$  as a consequence of the mass defect [16–18], where relative and c.m. degrees of freedom couple to each other. Relativistic corrections to the relative Hamiltonian  $\hat{h}_{\text{rel}}^{(1)}$  are not included in the mass-defect term for consistency, since these couplings are of order  $c^{-4}$ . The mass defect implies an internal-state-dependent c.m. motion that can be identified with a state-dependent mass [16, 17, 24–26, 30–34], which we show in detail later.

The fact that our description allows also for charged cobosons (ions) manifests in a monopole coupling where the total charge  $Q = q_n + q_e$  and the vector potential evaluated at the c.m. position  $\hat{\mathbf{A}}(\mathbf{R})$  appear in minimally-coupled momenta  $\hat{\mathbf{P}}_Q = \hat{\mathbf{P}} - Q\hat{\mathbf{A}}(\mathbf{R})$ . The kinetic c.m. degrees of freedom are completed by the c.m. relativistic kinetic correction proportional to  $\hat{\mathbf{P}}_Q^4$ , analogously [16] to the case of neutral atoms with  $Q = 0$ . For ions ( $Z > 1$ ), the Hamiltonian

$$\hat{h}_{\mathbf{r} \times \hat{\mathbf{P}}_Q} = -\frac{q_e q_n}{8\pi\epsilon_0 m_n M c^2} \frac{Z-1}{|\mathbf{r}|^3} \left( \mathbf{r} \times \hat{\mathbf{P}}_Q \right) \cdot \hat{\mathbf{s}}_n \quad (25)$$

describes a coupling of the coboson’s total angular momentum  $\mathbf{r} \times \hat{\mathbf{P}}_Q$  to the nucleus spin  $\hat{\mathbf{s}}_n$ , encoding the fact that the nucleus gives rise to charged cobosons. This additional coupling between c.m. and relative degrees of freedom arises analogously to the mass defect due to our extension to spin-carrying and possibly charged cobosons, and has not yet been derived to the best of our knowledge.

Further, external EM fields interact with the coboson in

leading order via

$$\hat{h}_1^{(0)} = \hat{h}_{\text{ME}} + \hat{h}_{\text{MM}} + \hat{h}_{\text{R}} + \hat{h}_{\text{Dia}} + \hat{h}_{\text{Self}}. \quad (26)$$

The explicit form of the components are summarized in Table III, where all EM fields depend on the integration variable  $\mathbf{y}$  if not stated otherwise. The polarization  $\mathcal{P}$  and the magnetization  $\hat{\mathbf{M}}$  [see Eq. (27)] depend on  $\mathbf{y}$ , as well as on coboson coordinates  $\mathbf{x}_e$  and  $\mathbf{x}_n$  that have to be expressed by c.m. and relative coordinates.

Table III. Contributions to the leading-order light-matter interaction  $\hat{h}_1^{(0)}$ . The individual terms  $\hat{h}_v$  describe a coupling of generalized electric (ME) and magnetic (MM) moments as well as the Röntgen (R) and diamagnetic (Dia) interaction together with the self-energy (Self). They describe a coupling of the polarization field  $\mathcal{P}$ , the magnetization  $\hat{\mathbf{M}}$ , magnetic moments  $\hat{\boldsymbol{\mu}}_i$  to c.m. momenta  $\hat{\mathbf{P}}_Q$ , magnetic fields  $\hat{\mathbf{B}}$ , and the transverse electric field  $\hat{\mathbf{E}}^\perp$ .

$v$	$\hat{h}_v$
ME	$-\int d^3y \mathcal{P}^\perp \cdot \hat{\mathbf{E}}^\perp$
MM	$-\frac{1}{2} \int d^3y (\hat{\mathbf{M}} \cdot \hat{\mathbf{B}} + \text{H.c.}) - \sum_{i=e,n} \hat{\boldsymbol{\mu}}_i \cdot \hat{\mathbf{B}}(\mathbf{x}_i)$
R	$\frac{1}{2M} \{ \hat{\mathbf{P}}_Q, \int d^3y \mathcal{P} \times \hat{\mathbf{B}} \}$
Dia	$\frac{(\int d^3y \mathcal{P} \times \hat{\mathbf{B}})^2}{2M} + \frac{\left[ \sum_i q_i \frac{m_r}{m_i^2} \mathbf{r} \times \int_0^1 d\rho \rho \hat{\mathbf{B}} \left( \mathbf{R} - \rho \frac{q_i}{ q_i } \frac{m_r}{m_i} \mathbf{r} \right) \right]^2}{2m_r}$
Self	$\frac{1}{2\epsilon_0} \int d^3y (\mathcal{P}^\perp)^2$

The term  $\hat{h}_{\text{ME}}$  couples the transverse electric field  $\hat{\mathbf{E}}^\perp$  to the transverse part of the polarization field from Eq. (19), giving rise to generalized electric moments (ME). For instance, a multipole expansion of the polarization field in  $\mathbf{R}$  implying small relative coordinates, we find in lowest order the dipole moment  $\mathbf{d} = m_r(q_e/m_e - q_n/m_n)\mathbf{r}$ .

Similarly, the magnetic field couples to magnetic moments (MM) in  $\hat{h}_{\text{MM}}$  and has two contributions: The particles' spin, *i. e.*, the magnetic moment  $\boldsymbol{\mu}_i = c_F^{(i)} q_i \mathbf{s}_i / m_i$ , couples to the magnetic field  $\hat{\mathbf{B}}(\mathbf{x}_i)$ , where the single-fermion coordinates have to be replaced by c.m. and relative coordinates  $\mathbf{x}_i = \mathbf{R} - \frac{q_i}{|q_i|} \frac{m_r}{m_i} \mathbf{r}$ . Moreover, constituents of composite particles carry orbital angular momentum  $\hat{\boldsymbol{\ell}}$  that induces an orbital magnetic moment contained in the quantum magnetization

$$\hat{\mathbf{M}}(\mathbf{y}) = \sum_i \frac{m_r}{m_i} q_i \frac{\hat{\boldsymbol{\ell}}}{m_i} \int_0^1 d\rho \rho \delta[\mathbf{y} - \mathbf{R} - \rho(\mathbf{x}_i - \mathbf{R})] \quad (27)$$

similar to the relation between polarization fields and electric moments. A multipole expansion of the magnetization and the magnetic field leads in lowest order to the magnetic moment of a coboson  $\hat{\boldsymbol{\mu}}_\ell + \hat{\boldsymbol{\mu}}_n + \hat{\boldsymbol{\mu}}_e$ , with  $\hat{\boldsymbol{\mu}}_\ell = m_r(q_e/m_e^2 + q_n/m_n^2)\hat{\boldsymbol{\ell}}/2$ , *i. e.*, the sum of orbital, electron, and nucleus spin magnetic moments giving rise to the Zeeman shift [80].

In addition, the c.m. motion of the coboson also yields the c.m. Röntgen Hamiltonian  $\hat{h}_{\text{R}}$  [81–85]. Further, we find that the diamagnetic interaction  $\hat{h}_{\text{Dia}}$  with c.m. and relative contribution corresponds to an induced magnetic moment due to the external fields, being part of the quadratic Zeeman effect [86]. Moreover, the cobosonic self-energy  $\hat{h}_{\text{Self}}$  is generally divergent, but can be renormalized [87] and contributes to the Lamb shift [40].

The last contributions to the single-coboson Hamiltonian are relativistic corrections to the light-matter interaction and in general depend on the electric or the magnetic field. In many applications light-matter interactions are dominated by electric fields. Here, we present these dominant electric terms and suppress the influence of magnetic fields in  $c^{-2}$ . The full Hamiltonian including magnetic-field contributions is given in Appendix D, while the electric-field contribution resolves to

$$\hat{h}_1^{(1)} = \sum_i c_S^{(i)} q_i \hat{\mathbf{s}}_i \cdot \frac{\left( \frac{m_i}{M} \hat{\mathbf{P}}_Q - \frac{q_i}{|q_i|} \hat{\mathbf{p}} \right) \times \hat{\mathbf{E}} + \text{H.c.}}{8m_i^2 c^2} + \frac{1}{2} \sum_i \left[ \hat{\mathbf{E}}^\perp(\mathbf{x}_i) \cdot \hat{\mathbf{d}}_i^{(1)} + \hat{\mathbf{d}}_i^{(1)} \cdot \hat{\mathbf{E}}^\perp(\mathbf{x}_i) \right]. \quad (28)$$

The second line originates from relativistic corrections to c.m. and relative coordinates and describes the coupling of the transverse electric field  $\hat{\mathbf{E}}^\perp$  to dipole-moment corrections

$$\hat{\mathbf{d}}_i^{(1)} = \frac{\mathbf{r}}{4M^2 c^2} \left( \hat{\mathbf{p}} \cdot \hat{\mathbf{P}}_Q + \frac{\Delta m}{m_r} \hat{\mathbf{p}}^2 + \frac{\Delta m q_e q_n}{4\pi \epsilon_0 |\mathbf{r}|} \right) + \text{H.c.} + \frac{\mathbf{r} \cdot \hat{\mathbf{P}}_Q}{4M^2 c^2} \left[ \left( 1 - 2 \frac{\Delta m}{m_i} \frac{q_i}{|q_i|} \right) \hat{\mathbf{p}} - \frac{m_r}{m_i} \frac{q_i}{|q_i|} \hat{\mathbf{P}}_Q \right] + \text{H.c.} + \frac{1}{2m_r M c^2} \left( \frac{m_r}{m_i} \frac{q_i}{|q_i|} \hat{\mathbf{P}}_Q + \hat{\mathbf{p}} \right) \times \hat{\mathbf{s}} \quad (29)$$

in accordance [77] with the limiting case of  $Q = 0$  and arbitrary loosely bound cobosons.

## B. Scattering potential

The scattering potential has the general form

$$\hat{\mathcal{V}}_{\text{Scatt}} = \sum_{i,j} \left[ \hat{\mathcal{V}}_{\text{C}}^{(ij)} + \hat{\mathcal{V}}_{\text{LL}}^{(ij)} + \hat{\mathcal{V}}_{\text{LS}}^{(ij)} + \hat{\mathcal{V}}_{\text{SS}}^{(ij)} \right] + \hat{\mathcal{V}}_{\text{Self}}, \quad (30)$$

where the components are summarized in Table IV. For simplicity, we include only the most dominant c.m. contribution to the scattering for all  $c^{-2}$ -terms by omitting terms directly proportional to  $\mathbf{r}_i$ , while keeping the general distance between two different constituents  $\chi_{ij} = \mathbf{x}_{1,i} - \mathbf{x}_{2,j}$  and neglecting all terms proportional to the relative momentum  $\hat{\mathbf{p}}_i$ . Besides, we also exclude the influence of light-matter interaction in the scattering processes presented in the Table. The full scattering potential including light-matter interactions and relative contributions is given in Appendix D. As expected, the leading-order contribution of scattering is the Coulomb (C) interaction between fermion  $i$  of coboson 1 and fermion  $j$  of coboson 2. However, we find a second Coulomb-like correction including the unit

Table IV. Contributions to the scattering potential  $\hat{\mathcal{V}}_{\text{Scatt}}$ . The individual terms  $\hat{\mathcal{V}}_v^{(ij)}$  mediate the interaction between two fermions  $i, j$  of different cobosons and include a Coulomb (C) interaction, a coupling of orbital magnetic moments through angular momenta including a retardation correction (LL), a spin-orbit interaction (LS), a magnetic dipole potential (SS) and the self-energy (Self).

$v$	$\hat{\mathcal{V}}_v^{(ij)}$
C	$\frac{q_i q_j}{8\pi\epsilon_0 \chi_{ij} } + \frac{\Delta m}{M} \frac{e_{\chi_{ij}} \cdot (e_{r_1} - e_{r_2})}{Mc^2} \frac{q_e q_n}{q_i q_j} \left( \frac{q_i q_j}{8\pi\epsilon_0 \chi_{ij} } \right)^2$
LL	$-\frac{\mu_0 q_i q_j}{8\pi M^2} \frac{1}{ \chi_{ij} ^3} \left( \frac{1}{2} \hat{\mathbf{L}}_1^{(ij)} \cdot \hat{\mathbf{L}}_2^{(ij)} + (\chi_{ij} \cdot \hat{\mathbf{P}}_1) (\chi_{ij} \cdot \hat{\mathbf{P}}_2) \right)$
LS	$-\frac{\mu_0}{8\pi \chi_{ij} ^3} \left[ \frac{q_i}{M} (\hat{\mathbf{L}}_1^{(ij)} - \hat{\mathbf{L}}_2^{(ij)}) \left( \frac{q_j}{q_i} \hat{\boldsymbol{\mu}}_{1,i} + \hat{\boldsymbol{\mu}}_{2,j} \right) \right. \\ \left. - \frac{Z_i}{2} \frac{q_j q_i}{M m_i} \hat{\mathbf{L}}_1^{(ij)} \cdot \hat{\boldsymbol{s}}_{1,i} + \frac{Z_j}{2} \frac{q_i q_j}{M m_j} \hat{\mathbf{L}}_2^{(ij)} \cdot \hat{\boldsymbol{s}}_{2,j} \right]$
SS	$-\frac{\mu_0}{8\pi \chi_{ij} ^3} \left[ \hat{\boldsymbol{\mu}}_{1,i} \cdot \hat{\boldsymbol{\mu}}_{2,j} - 3 (\hat{\boldsymbol{\mu}}_{1,i} \cdot e_{\chi_{ij}}) (\hat{\boldsymbol{\mu}}_{2,j} \cdot e_{\chi_{ij}}) \right]$
Self	$\frac{1}{2\epsilon_0} \int d^3y \mathcal{P}_1^\perp \cdot \mathcal{P}_2^\perp$

vector  $e_w$  in  $w$ -direction, where  $w$  is either the distance  $\chi_{ij}$  between constituents of different cobosons or relative distances between each coboson's constituents  $r_1$  and  $r_2$ . Corrections to the Coulomb potential are interactions between all possible magnetic moments among different cobosons. Consequently, in  $\hat{\mathcal{V}}_{\text{LL}}^{(ij)}$  we find orbital magnetic moments coupling to each other through orbital angular momenta  $\hat{\mathbf{L}}_k^{(ij)} = \chi_{ij} \times \hat{\mathbf{P}}_k$ . Moreover, we find also in the scattering potential an additional term containing momentum operators that corresponds to the so-called *retardation correction* [60]. The spin-orbit (LS) interaction includes an interaction of an effective orbital magnetic moment proportional to  $\hat{\mathbf{L}}_1^{(ij)} - \hat{\mathbf{L}}_2^{(ij)}$  with an effective spin magnetic moment  $q_j \hat{\boldsymbol{\mu}}_{1,i}/q_i + \hat{\boldsymbol{\mu}}_{2,j}$ , complemented by pure spin-orbit coupling. These potentials are completed by the known [88, 89] magnetic dipole-dipole potential  $\hat{\mathcal{V}}_{\text{SS}}^{(ij)}$ .

Moreover, one effect of the PZW transformation becomes apparent only in second quantization, which is the scattering self-energy [ $\hat{\mathcal{V}}_{\text{Self}}$ , Eq. (30)], arising analogously (and additionally) to the cobosonic self-energy [ $\hat{h}_{\text{Self}}$  in Eq. (26)] in the single-coboson sector. Because of the multi-coboson nature, this contribution may be associated as one part of the collective (or cooperative) Lamb shift [90, 91].

With these results, we have introduced a multipolar CbQFT. The single-coboson Hamiltonian includes consistently  $c^{-2}$  corrections for all scales, involving the corrected internal structure, the mass defect in the c.m. motion, but also light-matter interactions beyond a multipole expansion, and relativistic corrections. We derived scattering potentials based on lowest-order two-particle scattering, yielding the Coulomb potential with several corrections in form of interactions between magnetic moments.

## VI. DISCUSSION

In the following section, we identify different physical systems and issues that can be described or addressed by our multipolar CbQFT, such as models for atomic systems, bound-state energies, the scattering between atoms, as well as ultracold quantum gases. The examples demonstrate that our theory contributes to the fundamental understanding of various subfields, complementing and connecting existing approaches. While illustrative, these examples are not exhaustive but only represent a small portion of what might be achieved with such effective models.

### A. Models for atomic systems

First-quantized Lagrangian or Hamiltonian treatments of atomic dynamics restricted to single-particle systems have been studied extensively [80]. There are relativistic treatments, *e. g.*, extending the NR Schrödinger equation for a hydrogen atom to relativistic equations [92] or formulating equations of motion for c.m. coordinates of a system of relativistic Dirac particles, which allows for a description of relativistic bound-state systems [93]. However, the dynamics of atomic ensembles are often studied in NR regimes since atomic quantum gases are mostly restricted to low-energy scales. One accurate model of bound-state particles that includes relativistic corrections follows from two coupled Dirac equations in the respective NR limit [60–62], and is known as Breit-Pauli Hamiltonian. This Hamiltonian does not account for field-theoretical QED corrections and is derived with respect to single-fermion coordinates. As a result, additional relativistic corrections enter the Hamiltonian [77, 78] once NR c.m. and relative coordinates are introduced to separate the inner-atomic structure from the c.m. motion. In the simplified case where one ignores the spin of fermions, such a description of atoms gives rise to a coupling of c.m. to relative degrees of freedom as a consequence of the mass defect [16–18, 22]. In contrast to calculating relativistic corrections to the NR bound-state atoms and their dynamics, there are other models that focus on corrections arising from a finite extension of atoms via hard-sphere models, *i. e.*, atoms confined in spherical impenetrable boxes, and they have been studied for hydrogen [94–103], hydrogen-like [104], and many-electron atoms [105–108]. In this case, different deviations from the standard NR treatment of hydrogen-like atoms than the relativistic ones follow.

Based on such first-quantized models, one usually postulates a corresponding effective field theory [21, 109], and rigorous field-theoretical top-down derivations for atoms are not addressed. Conversely, our work embeds established first-quantized concepts mentioned above into a field-theoretical formulation. As a result, the Breit-Pauli Hamiltonian is further modified by QED corrections. Via our projection formalism, we naturally introduce length scales defining the extension of an atom, similar to hard-sphere impenetrable boxes. Introducing c.m. and relative coordinates leads also to the mass defect, where we extend known derivations [16, 17] to arbitrary numbers of spin-carrying and charged cobosons in a field-theoretical

framework, yet restricted to special relativity.

Models for atomic systems include not only isolated atoms but also the description of their interaction with external fields, *e. g.*, light and gravity. In quantum and atom optics for instance, atoms are manipulated via the interaction with light, leading *e. g.*, to magneto-optical traps [110–113] for neutral atoms as well as Paul [114–117] and Penning [118–121] traps for ions. Instead of trapping atoms, light pulses [122–124] or Bloch oscillations [125–130] are used to manipulate the atoms' momenta and might also induce transitions between internal states [131, 132]. In the context of cold atoms, magnetic fields give control over scattering dynamics between atoms via Feshbach resonances [133–137] but are also crucial to implement, *e. g.*, *E1M1* [138–140] or magnetically-induced single-photon [131] pulses. All of these light-matter interactions and processes are included in our multipolar CbQFT.

In many applications [141, 142] it is sufficient to take only the lowest-order multipole expansion of the EM field into account. Further contributions, such as higher-order multipole moments driving transitions [143] or respective energy shifts [144], are then considered individually to the desired order [85]. In our present work, we use the generalized polarization-field approach [79] for the PZW transformation [40, 41, 76]. Thus, all possible contributions from light-matter interactions are covered similar to single-atomic treatments [145] but incorporated into a field-theoretical framework. Moreover, relativistic corrections to light-matter interaction on the level of elementary fermions are known most accurately in the field of NRQED [53]. Once we move to the multipolar form defined with respect to NR c.m. and relative coordinates, additional relativistic corrections arise also for EM fields. These have been studied for electric-field contributions [77, 146] but magnetic-field contributions have not been discussed explicitly yet. Our treatment includes, in a field-theoretical framework, all relativistic corrections to EM fields appearing in light-matter interactions, in particular also magnetic-field contributions.

The simple first-quantized model of atoms falling in gravitational potentials [147], as another external field, has been extended to a post-Newtonian description for an atomic Hamiltonian considering relativistic corrections associated with the coupling of gravity to atoms [17, 22, 148, 149] for single, spinless, and neutral atoms. Some of these works derived the mass defect under gravity [17], confirming original ideas for quantum interferometry [23–25]. The mass defect shows a connection to proper time associated with the c.m. of the atom and can be encoded by atomic [22] and quantum [26, 32, 150] clocks in gravitational backgrounds. Some theories even predict effective gravitational decoherence mechanisms [151]. In addition, quantum-clock interferometry allows for tests of general relativity [30–32, 34]. However, also in the gravity-free case, a coupling of internal degrees of freedom to the atomic c.m. via the mass defect leads to possible measurements of a quantum twin paradox [26, 152, 153] or allows for dark-matter detection [27–29, 33]. Our work does not include gravity so far, but the mass defect is yet derived consistently in a field-theoretical framework and augmented by other relativistic corrections to the internal Hamiltonian. With QFT on curved spacetime and a generalization of the respective coordinate

transformations, an extension to gravitational fields seems in principle possible.

## B. Bound-state energies

Most models of atoms focus on their internal structure, allowing for calculations of bound-state energies. Consequently, in most accurate treatments radiative QED corrections [11–14] and effects from the composite-particle nature of the nucleus [55, 154] enter bound-state energies [37] of composite particles. These can be calculated with relativistic approaches [155], *e. g.*, for hydrogen-like atoms with bound-state QED [156–159] or with the Bethe-Salpeter equation [160–163]. Bound states and their properties for atoms have also been derived from field theory via flow equations and the functional renormalization group [164–166].

In contrast to these fully relativistic treatments, relativistically-corrected bound-state energies for hydrogen-like atoms can be obtained from EFTs in the NR regime, *e. g.*, NRQED [7, 45, 46, 59, 167–170] or pNRQED [35–37, 171]. These approaches exploit simplifications arising in inherent NR regimes while radiative corrections and effects from the nucleus are still taken into account via Wilson coefficients [7, 53]. However, bound-state calculations within these EFTs are usually restricted to a single atom that is assumed to be trapped. Consequently, the c.m. motion as well as its relativistic corrections and corrections to the relative coordinates become irrelevant [74, 77, 78]. Naturally, in the single-atom limit no atom-atom interactions occur and usually only basic light-matter interaction is considered, such as electric-dipole coupling for neutral atoms. These approaches for calculating bound-state energies of trapped atoms may include contributions to the NR Lamb shift [35, 171–174] but can also be used for fundamental tests [175], the determination of the proton charge radius [15, 154, 171, 173, 174], and dark-matter searches [176]. Since they typically focus only on the atomic spectrum, there are calculations, *e. g.*, for hydrogen [46], going beyond the precision of the internal energies derived in our work. In particular, a pNRQED treatment [37] may include next-order loop corrections that are omitted in the present article for simplicity but can be incorporated straightforwardly. Moreover, these pNRQED derivations focus on positronium (equal-mass case of constituents) or neutral atoms, without taking c.m. degrees of freedom into account, while light-matter interactions enter solely through electric-dipole couplings. As a result, light-induced internal energy shifts or shifts arising from the interaction with other atoms are not covered in these treatments. Finally, in pNRQED Wilson coefficients have to be determined for each particular system, which, *e. g.*, has been carried out explicitly for positronium [37]. Compared to that, we derived a Hamiltonian for hydrogen-like, possibly charged atoms, where constituents differ in their masses, considering the c.m. coordinates including the relevant relativistic corrections, and leading to the mass defect as well as to relativistically-corrected light-matter interactions. In the following applications, we will thus determine bound-state energies, *i. e.*, the QED-corrected hyperfine structure of hydrogen-like atoms, including parts

of the NR Lamb shift [40, 64, 65], where we keep arbitrary Wilson coefficients such that our results remain valid for generic hydrogen-like atoms. Because we also extend single-atomic considerations to an arbitrary number of atoms, scattering dynamics arise in addition to the usual pNRQED approaches.

### C. Scattering between atoms

Since we aim to describe ultracold quantum gases, these atom-atom interactions become highly relevant. There are several theoretical models [177] describing NR atomic scattering. One possible description is based on interaction potentials between two scattering partners, where higher-order scattering events [178] are neglected. The NR scattering of neutral atoms is then dominated by van der Waals interactions [179–182]. In this context, theoretical models have been developed to determine van der Waals scattering potentials [183, 184] and cover also density-functional-theory approaches [185–188]. Approximations to the van der Waals interaction are often performed according to an expansion of the form  $-C_6/\Delta R^6 - C_7/\Delta R^7 + \dots$  with real constants  $C_n$  [189], where  $\Delta R$  is the distance between the c.m. of two atoms. Hence, the long-range behavior may be observed in lowest order. For example, the  $C_6$  coefficient for hydrogen [190, 191] can be obtained by second-order perturbation theory [192] of the dipole-dipole potential [193] in first-quantized regimes [180]. Retardation effects may also be taken into account and correspond to the  $C_7/R^7$  term [180, 194]. Another approximation of the van der Waals potential is the Lennard-Jones potential [195]. In contrast to such first-quantized approaches, there are also EFTs [196, 197] dealing with van der Waals interactions directly. For the case of charged cobosons, ion-ion scattering [198, 199] is characterized by the Coulomb repulsion to lowest order. We augment these existing approaches for neutral and charged cobosons by deriving relativistic corrections to the lowest-order Coulomb scattering potentials and cover the interactions between magnetic moments associated with orbit-orbit, spin-orbit, and spin-spin (magnetic dipole-dipole potential) interactions. Spin-orbit and spin-spin magnetic-moment interactions are known, *e.g.*, from magnetic scattering in the context of neutrons [200–204]. Since neutrons are free of charge, no Coulomb interaction is present and such interactions dominate the process. Magnetic moments coupling in atomic scattering processes are partly discussed in the context of spinor BECs [10, 205]. However, to the best of our knowledge, the influence of relativistic corrections to the Coulomb potential in atomic scattering derived from first principles has not been discussed explicitly yet. In addition to the Coulomb potential and its corrections, we find a scattering self-energy, that is part of the collective Lamb shift and was postulated before by embedding light-matter interaction into a field-theoretical framework [109].

### D. Ultracold quantum gases

The combination of bound-state energies with scattering dynamics together allows for a consistent treatment of ultracold

quantum gases including their internal structure. So far, the description of ultracold quantum gases often relies on bottom-up approaches for EFTs based on extensions of NR first-quantized theories. Consequently, there are successful field-theoretical descriptions of scalar BECs [21, 206–208] as well as spinor BECs including internal states [10, 205]. Although their realization is challenging [209, 210], due to the Coulomb repulsion among charged bosons, also ionized BECs [211–215] have been studied. All these descriptions usually do not address relativistic corrections, the inner-atomic structure is often of minor importance, and light-matter interaction is only partly accounted for. In our work, we derived an EFT for ultracold quantum gases from first principles, including possibly charged atoms and relativistic corrections to the c.m. and relative degrees of freedom of both the single-coboson energy and the scattering dynamics, as well as to light-matter interactions. Our basic assumption for cobosonic QFT, to introduce different length scales, enters our description of an ultracold quantum gas in terms of hard-sphere atoms, and naturally the scattering dynamics in our model remain perturbations to the single-coboson contribution.

Moreover, this scattering dynamics is usually treated with approximations, leading to effective scattering lengths from *s*-wave scattering [21] as well as introducing effective pseudo potentials for scattering from hard-sphere interactions [67, 216] instead of the full scattering potential. Within these approximations, we may derive the Gross-Pitaevskii equation (GPE) [42, 43, 217] that describes a Schrödinger-type equation complemented by a nonlinear collision term corresponding to the lowest-order effects of the condensate mean-field contribution [10, 21, 218]. Here, the field operator can be approximated by a wave function of the condensate by symmetry-breaking [219] or number-conserving approaches [220, 221]. Higher-order corrections such as fluctuations [218, 222] arising from the coupling of the condensate to a noncondensed thermal cloud may also be taken into account. There are extensions to coupled GPEs, both for different modes [223, 224] and quantized light fields [109, 225], which are usually postulated extensions of first-quantized considerations. Some studies [226, 227] generalize the GPE to a relativistic equation by postulating an invariant Klein-Gordon-type equation [3, 228, 229] to account for relativistic effects. The modified GPE then follows in these approaches in the NR limit by separating a rest-energy phase from the condensate function [230], resulting into a relativistic correction proportional to a second derivative in time of the condensate function. However, such a treatment does not include relativistic effects and the mass defect as derived in our work. Consequently, as another application, we will derive a GPE including the mass defect, relativistic corrections, also for light-matter interactions, and a coupling of different internal states of the coboson. This modified GPE differs significantly from previous Klein-Gordon-type derivations and might lead to fundamentally different predictions. The deviation originates from the fact that atoms, as composite particles, are not fundamental bosons but rather cobosonic in their nature and, thus, they do not obey a Klein-Gordon equation describing spin-0 particles.

## VII. APPLICATIONS

Following the discussion above, we aim to derive the dynamics of interacting quantum gases and their internal structure encoded in the coboson field operator  $\hat{\varphi}$ . This includes modified bound-state energies associated with the fine and hyperfine structure of the coboson and a coupling via the mass defect to its c.m. motion. We determine the scattering potentials between two internal states of the coboson with respect to internal degrees of freedom giving access to generalized van der Waals potentials. The mean-field contribution of the field operator gives rise to a GPE modified by relativistic corrections and the mass defect.

### A. Modes of relative motion

In the spirit of composite particles, we introduced c.m. and relative coordinates for the multipolar CbQFT. As a next step, we explicitly describe the equation of motion of cobosons and separate between the c.m. and modes for the relative motion between constituents.

#### 1. Cobosonic equation of motion

First, we derive the equation of motion for the cobosonic field operator  $\hat{\varphi}$  based on the Heisenberg equation  $i\hbar d\hat{\varphi}/dt = [\hat{\varphi}, \hat{H}_{\text{MpCb}}]$ , neglecting the influence of the environment that lies outside of our cobosonic subspace. We recall that the equation of motion follows from the cobosonic commutation relation, generating additional terms compared to a purely bosonic field operator. However, these additional terms correspond to processes that lie outside of the projected Hilbert space, such as the annihilation of an electron and a nucleus of different cobosons. To derive the effective equation of motion, we rely on the projected equation of motion  $i\hbar \hat{\pi}_{\text{Cb}} d\hat{\varphi}/dt \hat{\pi}_{\text{Cb}} = \hat{\pi}_{\text{Cb}} [\hat{\varphi}, \hat{H}_{\text{MpCb}}] \hat{\pi}_{\text{Cb}}$  that resolves to

$$i\hbar \frac{d}{dt} \hat{\varphi} = \Theta(a - |\mathbf{r}|) \left( \hat{h}_{\text{MpCb}} + \int_{C_2} d^6 \mathcal{R}_2 \hat{\varphi}_2^\dagger \hat{\mathcal{V}}_{\text{Scatt}} \hat{\varphi}_2 \right) \hat{\varphi}. \quad (31)$$

The Heaviside step function  $\Theta(x)$  accounts for creation and annihilation of only such cobosons whose constituents possess relative distances  $|\mathbf{r}| \leq a$ . The equation of motion yields a Schrödinger-like equation for the single-coboson energy governed by  $\hat{h}_{\text{MpCb}}$ , while the second term accounts for the influence of all other cobosons in the system via scattering.

#### 2. Expansion into unperturbed hydrogen-like modes

While the dynamics implied by Eq. (31) is involved, the limits of integration restrict the relative distances between constituents of different cobosons to  $|\mathbf{x}_{1,i} - \mathbf{x}_{2,j}| > b \gg a$ , and allow for a perturbative treatment of the scattering potentials.

The remaining dominant term denotes the single-coboson contribution associated with  $\hat{h}_{\text{MpCb}}$ , where the leading-order contribution  $\hat{h}_{\text{rel}}^{(0)} = \hat{\mathbf{p}}^2/(2m_r) + q_e q_n/(4\pi\epsilon_0|\mathbf{r}|)$  is followed by other perturbative terms contained in  $\hat{h}_{\text{rel}}^{(1)}$ . Consequently, we use an expansion into eigenmodes of  $\hat{h}_{\text{rel}}^{(0)}$ , *i. e.*, into hydrogen-like modes of the relative motion, and find

$$\hat{\varphi} = \sum_{\beta} \psi_{\beta}(\mathbf{r}) \hat{\Psi}_{\beta}(\mathbf{R}, t), \quad (32)$$

where  $\psi_{\beta}$  is the (first-quantized) wave function of the relative motion associated with internal state  $\beta$ . The field operator  $\hat{\Psi}_{\beta}(\mathbf{R}, t)$  annihilates a coboson in state  $\beta$  at c.m. position  $\mathbf{R}$ . The commutation relation of the remaining field operator  $\hat{\Psi}_{\beta}(\mathbf{R}, t)$  is completely defined through the original cobosonic commutator from Eq. (14). Furthermore, the cobosonic equation of motion requires the wave functions to vanish at  $|\mathbf{r}| = a$ , similar to the case of atoms in an impenetrable spherical box [94–103]. This condition is numerically solvable, with an energy depending on the particular choice of  $a$  and converging to the known energies of hydrogen-type atoms for  $a \rightarrow \infty$ . In the following, we choose the standard hydrogen-like wave functions for the relative motion, because for suitable values of  $a$  the probability density is exponentially suppressed in regions  $|\mathbf{r}| > a$ . However, a numerical treatment is possible as well [98]. Hence, the hydrogen-like wave function  $\psi_{\beta}(\mathbf{r})$  is associated with a generalized quantum number  $\beta$  encompassing all quantum numbers, *i. e.*, the principal quantum number  $n$  with energy eigenvalues  $E_n^{(0)} = -m_r(Z\alpha c)^2/(2n^2)$ , the quantum number  $j$  associated with total angular momentum  $\hat{\mathbf{j}} = \hat{\mathbf{l}} + \hat{\mathbf{S}}$ , its projection to the  $z$ -axis ( $m_j$ ), the orbital angular momentum ( $\ell$ ) and the quantum number of the total spin  $S$  associated with the spin  $\hat{\mathbf{S}} = \hat{\mathbf{s}}_e + \hat{\mathbf{s}}_n$ . We present the angular momentum basis in Appendix E, where  $\psi_{\beta}$  takes also the spin degrees of freedom of the coboson into account, *i. e.*, it contains in total four components from the two spin-1/2 fermions.

By inserting the field-operator expansion from (32) into the equation of motion, multiplying with the conjugate wave function  $\psi_{\alpha}^*$ , and using the orthonormality of the relative modes when integrating over the relative coordinate, the equation of motion for the c.m. field operator of mode  $\alpha$  resolves to

$$i\hbar \frac{d}{dt} \hat{\Psi}_{\alpha} = \hat{h}_{\text{MpCb},\alpha} \hat{\Psi}_{\alpha} + \sum_{\beta \neq \alpha} \hat{T}_{\alpha\beta} \hat{\Psi}_{\beta} + \sum_{\beta\nu\mu} \int_{|\Delta\mathbf{R}| > b'} d^3 R' \hat{\Psi}_{\nu}^{\dagger} \hat{\mathcal{V}}_{\alpha\nu;\beta\mu} \hat{\Psi}_{\mu} \hat{\Psi}_{\beta}. \quad (33)$$

It only contains an integration with respect to c.m. coordinates. The inter-cobosonic scale was introduced through the nucleus coordinate. Thus, for consistency with the previous definition, we replace  $b$  with  $b' = b + a$  for the distance  $\Delta\mathbf{R} = \mathbf{R} - \mathbf{R}'$  between the c.m. positions of two cobosons. Next, we present the internal Hamiltonian  $\hat{h}_{\text{MpCb},\alpha}$ , the transition elements  $\hat{T}_{\alpha\beta}$  between internal states, and scattering matrix elements  $\hat{\mathcal{V}}_{\alpha\nu;\beta\mu}$  in the following two subsections.

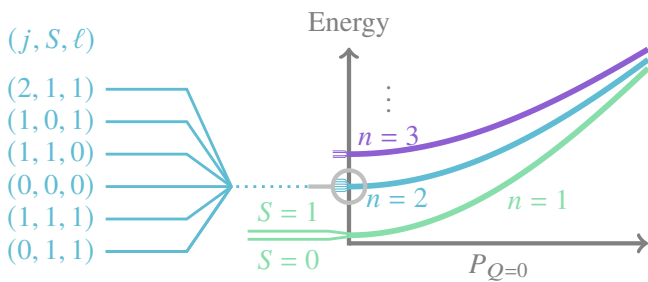


Figure 6. Due to the mass defect, the energy-momentum dispersion of a neutral coboson (with  $Q = 0$ ) depends on the unperturbed internal state defined by the principal quantum number  $n = 1, 2, 3, \dots$ . Additional relativistic corrections cause a splitting into sublevels that correspond to the fine and hyperfine structure given by the set of quantum numbers  $(j, S, \ell)$ . These structures do not enter the modified energy-momentum dispersion at our level of approximation in  $c^{-2}$ . The quantum number  $j$  coincides with the quantum number  $f$  that is the standard form for the hyperfine splitting in atomic physics and results from coupling the electron's spin with the relative angular momentum, before coupling the nuclear spin.

### B. Modified bound-state energies

The equation of motion for the field operator  $\hat{\Psi}_\alpha$  associated with the annihilation of a coboson in mode  $\alpha$  at c.m. position  $\mathbf{R}$  includes the bound-state energy

$$\hat{h}_{\text{MpCb},\alpha} = M_\alpha c^2 + E_\alpha^{(1)} + \frac{\hat{\mathbf{P}}_Q^2}{2M_\alpha} - \frac{\hat{\mathbf{P}}_Q^4}{8M_\alpha^3 c^2} + \langle \hat{h}_1 \rangle_\alpha, \quad (34)$$

of a coboson in internal state  $\alpha$ . Figure 6 shows the energy-momentum dispersion for the Hamiltonian  $\hat{h}_{\text{MpCb},\alpha}$  for different modes  $\alpha$ . By introducing an internal-state dependent rest mass  $M_\alpha = M[1 + E_\alpha^{(0)}/(Mc^2)]$ , the spectrum of the atom enters the rest energy  $M_\alpha c^2$  and, through the relativistic mass defect, the minimally-coupled kinetic energy  $\hat{\mathbf{P}}_Q^2/(2M_\alpha)$ , where the latter implies a lowest-order Taylor expansion. As a result, the energy-momentum dispersion depends on the internal energy of the coboson. Fine and hyperfine splittings [36] enter through relativistic internal corrections  $E_\alpha^{(1)} = \langle \hat{h}_{\text{int}}^{(1)} \rangle_\alpha$ , where  $\langle \hat{\delta} \rangle_\alpha = \int d^3r \psi_\alpha^* \hat{\delta} \psi_\alpha$  denotes the expectation value with respect to internal state  $\alpha$  of an arbitrary operator  $\hat{\delta}$ , see Appendix E for details. Due to these corrections, there is a splitting of the unperturbed hydrogen-like energy levels also presented in Fig. 6. In the presence of EM fields, energy shifts occur in the form of  $\langle \hat{h}_1 \rangle_\alpha = \langle \hat{h}_1^{(0)} + \hat{h}_1^{(1)} \rangle_\alpha$ , accounting for first-order perturbative shifts such as, *e. g.*, the linear Zeeman shift [80]. Contrarily, second-order effects like the quadratic Stark effect [86] are not explicitly accounted for in the diagonal matrix elements. Further nonperturbative EM fields, giving rise to shifts such as AC-Stark [231] and other light shifts [232, 233] are also not solely represented by these diagonal elements. To cover such additional effects, the second term in Eq. (33),

including all off-diagonal transition elements

$$\hat{T}_{\alpha,\beta} = \int d^3r \psi_\alpha^* \left( \hat{h}_{\text{rel}}^{(1)} + \hat{h}_{\mathbf{r} \times \hat{\mathbf{P}}_Q} + \hat{h}_1 \right) \psi_\beta \quad (35)$$

from internal state  $\beta$  to  $\alpha$ , cannot necessarily be treated perturbatively.

In summary, using the expansion into relative hydrogen-like modes, we find both the bound-state energy of a coboson, including energy shifts due to internal relativistic corrections, as well as transitions between different internal-coboson states driven by both internal interactions and light fields.

### C. Modified scattering potentials

The multi-coboson aspect of our theory enters via the scattering matrix elements

$$\hat{\mathcal{V}}_{\alpha\nu;\beta\mu} = \int d^3r \int d^3r' \psi_\alpha^* \psi_\nu^* 2\hat{\mathcal{V}}_{\text{Scatt}} \psi'_\mu \psi'_\beta, \quad (36)$$

describing the scattering from internal modes  $\beta\mu$  into  $\alpha\nu$ , where  $\hat{\mathcal{V}}_{\alpha\nu;\beta\mu}$  is a function of both  $\mathbf{R}$  and  $\mathbf{R}'$ . Similar to the splitting of the single-coboson energy into the bound-state energies and internal transitions, we divide the scattering matrix elements into one part without transitions, *i. e.*,  $\alpha = \beta$ , and a part including actual transitions, *i. e.*,  $\alpha \neq \beta$ , that corresponds to internal state changing collisions. As a result, the equation of motion

$$i\hbar \frac{d}{dt} \hat{\Psi}_\alpha = \left( \hat{h}_{\text{MpCb},\alpha} + \sum_{\nu\mu} \int_{|\Delta\mathbf{R}|>b'} d^3R' \hat{\Psi}'_\nu \dagger \hat{\mathcal{V}}_{\alpha\nu;\alpha\mu} \hat{\Psi}'_\mu \right) \hat{\Psi}_\alpha + \sum_{\beta \neq \alpha} \left( \hat{T}_{\alpha\beta} + \sum_{\nu\mu} \int_{|\Delta\mathbf{R}|>b'} d^3R' \hat{\Psi}'_\nu \dagger \hat{\mathcal{V}}_{\alpha\nu;\beta\mu} \hat{\Psi}'_\mu \right) \hat{\Psi}_\beta \quad (37)$$

for internal state  $\alpha$  includes the single-coboson energy  $\hat{h}_{\text{MpCb},\alpha}$  and is augmented by the scattering accounting for the mean field created by all other cobosons interacting with the coboson of mode  $\alpha$ . Transitions from mode  $\beta$  to  $\alpha$  are either induced via internal or light-matter interactions but also by scattering with other cobosons that change its internal state from  $\mu$  to  $\nu$ . By integrating over relative degrees of freedom to obtain the scattering matrix elements from Eq. (36), we gain via Eq. (37) access to exact scattering potentials predicted by our model.

We obtain analytic expressions for the potentials approximated order by order, at least for the regime where  $b' \gg a$ , via the Taylor expansion of  $\hat{\mathcal{V}}_{\text{Scatt}}$  around  $\mathbf{x}_i - \mathbf{x}'_j \cong \Delta\mathbf{R}$  in Eq. (36). The dominant contribution in this regime follows from the Coulomb potential. We find the generalized electric dipole-dipole potential



$$\mathcal{V}_{\text{Scatt}} \approx \frac{1}{8\pi\epsilon_0} \left\{ \frac{Q^2}{|\Delta\mathbf{R}|} + Q \frac{e_{\Delta\mathbf{R}} \cdot (\mathbf{d} - \mathbf{d}')}{|\Delta\mathbf{R}|^2} + Q \frac{\sum_u (Q_{uu} + Q'_{uu}) - 3 \sum_{u,v} e_{\Delta\mathbf{R}}^{(u)} (Q_{uv} + Q'_{uv}) e_{\Delta\mathbf{R}}^{(v)}}{|\Delta\mathbf{R}|^3} + \frac{\mathbf{d} \cdot \mathbf{d}' - 3 (e_{\Delta\mathbf{R}} \cdot \mathbf{d}) (e_{\Delta\mathbf{R}} \cdot \mathbf{d}')}{|\Delta\mathbf{R}|^3} \right\} \quad (38)$$

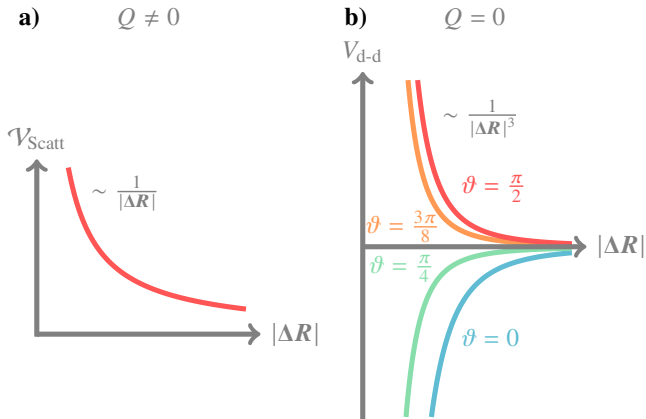


Figure 7. Form of the scattering potential. a) Two ionized cobosons with  $Q \neq 0$  experience a repulsive Coulomb potential as the dominant contribution of their interaction. b) For neutral cobosons with  $Q = 0$  higher-order dipole terms are dominating the interaction. The panel shows the dipole-dipole potential  $V_{\text{d-d}} \propto (Z-1)^2/|\Delta\mathbf{R}| + Za^2(1-3\cos^2\vartheta)/|\Delta\mathbf{R}|^3$  for the simplified case of  $\mathbf{r} = \mathbf{r}' = a\mathbf{e}_r$ , where  $\vartheta$  is the angle  $\mathbf{r}$  and  $\Delta\mathbf{R}$ . Depending on the orientation, the potential is either attractive or repulsive.

that accounts in general for cobosonic ions. For  $Q \neq 0$ , the leading order corresponds to a repulsive Coulomb potential proportional to  $Q^2$  as indicated in Fig. 7b). It is followed by corrections in which the difference of generalized dipole moments  $\mathbf{d} = m_r(q_e/m_e - q_n/m_n)\mathbf{r}$  enters as well as the quadrupole-moment tensor  $\mathbf{Q}_{uv} = -r_u r_v m_r^2 (q_e/m_e^2 + q_n/m_n^2)/2$  with components  $u, v = x, y, z$ . The last term, the only one remaining in the limit of neutral cobosons with  $Q = 0$ , corresponds to the standard electric dipole-dipole potential whose dipole moment simplifies to  $\mathbf{d} = q_e \mathbf{r}$  for  $q_e = -q_n$ . Such a potential is the starting point to describe inter-atomic interactions in dipolar quantum gases [234–236]. We plot it in Fig. 7a) for parallel  $\mathbf{r}$  and  $\mathbf{r}'$ , as well as for different values of the angle between  $\Delta\mathbf{R}$  and  $\mathbf{r}$ . For instance, using second-order perturbation theory in first quantization, the dipole-dipole potential gives rise to the energy shift associated with the van der Waals potential [136, 179, 180] of the form  $-C_6/|\Delta\mathbf{R}|^6$  with a real constant  $C_6$ . As a consequence, using the full Coulomb potential together with all relativistic corrections and explicitly integrating over relative degrees of freedom gives access to generalized van der Waals scattering potentials between cobosonic modes. This approach has not been carried out and can serve as the cobosonic-model prediction to van der Waals potentials that may be compared with experimental results. In addition, as we derived scattering dynamics with respect to internal states

of the coboson, we are able to model cobosonic entanglement through scattering. Since scattering can also be used for squeezing of internal states of atoms [237–240] and its description requires a field-theoretical formulation, our multipolar QFT can be embedded into the field of quantum metrology.

#### D. Modified Gross-Pitaevskii equation

The derivation of approximate solutions to the equation of motion from Eq. (33) for the c.m. field operator often follows a mean-field approach [241]. Such a treatment leads to the celebrated *Gross-Pitaevskii equation* (GPE) [42, 43] which we derive below in favor of approaches following, *e. g.*, density-functional theory [242].

The scattering potentials in Eq. (37) have the form of a hard-sphere interaction [67, 216] characterized by a nonvanishing potential only at distances  $|\Delta\mathbf{R}| > b'$ , which is ensured by integration regions in our model. In this case and for low temperatures as well as weakly interacting, dilute gases, such hard-sphere potentials can be replaced by a pseudopotential [216] of the form  $\eta_{\alpha\nu;\alpha\mu}\delta(\mathbf{R} - \mathbf{R}')$ , where no integration region appears [243]. Instead, we find an effective, renormalized [218, 244, 245] scattering length [246]  $\eta_{\alpha\nu;\alpha\mu}$ , mediating scattering between cobosons of mode  $\alpha$  with that of mode  $\mu$  transitioning into mode  $\nu$ . An analogous replacement in the collision-induced coupling between modes  $\alpha$  and  $\beta$  in the second line of Eq. (37) with an effective scattering length  $\eta_{\alpha\nu;\beta\mu}$  can be made. Within this approximation the equation of motion for the field operator takes the form

$$i\hbar \frac{d}{dt} \hat{\Psi}_\alpha = \left( \hat{h}_{\text{MPCb},\alpha} + \sum_{\nu\mu} \eta_{\alpha\nu;\alpha\mu} \hat{\Psi}_\nu^\dagger \hat{\Psi}_\mu \right) \hat{\Psi}_\alpha + \sum_{\beta \neq \alpha} \left( \hat{T}_{\alpha,\beta} + \sum_{\nu\mu} \eta_{\alpha\nu;\beta\mu} \hat{\Psi}_\nu^\dagger \hat{\Psi}_\mu \right) \hat{\Psi}_\beta. \quad (39)$$

Such an approximation is often applied in the context of ultracold quantum gases [21, 247] and corrections may also be taken into account [248, 249].

However, already in a mean-field theory we observe a difference to the conventional treatment, *i. e.*, we have access to relative and c.m. relativistic corrections, as well as to the full coupling to external EM fields. To this end, we approximate Eq. (39) by moving to a first-quantized equation of motion  $\hat{\Psi}_\alpha \rightarrow \Psi_\alpha$  where  $\Psi_\alpha$  represents the mean field of the condensate [241]. There are several ways to introduce the mean field as lowest-order contribution of the equation of motion [218, 250, 251]. Extending the lowest-order contribution

to beyond mean-field theory [252–255] may be achieved by including also an operator-valued noncondensate part of the field operator in terms of a thermal cloud that couples to the mean field [218]. Within the mean-field approach, we find new

$$i\hbar \frac{d}{dt} \Psi_\alpha = \left( M_\alpha c^2 + E_\alpha^{(1)} + \langle \hat{h}_1 \rangle_\alpha + \frac{\hat{\mathbf{P}}_Q^2}{2M_\alpha} - \frac{\hat{\mathbf{P}}_Q^4}{8M^3 c^2} + \sum_{\nu\mu} \tilde{\eta}_{\alpha\nu;\alpha\mu} \Psi_\nu^* \Psi_\mu \right) \Psi_\alpha + \sum_{\beta \neq \alpha} \left( \hat{T}_{\alpha,\beta} + \sum_{\nu\mu} \tilde{\eta}_{\alpha\nu;\beta\mu} \Psi_\nu^* \Psi_\mu \right) \Psi_\beta \quad (40)$$

that contains, compared to the NR bosonic GPE [42, 43], first-order relativistic corrections. It is valid for spinor Bose-Einstein condensates [10] and has a state-dependent mass  $M_\alpha$  differing from previous derivations [226, 227, 230] significantly. Even more, our derivation applies also to cobosonic ions (coupling via  $\hat{\mathbf{P}}_Q$ ), as long as the gas can still be treated as weakly-interacting. In addition, we find the energy shift  $E_\alpha^{(1)}$  from the internal cobosonic structure and we account for light-matter interaction in  $\langle \hat{h}_1 \rangle_\alpha$ . Moreover, we observe that the GPE for mode  $\alpha$  may couple to other modes through  $\Psi_\nu^* \Psi_\mu$  terms [256], where usually only the contributions proportional to  $|\Psi_\mu|^2$  are taken into account. The coupling to other modes enters via nonvanishing internal transition elements  $\hat{T}_{\alpha,\alpha'}$ , as well as via a scattering element including transitions from mode  $\mu$  to  $\nu$ .

To our knowledge, a modified GPE for c.m. degrees of freedom, taking into account internal degrees of freedom and incorporating the mass defect, has not yet been derived in a top-down approach. Moreover, previous derivations of relativistically-corrected GPEs [226, 227, 230] differ significantly from our results.

### E. Reduction to mass defect

With the modified GPE we reproduce two special cases: (i) We find the typical atomic physics NR GPE by neglecting all relativistic contributions. (ii) By restricting the treatment for  $Q = 0$  to two modes, *i. e.*, ground ( $g$ ) and excited ( $e$ ) state, and by neglecting the  $\hat{\mathbf{P}}^4$  term, internal relativistic corrections in  $E_\alpha^{(1)}$ , as well as the influence of any scattering, we reproduce a Hamiltonian [16, 17] that is relevant in an atomic- [18, 22] and quantum-clock context [23, 24, 26, 30–34]. For sake of presentation, we neglect light-matter interactions for the moment. In this limit, the equation of motion for both, ground and excited state, reduces to  $i\hbar d|j\rangle/dt = \hat{h}_j |j\rangle$  with a first-quantized Hamiltonian  $\hat{h}_j = M_j c^2 + \hat{\mathbf{P}}^2/(2M_j)$ , including the abstract form of the wave function in position representation  $\Psi_j = \langle \mathbf{R} | j \rangle$ , with  $j = g, e$ . Since the differential equations for the internal states are now decoupled, we find a Schrödinger equation for the general state  $|\psi\rangle = \psi_g |g\rangle + \psi_e |e\rangle$  with  $|\psi_g|^2 + |\psi_e|^2 = 1$ . After Taylor expanding the state-dependent mass  $M_j$ , the system Hamiltonian, *i. e.*, the sum of the two Hamiltonians

effective scattering lengths  $\tilde{\eta}_{\alpha\beta}$  and  $\tilde{\eta}_{\alpha\beta;\alpha'\beta'}$  that may differ from the previous values. These approximations result in the modified GPE

$\hat{h}_j$ , takes the form

$$\hat{h} = M c^2 \mathbb{1} + \hat{h}_{\text{rel}}^{(0)} + \frac{\hat{\mathbf{P}}^2}{2M} \left( \mathbb{1} - \frac{\hat{h}_{\text{rel}}^{(0)}}{M c^2} \right), \quad (41)$$

which is the limit of addressing only two internal states of  $\hat{h}_{\text{rel}}^{(0)} = E_g |g\rangle\langle g| + E_e |e\rangle\langle e|$  in Eq. (22), as expected. This Hamiltonian can be recast into the form

$$\hat{h} = \bar{M} c^2 \mathbb{1} + \hat{h}_{\text{cl}} + \frac{\hat{\mathbf{P}}^2}{2\bar{M}} \left( \mathbb{1} - \frac{\hat{h}_{\text{cl}}}{\bar{M} c^2} \right) \quad (42)$$

by introducing a new mean mass  $\bar{M} = M + (E_e^{(0)} + E_g^{(0)})/(2c^2)$  together with replacing the unperturbed Hamiltonian of the relative degrees of freedom  $\hat{h}_{\text{rel}}^{(0)}$  by the clock Hamiltonian

$$\hat{h}_{\text{cl}} = \frac{E_e^{(0)} - E_g^{(0)}}{2} [|e\rangle\langle e| - |g\rangle\langle g|]. \quad (43)$$

This clock Hamiltonian describes the internal (relative) dynamics and constitutes the basis of atomic and quantum clocks [16–18, 22–24, 26, 30–34], in our case without gravity. In particular, the preceding two equations are related by the fact that in the order  $c^{-2}$  the equivalence

$$\hat{h}(M, \hat{h}_{\text{rel}}^{(0)}) = \hat{h}(\bar{M}, \hat{h}_{\text{cl}}) \quad (44)$$

holds. Moreover, the energy difference  $E_e^{(0)} - E_g^{(0)}$  can be associated with the transition frequency of a clock as well as the mass difference between both internal states. This equivalence can be extended in the order  $c^{-2}$  to the case where the total momentum  $\hat{\mathbf{P}}$  is replaced by its minimally-coupled version  $\hat{\mathbf{P}}_Q$ . Similarly, the equivalence holds in the order  $c^{-2}$  also for the corrected relative degrees of freedom  $\hat{h}_{\text{rel}}^{(1)}$ , the angular momentum to spin coupling term  $\hat{h}_{r \times \hat{\mathbf{P}}_Q}$ , and the corrected EM interaction  $\hat{h}_1^{(1)}$  in Eq. (22). However, replacing  $M$  by  $\bar{M}$  would lead to additional relativistic modifications for some parts of the NR EM interaction  $\hat{h}_1^{(0)}$ , especially when considering magnetic fields, while its leading-order NR contributions maintain of the same form.

The Hamiltonian accounts for a modified c.m. motion and dispersion relation for atoms in different internal states through the mass defect. To underline the implications of the mass defect, we observe that wave packets associated with

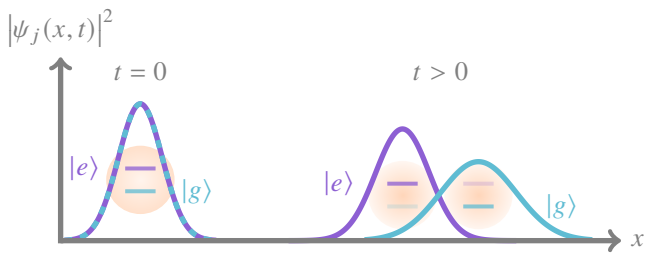


Figure 8. Sketch of the time evolution of noninteracting cobosons in a superposition of ground  $|g\rangle$  and excited  $|e\rangle$  state. The c.m. probability distribution  $|\psi_j(x, t)|^2$  of the atom in state  $|j\rangle$  is shown by different wave packets. Their form depends on the internal states due to different dispersion relations, which depend on the masses  $M_g$  and  $M_e$  due to the mass defect. Moreover, if both wave packets have the same initial momentum, the ground state propagates with a higher velocity.

the ground and excited state of a free coboson disperse and propagate differently over time, as indicated in Fig. 8. Due to the state-dependent mass, the amplitude and the uncertainty differ. Since both wave packets share the same initial momentum they evolve with a different velocity. In the context of atomic clocks, energy shifts and phase contributions caused by the modified kinetic terms cause special-relativistic time dilation or second-order Doppler effects [18, 22] and have to be taken into account for the analysis of high-accuracy frequency standards.

### VIII. CONCLUSIONS

In this article, we derived an EFT for (possibly) charged, spin-carrying, and interacting composite bosons based on their constituents. Our top-down approach includes relativistic contributions such as radiative corrections, mass defects, atom-atom scattering, and light-matter interactions. We therefore unified low-energy aspects of particle physics, quantum optics, and atomic physics into one effective multipolar cobosonic QFT with a broad range of applications, *e. g.*, to scattering experiments [177, 257], ultracold quantum gases [4, 5, 21], and high-precision measurements based on quantum clocks [18, 22–24, 26–32, 34].

In particular, our effective QFT is valid for an arbitrary number of (possibly) charged cobosons and therefore goes beyond previous single-atom descriptions. By considering their c.m. motion, we found inter-cobosonic interactions via relativistically-corrected scattering potentials and a coupling between c.m. and relative degrees of freedom that arises from the relativistic mass defect. Moreover, our projection technique closes the gap between EFTs for ultra cold quantum gases and elementary quantum field theories such as QED. This procedure is universal in the sense that it can be applied to arbitrary single-fermion Hamiltonians  $\hat{h}_i$  and potentials  $\hat{V}^{(ij)}$ . We also introduced field-theoretical unitary transformations and reduced them to well-known single-particle unitaries. In our case these transformations led to relativistic corrections to c.m. and relative coordinates together with the multipolar version of our effective QFT. The extension to spin-carrying

charged cobosons unveiled another coupling between the c.m. and relative motion, *i. e.*, a spin-orbit coupling  $\hat{h}_{r \times \hat{p}_Q}$  of ions, in addition to the coupling induced by the mass defect. To the best of our knowledge, relativistically-corrected scattering potentials to this extent are given for the first time, including a scattering self-energy term. In addition, we presented a new modified, coupled GPE including light-matter interactions, other relativistic corrections, and the mass defect.

Our projection formalism introduces length scales associated with atoms composed of electron-nucleus pairs. Introducing further different length scales may result into EFTs for other types of composite particles, *e. g.*, multi-electron atoms and molecules. An EFT for molecules would directly connect to and extend existing approaches [258] and lead to a field-theoretical description of interacting ultracold molecules. Such an effective theory revolves around established concepts such as the Born-Oppenheimer approximation [259] and other bound-state calculations for many-body bound systems such as density functional theory [260]. Furthermore, our model describing single-species ensembles may be extended to mixtures, *e. g.*, of cobosons and free fermions, different species, isotopes, as well as ions within neutral quantum gases, the latter giving rise to respective spinor quantum gases. Moreover, effects of the environment that lie outside of our cobosonic subspace could in principle be incorporated by techniques known from open quantum systems [71, 72], and will lead to additional energy shifts as well as to decoherence mechanisms.

Including external nonelectromagnetic fields such as gravity or violation fields in a similar fashion would set a quantum-field-theoretical foundation for established single-particle descriptions, being of essence for quantum-clock interferometry but also for atomic clocks exposed to micromotion [18, 22], tests of special and general relativity [30–32, 34], as well as dark-matter detection [27–29, 33]. By determining c.m. scattering potentials between two cobosons by integrating over relative degrees of freedom numerically, we expect to find corrected *van der Waals* scattering potentials [183, 184] predicted by our model. Moreover, our results facilitate a field-theoretical description of both the c.m. motion as well as the internal states of atomic quantum gases. Since quantum-metrological methods enhancing the precision through techniques like squeezing rely on such a treatment and might be even generated through scattering, our results lay the basis for the description and modeling of super-sensitive measurements below the shot-noise limit and can be applied to spin-squeezed experiments [237, 238] or momentum-squeezed atom interferometry [239, 240].

In summary, our multipolar cobosonic QFT can be applied to a large class of atomic ensembles, *e. g.*, Bose-Einstein condensates [10, 21, 88, 89, 235], ionized quantum gases [211–215], and thermal clouds [261, 262] that may be exposed to arbitrary light-matter interactions including trapping potentials [263] and light pulses [122–124]. It also includes relativistic corrections to the relative Hamiltonian, the mass defect, light-matter interaction in its most general form, and scattering potentials. Therefore, our results are a basis for studies of composite particles, both for fundamental physics but also for applied quantum systems in a vast area of different subfields.

## ACKNOWLEDGMENTS

We are grateful to W. P. Schleich for his stimulating input and continuing support. Moreover, we are thankful to A. Friedrich for helpful support and instructive feedback throughout the whole project, as well as proofreading our manuscript. We also thank O. Buchmüller, C. Kiefer, R. Lopp, C. Niehof, G. Paz, R. Walser, as well as the QUANTUS and INTENTAS teams for fruitful and interesting discussions. The projects “Building composite particles from quantum field theory on dilaton gravity” (BOnD) and “Metrology with interfering Unruh-DeWitt detectors” (MIUnD) are funded by the Carl Zeiss Foundation (Carl-Zeiss-Stiftung). The QUANTUS and INTENTAS projects are supported by the German Space Agency at the German Aerospace Center (Deutsche Raumfahrtagentur im Deutschen Zentrum für Luft- und Raumfahrt, DLR) with funds provided by the Federal Ministry for Economic Affairs and Climate Action (Bundesministerium für Wirtschaft und Klimaschutz, BMWK) due to an enactment of the German Bundestag under Grant Nos. 50WM2250D-2250E (QUANTUS+), as well as 50WM2177-2178 (INTENTAS). The Qu-Gov project in cooperation with the “Bundesdruckerei GmbH” is supported by the Federal Ministry of Finance (Bundesministerium der Finanzen, BMF). E.G. thanks the German Research Foundation (Deutsche Forschungsgemeinschaft, DFG) for a Mercator Fellowship within CRC 1227 (DQ-mat). F.D.P. is grateful that this work has been supported by funding programs for junior researchers of the Graduate & Professional Training Center at Ulm University within the project “Long-Baseline-Atominterferometer Gravity and Standard-Model Extensions tests” (LArGE).

## Appendix A: Potential matching

Starting from the Hamiltonian given in Eq. (1), we move to an interaction picture with respect to the Hamiltonian

$$\hat{H}_0 = \sum_i \int d^3x_i \hat{\psi}_i^\dagger \left( m_i c^2 + \frac{\hat{\mathbf{p}}_i^2}{2m_i} \right) \hat{\psi}_i + \hat{H}_{\text{EM}} \quad (\text{A1})$$

accounting for the free EM and fermion fields. The resulting interaction Hamiltonian density

$$\begin{aligned} \hat{\mathcal{H}}_I = \sum_i \hat{\psi}_i^\dagger & \left( q_i \hat{\phi} + \frac{-\{\hat{\mathbf{p}}, q_i \hat{\mathbf{A}}\} + q_i^2 \hat{\mathbf{A}}^2}{2m_i} - c_F^{(i)} q_i \frac{\hat{\mathbf{s}}_i \cdot \hat{\mathbf{B}}}{m_i} \right. \\ & \left. - c_D^{(i)} q_i \hbar^2 \frac{\nabla \cdot \hat{\mathbf{E}}}{8m_i^2 c^2} - c_S^{(i)} q_i \hat{\mathbf{s}}_i \cdot \frac{\hat{\mathbf{p}}_i \times \hat{\mathbf{E}} - \hat{\mathbf{E}} \times \hat{\mathbf{p}}_i}{4m_i^2 c^2} \right) \hat{\psi}_i \end{aligned} \quad (\text{A2})$$

shows only those terms relevant for the matching in the order  $c^{-2}$ . In particular, the kinetic correction and the last two terms of  $\hat{h}_i$  in Eq. (1) give only rise to Feynman diagrams of orders higher than  $c^{-2}$ . Moreover, the contact interaction has already the form of first-order scattering so that it does not give rise to additional second-order Feynman diagrams. In this interaction picture, all field operators  $\hat{\psi}_i$ ,  $\hat{\phi}$ , and  $\hat{\mathbf{A}}$

depend on  $x^\varrho = (ct, \mathbf{x})$  with  $\varrho = 0, 1, 2, 3$ , *i. e.*, they become explicitly time dependent. The EM fields are connected to the four potential  $\hat{A}^\varrho = (\hat{\phi}/c, \hat{\mathbf{A}})$  via  $\hat{\mathbf{E}} = -\partial \hat{\mathbf{A}}/\partial t - \nabla \hat{\phi}$  and  $\hat{\mathbf{B}} = \nabla \times \hat{\mathbf{A}}$ . With the interaction Hamiltonian density from Eq. (A2) and the time ordering operator  $\hat{\mathcal{T}}$ , we define the scattering matrix  $\hat{\mathcal{S}} = \hat{\mathcal{T}} \exp\left\{-\frac{i}{\hbar c} \int d^4x \hat{\mathcal{H}}_I(x)\right\}$ . The actual matching corresponds to determining scattering-matrix elements up to a given order for the desired interactions [37]. In our case, we match up to the order  $c^{-2}$  for virtual photons between two fermions. Hence, second-order scattering

$$\hat{\mathcal{S}}^{(2)} = \frac{1}{2!} \left( -\frac{i}{\hbar c} \right)^2 \int d^4x \int d^4x' \hat{\mathcal{T}} \left\{ \hat{\mathcal{H}}_I(x) \hat{\mathcal{H}}_I(x') \right\} \quad (\text{A3})$$

is the first and only relevant scattering-matrix element whose time ordering is resolved by Wick’s theorem [3, 264], giving rise to only normally-ordered contractions. As a result, we select all contractions with two (real) fermions entering and exiting the scattering (constituents of the cobosons), *i. e.*, only contractions of EM fields, scalar photons  $\hat{A}_0 \hat{A}'_0$ , and vector photons  $\hat{A}_r \hat{A}'_s$  with  $r, s = 1, 2, 3$ , are involved. After power counting [37], we find that consistent matching up to the order  $c^{-2}$  requires the contraction of all scalar and vector photons between terms in the first line of Eq. (A2). The terms in the second line can only be contracted via a scalar photon with the Coulomb potential (compare with the Feynman diagrams depicted in Fig. 3).

### 1. Coulomb gauge

To determine the matrix elements, a choice of gauge is required to resolve the contractions. First, we move to Coulomb gauge where contractions of the scalar and vector photon take the form [265]

$$\hat{A}_0 \hat{A}'_0 = i\hbar \frac{\delta(x_0 - x'_0)}{4\pi\epsilon_0 c |\mathbf{x} - \mathbf{x}'|} \quad (\text{A4a})$$

and

$$\begin{aligned} \hat{A}_r \hat{A}'_s = \frac{\hbar\mu_0 c}{2} \frac{1}{(2\pi)^3} \int d^3k e^{i\mathbf{k} \cdot (\mathbf{x} - \mathbf{x}')} & \left( \frac{\delta_{rs}}{|\mathbf{k}|} - \frac{k_r k_s}{|\mathbf{k}|^3} \right) \\ & \times \left( e^{-i|\mathbf{k}|(x_0 - x'_0)} \Theta(x_0 - x'_0) + (x_0 \leftrightarrow x'_0) \right) \end{aligned} \quad (\text{A4b})$$

with the Heaviside step function  $\Theta(x_0 - x'_0)$ . Further, contractions between the vector and scalar potential  $\hat{A}_r \hat{A}'_0 = 0$  vanish. Multiplying all elements of  $\hat{\mathcal{H}}_I(x) \hat{\mathcal{H}}_I(x')$  yields a term proportional to  $\hat{\phi} \hat{\phi}'$ , whose contraction leads to the Coulomb potential and corresponds to the first Feynman diagram in Fig. 3. This particular second-order matrix element

$$\hat{\mathcal{S}}_C^{(2)} = \left( -\frac{i}{\hbar} \right)^2 \sum_{i,j} \frac{q_i q_j}{2!} \int d^4x \int d^4x' \hat{\psi}_i^\dagger \hat{\psi}_j^\dagger \hat{A}_0 \hat{A}'_0 \hat{\psi}_j \hat{\psi}_i \quad (\text{A5})$$

contains abbreviations  $\hat{\psi}_i = \hat{\psi}_i(x)$  and  $\hat{\psi}'_j = \hat{\psi}_j(x')$ , where the order of fermion operators takes both commuting and anti-commuting field operators into account. Inserting the contraction of the scalar potential from Eq. (A4a) yields

$$\hat{S}_C^{(2)} = -\frac{i}{\hbar} \int dt \int d^3x \int d^3x' \sum_{i,j=e,n} \hat{\psi}_i^\dagger \hat{\psi}'_j{}^\dagger V_C^{(ij)} \hat{\psi}'_j \hat{\psi}_i \quad (\text{A6})$$

and the corresponding Coulomb potential  $\hat{V}_C^{(ij)} = q_i q_j / (8\pi\epsilon_0 |\mathbf{x} - \mathbf{x}'|)$ .

Moving to the contribution proportional to  $\{\hat{p}_r, \hat{A}^{(r)}\} \{\hat{p}'_s, \hat{A}'^{(s)}\}$ , we find the matrix element

$$\hat{S}_{LL}^{(2)} = \left(-\frac{i}{\hbar c}\right)^2 \frac{1}{2!} \sum_{i,j=e,n} \frac{q_i q_j}{m_i m_j} \int d^4x \int d^4x' \times \hat{\psi}_i^\dagger \hat{\psi}'_j{}^\dagger \hat{A}_r \hat{A}'_s \hat{p}_r \hat{p}'_s \hat{\psi}'_j \hat{\psi}_i \quad (\text{A7})$$

with the help of  $\hat{\mathbf{p}}_\ell \cdot \hat{\mathbf{A}}_\ell = \hat{\mathbf{A}}_\ell \cdot \hat{\mathbf{p}}_\ell$  in Coulomb gauge. The contraction of the vector photon is not an exact delta function in time, *i. e.*, not instantaneous. However, by partial integration with respect to one temporal coordinate we extract from the instantaneous part of the matrix element

$$\hat{S}_{LL}^{(2)} = \frac{-i}{\hbar} \int dt \int d^3x \int d^3x' \sum_{i,j} \hat{\psi}_i^\dagger \hat{\psi}'_j{}^\dagger \hat{V}^{(ij)}_{LL} \hat{\psi}'_j \hat{\psi}_i \quad (\text{A8})$$

the potential

$$\hat{V}_{LL}^{(ij)} = \frac{4\pi\kappa_{ij}}{(2\pi)^3} \int d^3k e^{i\mathbf{k}\cdot(\mathbf{x}-\mathbf{x}')} \left( \frac{\delta_{rs}}{|\mathbf{k}|^2} - \frac{k_r k_s}{|\mathbf{k}|^4} \right) \hat{p}_r \hat{p}'_s \quad (\text{A9})$$

associated with the orbit-orbit coupling, while the remainder of the integral is of higher order and thus neglected. Here, we introduce  $\kappa_{ij} = -q_i q_j / (8\pi\epsilon_0 m_i m_j c^2)$  as before. After performing the Fourier transform we find

$$\hat{V}_{LL}^{(ij)} = \frac{\kappa_{ij}}{2} \left( \frac{1}{|\mathbf{r}|} \hat{\mathbf{p}} \cdot \hat{\mathbf{p}}' + \frac{1}{|\mathbf{r}|^3} \mathbf{r} \cdot (\mathbf{r} \cdot \hat{\mathbf{p}}) \hat{\mathbf{p}}' \right). \quad (\text{A10})$$

It is straightforward to show the equivalence to the form given in Fig. 3. The remaining potentials are derived in a completely analogous procedure.

## 2. Lorenz gauge

When we use Lorenz gauge instead of Coulomb gauge to determine the potentials, the general procedure remains identical but we need to take into account that  $\hat{\mathbf{p}}_\ell \cdot \hat{\mathbf{A}}_\ell \neq \hat{\mathbf{A}}_\ell \cdot \hat{\mathbf{p}}_\ell$ . The contraction then reads

$$\hat{A}_\mu \hat{A}'_\nu = -\frac{\hbar\mu_0 c}{2} \frac{\eta_{\mu\nu}}{(2\pi)^3} \int d^3k \frac{e^{i\mathbf{k}\cdot(\mathbf{x}-\mathbf{x}')}}{|\mathbf{k}|} \times \left( e^{-i|\mathbf{k}|(x_0-x'_0)} \Theta(x_0 - x'_0) + (x_0 \leftrightarrow x'_0) \right). \quad (\text{A11})$$

All potentials are identical to the ones obtained in Coulomb gauge except for the orbit-orbit and Coulomb potentials. For the first, we find

$$\hat{V}_{LL}^{(ij)} = \frac{\kappa_{ij}}{|\mathbf{r}|^3} \left( \hat{\boldsymbol{\ell}} \cdot \hat{\boldsymbol{\ell}}' + (\mathbf{r} \cdot \hat{\mathbf{p}}) (\mathbf{r} \cdot \hat{\mathbf{p}}') \right) - \kappa_{ij} \pi \hbar^2 \delta(\mathbf{r}). \quad (\text{A12})$$

The Coulomb potential is of order  $c^0$ , but in Lorenz gauge the scalar photon propagator is not instantaneous in time. As a consequence, there is a nonnegligible remaining integral after a partial integration. The instantaneous part of this matrix element corresponds to the Coulomb potential and the remainder yields a term of order  $c^{-2}$ . We resolve the second part as well with the help of partial integration in time and use consecutively the continuity equation

$$\frac{\partial}{\partial t} (\hat{\psi}_i^\dagger \hat{\psi}_i) = \frac{i\hbar}{2m_i} \nabla \cdot (\hat{\psi}_i^\dagger [\nabla \hat{\psi}_i] + [\nabla \hat{\psi}_i^\dagger] \hat{\psi}_i) \quad (\text{A13})$$

to remove partial derivatives in time. This procedure leads to the potential

$$\hat{V}_C^{(ij)} = \frac{q_i q_j}{8\pi\epsilon_0 |\mathbf{r}|} - \kappa_{ij} \frac{1}{2|\mathbf{r}|^3} \hat{\boldsymbol{\ell}} \cdot \hat{\boldsymbol{\ell}}' + \kappa_{ij} \pi \hbar^2 \delta(\mathbf{r}) \quad (\text{A14})$$

showing that the sum of all potentials is identical in both gauges.

## Appendix B: Coboson subspace

### 1. Projection operator

First, we discuss the projector nature of  $\hat{\pi}_{Cb}$  from Eq. (8) defined via subspace projectors  $\hat{\pi}_\ell$ . Projectors of different subspaces  $k \neq \ell$  are by construction orthogonal because of the different number of field operators, since annihilation operators acting on the vacuum state leads to a vanishing contribution. We confirm the normalization of  $1/j!$  by determining

$$\hat{\pi}_\ell^2 \propto \frac{1}{\ell!^2} \hat{\varphi}_1^\dagger \dots \hat{\varphi}_\ell^\dagger |0\rangle \langle 0| \hat{\varphi}_\ell \dots \hat{\varphi}_1 \hat{\varphi}_1^\dagger \dots \hat{\varphi}_\ell^\dagger |0\rangle \langle 0| \hat{\varphi}_\ell \dots \hat{\varphi}_1, \quad (\text{B1})$$

where for simplicity the corresponding integrals are suppressed. Thus, Eq. (B1) requires to calculate matrix elements

$$\begin{aligned} & \langle 0| \hat{\varphi}_\ell \dots \hat{\varphi}_1 \hat{\varphi}_1^\dagger \dots \hat{\varphi}_\ell^\dagger |0\rangle \\ &= \sum_{\substack{u_1 \dots u_\ell=1 \\ v_1 \dots v_\ell=1}} \varepsilon_{u_1 \dots u_\ell} \varepsilon_{v_1 \dots v_\ell} \prod_{t=1}^{\ell} \delta(\mathbf{x}_{t,e} - \mathbf{x}'_{u_t,e}) \delta(\mathbf{x}_{t,n} - \mathbf{x}'_{v_t,n}) \end{aligned} \quad (\text{B2})$$

as a consequence of a consecutive application of the fundamental fermion anti-commutation relations given in Sec. II. The Levi-Civita symbol is defined as  $\varepsilon_{12\dots\ell} = +1$ , changes its sign if two indices are interchanged, and vanishes if at least two indices coincide. When evaluating the integrals that were not displayed in Eq. (B1), not all terms in Eq. (B2) contribute because of the integration limits of the coboson projection

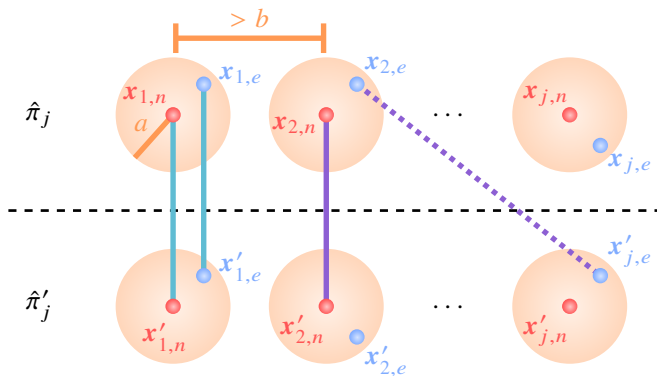


Figure 9. Top and bottom of the figure correspond to integration limits associated with projectors  $\hat{\pi}_j$  and  $\hat{\pi}'_j$ . Both project on  $j$  cobosons; and coboson coordinates of the same projector are restricted to pairwise combinations of nucleus-electron pairs confined in spheres of radius  $a$ , where different cobosons must not overlap. Connecting fermion coordinates of different subspace projectors accounts to the application of the commutation relation. The first case, connecting both electron and nucleus of coboson 1 and 1' (turquoise) corresponds to the bosonic part of the commutator. Connecting different coordinates amounts to the cobosonic part (purple). Due to restrictions given by integration regions, delta functions (lines) between more than two cobosons do not contribute and the cobosonic part of the commutator always vanishes.

operator. In fact, only terms where all sub-indices  $u_t = v_t$  coincide result in a nonvanishing contribution and all cross terms vanish, as motivated by Fig. 9.

One exemplary term is shown where the first and second line account for integration regions of projectors  $\hat{\pi}_j$  and  $\hat{\pi}'_j$  respectively. Each delta function  $\delta(\mathbf{x}_{t,i} - \mathbf{x}'_{u_t,i})$  is visualized by lines between coordinate  $\mathbf{x}_{t,i}$  and  $\mathbf{x}'_{u_t,i}$  of particle species  $i$ . Integrating over one coordinate gives rise to contributions where these coordinates coincide (turquoise lines) while the remaining fermions are still restricted to their respective regions. The purple lines, which correspond to one of the cross terms from Eq. (B2), imply that there are two electrons with coordinate  $\mathbf{x}'_{2,e}$  and  $\mathbf{x}'_{j,e}$  around nucleus  $\mathbf{x}'_{2,n}$ . As our projector does not allow such a situation, this term vanishes. Consequently, only such terms where  $u_t = v_t$  contribute, *i. e.*, only coordinates selected according to the blue lines in Fig. 9. After a relabeling of integration variables we find in total  $\ell!$  terms and, thus, the subspace projector is idempotent.

Comparing the nonvanishing terms from Eq. (B2) with the coboson commutator from Eq. (14), we observe that these correspond to the bosonic contribution of the commutator, emphasizing again that the integration regions in our projector enforce boson-like behavior.

## 2. Projection of Hamiltonian

In the following, we summarize essential identities that are required to perform the projection of the Hamiltonian. First, we may interchange  $\mathbf{x}_i = (\mathbf{x}_{i,n}, \mathbf{x}_{i,e})$  in integrands, *i. e.*, in the

case of two cobosons

$$\int_{C_1} d^6x_1 \int_{C_2} d^6x_2 f(\underline{\mathbf{x}}_1, \underline{\mathbf{x}}_2) = \int_{C_1} d^6x_1 \int_{C_2} d^6x_2 f(\underline{\mathbf{x}}_2, \underline{\mathbf{x}}_1) \quad (\text{B3a})$$

for any integrand  $f$ . This identity follows from relabeling integration variables and from the symmetry of the integration regions. The extension to  $N$  cobosons is straightforward.

Second, annihilating a coboson at position  $\mathbf{x}_1 = (\mathbf{x}_{1,n}, \mathbf{x}_{1,e})$ , before projecting onto the space of  $\ell - 1$  cobosons located anywhere but at  $\mathbf{x}_1$  is equivalent to projecting first onto the whole subspace of  $\ell$  cobosons, before annihilating a coboson at position  $\mathbf{x}_1$ , *i. e.*,

$$\int_{C_1} d^6x_1 \hat{\phi}_1^\dagger \hat{O}_1 \hat{\pi}_{\ell-1} \hat{\mathbf{x}}_1 \hat{\phi}_1 = \int_{C_1} d^6x_1 \hat{\phi}_1^\dagger \hat{O}_1 \hat{\phi}_1 \hat{\pi}_\ell. \quad (\text{B3b})$$

Here, the operator

$$\hat{\pi}_{\ell-1} \hat{\mathbf{x}}_1 = \int_{C_2} d^6x_2 \dots \int_{C_\ell} d^6x_\ell \hat{\phi}_2^\dagger \dots \hat{\phi}_\ell^\dagger |0\rangle \langle 0| \hat{\phi}_\ell \dots \hat{\phi}_2 \quad (\text{B4})$$

is the projector whose largest region of integration is  $C_2$  instead of  $C_1$ . A generalization to  $N$  cobosons is found analogously.

With the identities from Eq. (B3) we project the single-fermion part of the Hamiltonian  $\int d^3x \hat{\psi}_i^\dagger \hat{h}_i \hat{\psi}_i \hat{\pi}_\ell$  with the help of the fermionic anti-commutation relation for the same species, while different fermionic species commute trivially. We arrive at  $\ell$  terms which reduce by relabeling integration variables with help of the first identity to

$$\int d^3x \hat{\psi}_i^\dagger \hat{h}_i \hat{\psi}_i \hat{\pi}_\ell = \int_{C_1} d^6x_1 \hat{\phi}_1^\dagger \hat{h}_i \hat{\pi}_{\ell-1} \hat{\mathbf{x}}_1 \hat{\phi}_1. \quad (\text{B5})$$

Together with Eq. (B3b), we find the desired form from Eq. (11).

The projection of repulsive fermion-fermion interactions is performed similarly to the single-fermion operator case, but we exchange two annihilation operators with  $\ell$  creation operators. This case yields an effective factor of  $\ell(\ell - 1)$ , corresponding to all possible combinations of electron-electron (or nucleus-nucleus) interaction in the presence of  $\ell$  electrons (nuclei). Hence, the repulsive case with  $i = j$  resolves to

$$\begin{aligned} & \int d^3x_1 \int d^3x_2 \hat{\psi}_i^\dagger \hat{\psi}_j^\dagger \hat{V}^{(ij)} \hat{\psi}_j \hat{\psi}_i \hat{\pi}_\ell \\ &= \int_{C_1} d^6x_1 \int_{C_2} d^6x_2 \hat{\phi}_1^\dagger \hat{\phi}_2^\dagger \hat{V}^{(ij)} \hat{\pi}_{\ell-2} \hat{\mathbf{x}}_1, \hat{\mathbf{x}}_2 \hat{\phi}_2 \hat{\phi}_1. \end{aligned} \quad (\text{B6})$$

With the generalization of Eq. (B3b) we arrive at the projected form.

The attractive part contains field operators of two different species that define  $\hat{\phi}$  so that we apply the coboson commutator. There are  $\ell$  terms originating from the bosonic part and the corresponding coordinates are confined to the same region implying that these terms correspond to the binding potential. This projection can be performed analogously to the single-fermion part. On the other hand, the cobosonic part of the

commutator is responsible for  $\ell(\ell-1)$  terms that result in attractive interactions between different cobosons, similar to the repulsive interactions discussed above. In this derivation the importance of maintaining the elementary particle level becomes most evident as the bosonic part of the commutator generates the attractive part of the scattering potential.

### Appendix C: Coboson operator transformation

We determine the transformation of  $\hat{U}^\dagger \hat{\varphi} \hat{U}$  with the help of a Baker-Campbell-Hausdorff formula

$$\hat{U}^\dagger \hat{\varphi} \hat{U} = \sum_{k=0}^{\infty} \frac{1}{k!} \left( -\frac{i}{\hbar} \right)^k [\hat{\Lambda}, \hat{\varphi}]_k \quad (\text{C1})$$

where  $[\hat{\Lambda}, \hat{\varphi}]_k = [\hat{\Lambda}, [\hat{\Lambda}, \hat{\varphi}]_{k-1}]$  and  $[\hat{\Lambda}, \hat{\varphi}]_0 = \hat{\varphi}$ . Focusing first on the bosonic part of the coboson commutator, it can be shown that

$$[\hat{\Lambda}, \hat{\varphi}]_k = (-\hat{\lambda})^k \hat{\varphi}. \quad (\text{C2})$$

By definition,  $\hat{\Lambda}$  is the second-quantized generator of  $\hat{\lambda}$  and they are related to each other by Eq. (17). Regarding the additional parts of the coboson commutator, they do not vanish trivially but can be resolved with an argument similar to the case sketched in Fig. 9. Through the bosonic part of the commutator, we generate terms containing the annihilation of two electrons (nuclei) within the same sphere around one nucleus (electron) which lies outside of our projected subspace and thus vanishes. This fact may be made explicit by introducing the projected transformation  $\hat{\pi}_{\text{Cb}} \hat{U}^\dagger \hat{\varphi} \hat{U} \hat{\pi}_{\text{Cb}}$  as  $\hat{\varphi} = \hat{\pi}_{\text{Cb}} \hat{\varphi}$ . Consequently, the transformation reduces to

$$\hat{U}^\dagger \hat{\varphi} \hat{U} = \hat{u} \hat{\varphi}, \quad (\text{C3})$$

*i. e.*, the second-quantized unitary transformation given by  $\hat{U}$  reduces to the first-quantized unitary  $\hat{u}$  defined via their respective generator.

### Appendix D: Multipolar cobosonic Hamiltonian from unitary transformations

In this appendix, we present the transformation of the coboson Hamiltonian into its multipolar form including relativistic corrections of c.m. and relative coordinates, and provide the full expressions omitted in the main body of the article. In Sec. IV we demonstrated that the transformation of the field-theoretical Hamiltonian can be reduced to its single-particle counterpart, summarized in Eq. (20). This appendix gives details on the respective single-particle transformations.

As discussed in Sec. IV, we first perform a unitary transformation to introduce relativistic corrections to c.m. and relativistic coordinates, before we transform in a second step the resulting operators with the help of the PZW transformation. Because only the lowest-order relativistic correction is of relevance, we find for any single-particle operator  $\hat{O}$  the

transformation  $\hat{u}^{(\text{rel}) \dagger} \hat{O} \hat{u}^{(\text{rel})} = \hat{O} - i [\hat{\lambda}^{(\text{rel})}, \hat{O}] / \hbar = \hat{O} + \hat{O}^{(1)}$ . The generator  $\hat{\lambda}^{(\text{rel})}$  already given in Eq. (18) has the form

$$\hat{\lambda}_k^{(\text{rel})} = \frac{\mathbf{r}_k \cdot \hat{\mathbf{P}}_k}{4M^2 c^2} \left[ \hat{\mathbf{p}}_k \cdot \hat{\mathbf{P}}_k + \Delta m \left( \frac{\hat{\mathbf{p}}_k^2}{m_r} + \frac{q_e q_n}{4\pi \epsilon_0 |\mathbf{r}_k|} \right) \right] + \text{H.c.} \\ - \frac{1}{4m_r M c^2} \left( \hat{\mathbf{p}}_k \times \hat{\mathbf{P}}_k + \text{H.c.} \right) \cdot \hat{\mathbf{s}}_k. \quad (\text{D1})$$

The subsequent PZW transformation is performed with the help of the generator  $\hat{\lambda}_k^{(\text{PZW})} = \int d^3y \mathcal{P}_k(\mathbf{y}) \cdot \hat{\mathbf{A}}(\mathbf{y})$ , where  $\mathcal{P}_k$  is a polarization field of the  $k$ -th coboson and is defined in Eq. (19). According to Eq. (20), we discuss in the following the individual transformations of the single-coboson Hamiltonian, the coboson scattering potential, and the EM Hamiltonian.

#### 1. Single-coboson Hamiltonian

The single-coboson Hamiltonian from Eq. (20a) includes the operators  $\hat{\mathbf{P}}, \hat{\mathbf{p}}, 1/|\mathbf{r}|, \hat{\mathbf{B}}, \hat{\mathbf{s}}, \hat{\mathbf{E}}$ , and  $\nabla \cdot \hat{\mathbf{E}}$  [266] that have to be transformed.

##### a. Relativistic corrections

To compute the relativistic corrections  $\hat{O}^{(1)}$ , we first calculate the commutators between minimally-coupled momenta to

$$[\hat{P}_\ell, \hat{P}_m] = i\hbar \epsilon_{\ell mn} Q \hat{B}_{Q,n}, \quad (\text{D2a})$$

$$[\hat{p}_\ell, \hat{P}_m] = i\hbar \epsilon_{\ell mn} q_1 \hat{B}_{q_1,n}, \text{ and} \quad (\text{D2b})$$

$$[\hat{p}_\ell, \hat{p}_m] = i\hbar \epsilon_{\ell mn} q_2 \hat{B}_{q_2,n}. \quad (\text{D2c})$$

Here, we introduce the abbreviation  $\hat{\mathbf{B}}_{q_r} = \sum_i \text{sgn}(-q_i)^r q_i (m_r/m_i)^r \hat{\mathbf{B}}(\mathbf{x}_i)/q_r$  with  $r = 0, 1, 2, \dots$  that contains the weighted charge  $q_r = \sum_i \text{sgn}(-q_i)^r q_i (m_r/m_i)^r$  and is chosen such that the lowest-order multipole expansion of  $\hat{\mathbf{B}}_{q_r}$  coincides with  $\hat{\mathbf{B}}(\mathbf{R})$ . In the particular case  $q_0 = Q$  we write the total charge  $Q$  and  $\text{sgn}$  is the sign function. With the commutators of minimally-coupled momenta we determine all corrections which are presented in Table V. We see that c.m. and relative momentum are modified by light-induced corrections with the general  $\mathbf{r} \times \hat{\mathbf{B}}$  structure. In Table V we introduced the operators

$$\hat{\delta}_r = \frac{\mathbf{r} \cdot \hat{\mathbf{P}}}{4M^2 c^2} \left( \hat{\mathbf{P}} + 2 \frac{\Delta m}{m_r} \hat{\mathbf{p}} \right) - \frac{\hat{\mathbf{P}} \times \hat{\mathbf{s}}}{4m_r M c^2} \quad (\text{D3a})$$

$$\hat{\delta}_R = \frac{\mathbf{r} \cdot \hat{\mathbf{P}}}{4M^2 c^2} \hat{\mathbf{p}} + \frac{\hat{\mathbf{p}} \cdot \hat{\mathbf{P}} + \Delta m \left( \frac{\hat{\mathbf{p}}^2}{m_r} + \frac{q_e q_n}{4\pi \epsilon_0 |\mathbf{r}|} \right)}{4M^2 c^2} \mathbf{r} + \frac{\hat{\mathbf{p}} \times \hat{\mathbf{s}}}{4m_r M c^2} \quad (\text{D3b})$$

where  $\hat{\delta}_r$  and  $\hat{\delta}_R$  follow from a commutator involving the relative and c.m. momentum, respectively. Moreover, terms arise that are of the form of a second-order multipole expansion of the magnetic field  $\hat{\mathbf{B}}_{r,s} = q_r \hat{\mathbf{B}}_{q_r} + \frac{\Delta m}{m_r} q_s \hat{\mathbf{B}}_{q_s}$ .

Table V. Lowest-order relativistic corrections obtained by the transformation  $\hat{u}^{(\text{rel})} \dagger \hat{\mathcal{O}} \hat{u}^{(\text{rel})} = \hat{\mathcal{O}} + \hat{\mathcal{O}}^{(1)}$  for the c.m. momentum, the relative momentum, Coulomb-like terms, the magnetic field at the position of a fermion, and its spin. They are obtained by calculating  $\hat{\mathcal{O}}^{(1)} = -i \left[ \hat{\lambda}^{(\text{rel})}, \hat{\mathcal{O}} \right] / \hbar$ . They depend on the operators  $\hat{\delta}_r, \hat{\delta}_R$  and  $\hat{\delta}_B$  given in Eqs. (D3) and (D4) as well as the terms  $\hat{B}_{q_r} = \sum_i \text{sgn}(-q_i)^r q_i (m_r/m_i)^r \hat{B}(x_i)/q_r$  and  $\hat{B}_{r_s} = q_r \hat{B}_{q_r} + \frac{\Delta m}{m_r} q_s \hat{B}_{q_s}$  with a weighted charge  $q_r = \sum_i \text{sgn}(-q_i)^r q_i (m_r/m_i)^r$ .

$\hat{\mathcal{O}}$	$\hat{\mathcal{O}}^{(1)}$
$\hat{P}$	$-\hat{\delta}_R \times Q \hat{B}_Q - \hat{\delta}_r \times q_1 \hat{B}_{q_1} + \text{H.c.} - \frac{\hbar^2}{4M^2 c^2} (\mathbf{r} \cdot \nabla) \nabla \times \hat{B}_{12}$
$\hat{p}$	$-\hat{\delta}_R \times q_1 \hat{B}_{q_1} - \hat{\delta}_r \times q_2 \hat{B}_{q_2} + \text{H.c.} - \frac{\hbar^2}{4M^2 c^2} (\mathbf{r} \cdot \nabla) \nabla \times \hat{B}_{23} + \frac{1}{4M^2 c^2} \left[ \hat{P} (\hat{p} \cdot \hat{P} + \frac{\Delta m}{m_r} \hat{p}^2 + \frac{\Delta m q_e q_n}{4\pi \epsilon_0  \mathbf{r} }) - \frac{\Delta m q_e q_n}{4\pi \epsilon_0} \mathbf{r} \cdot \hat{P} \frac{\mathbf{r}}{ \mathbf{r} ^3} + \text{H.c.} \right]$
$1/ \mathbf{r} $	$\frac{1}{ \mathbf{r} ^3} (\hat{P} \cdot \mathbf{r})^2 + \frac{\Delta m}{2m_r M c^2} \left( \frac{1}{ \mathbf{r} ^3} (\hat{P} \cdot \mathbf{r}) (\mathbf{r} \cdot \hat{p}) + \text{H.c.} \right) - \frac{1}{2m_r M c^2} \frac{1}{ \mathbf{r} ^3} \mathbf{r} \times \hat{P} \cdot \hat{s}$
$\hat{B}(x_i)$	$(\hat{\delta}_B \cdot \nabla) \hat{B} + \text{H.c.} + \frac{\hbar^2}{4M^2 c^2} \frac{q_i}{ q_i } \frac{m_r}{m_i} \left( 1 - \frac{\Delta m}{m_i} \frac{q_i}{ q_i } \right) (\mathbf{r} \cdot \nabla) \nabla^2 \hat{B}$
$\hat{s}_i$	$\hat{s}_i \times \frac{q_i}{ q_i } \frac{\hat{p} \times \hat{P} + \text{H.c.}}{4m_i M c^2}$

While the c.m. momentum contains only light-induced corrections, the relative momentum has an additional correction that is not induced by magnetic fields. The correction to the Coulomb potential coincides [16] with the one when light-field corrections are neglected, but the canonical c.m. and relative momenta are exchanged by minimally-coupled ones. Finally, the correction to the magnetic field may be rewritten into a second-order multipole expansion form but with the operator

$$\hat{\delta}_B = - \frac{\hat{p} \cdot \hat{P} + \frac{\Delta m}{m_r} \hat{p}^2 + \frac{\Delta m q_e q_n}{4\pi \epsilon_0 |\mathbf{r}|}}{4M^2 c^2} \mathbf{r} + \frac{q_i}{|q_i|} \frac{m_r}{m_i} \frac{\hat{P} \cdot \mathbf{r}}{4M^2 c^2} \hat{P} - \left( 1 - 2 \frac{q_i}{|q_i|} \frac{\Delta m}{m_i} \right) \frac{\hat{P} \cdot \mathbf{r}}{4M^2 c^2} \hat{p} - \frac{\hat{p} + \frac{q_i}{|q_i|} \frac{m_r}{m_i} \hat{P}}{4m_r M c^2} \times \hat{s} \quad (\text{D4})$$

together with a contribution proportional to the Laplacian of the magnetic field. Since the electric fields are already of the order  $c^{-2}$  in the Hamiltonian, there are no further relevant corrections.

### b. PZW transformation

We perform the PZW transformation in Coulomb gauge where the vector potential commutes with itself and the magnetic field at any position. Thus, only the transformation of minimally-coupled momenta and the electric field is remaining. As a result, we find the transformations [79, 145]

$$\hat{P} \rightarrow \hat{P}_{\text{PZW}} = \hat{P}_Q + \hat{F}^{(\text{cm})} \quad (\text{D5a})$$

$$\hat{p} \rightarrow \hat{p}_{\text{PZW}} = \hat{p} + \hat{F}^{(\text{rel})} \quad (\text{D5b})$$

$$\hat{E}^\perp(\mathbf{y}) \rightarrow \hat{E}^\perp(\mathbf{y}) - \frac{1}{\epsilon_0} \mathcal{P}^\perp(\mathbf{y}). \quad (\text{D5c})$$

In the case of ions with  $Q \neq 0$ , the c.m. momentum couples minimally to a monopole evaluated at the c.m. position of the vector potential, *i. e.*,  $\hat{P}_Q = \hat{P} - Q \hat{A}(\mathbf{R})$ . Moreover, both

c.m. and relative momenta are modified by generalized  $\mathbf{r} \times \hat{B}$  summarized by

$$\hat{F}^{(\text{cm})} = \int d^3y \mathcal{P}(\mathbf{y}) \times \hat{B}(\mathbf{y}) \quad (\text{D6a})$$

$$\hat{F}^{(\text{rel})} = \sum_{j=e,n} q_j \frac{m_r^2}{m_j^2} \mathbf{r} \times \int_0^1 d\rho \rho \hat{B}(\mathbf{R} + \rho(\mathbf{x}_j - \mathbf{R})), \quad (\text{D6b})$$

where the c.m. momentum now includes the polarization field defined in Eq. (19). The electric fields in the single-coboson Hamiltonian are evaluated at positions  $x_i$ . Since the polarization field  $\mathcal{P}(x_i) = 0$  vanishes, there is no electric-field contribution from the single-coboson electric fields.

### c. Hamiltonian

After we insert the PZW-transformed momenta, also into the corrections from Table V, the transformed single-coboson Hamiltonian  $\hat{h}_{\text{Cb}}$  from Eq. (20a) resolves to

$$\hat{h}'_{\text{MpCb}} = M c^2 + \frac{\hat{P}_Q^2}{2M} \left( 1 + \frac{\hat{h}_{\text{rel}}^{(0)}}{M c^2} \right) - \frac{\hat{P}_Q^4}{8M^3 c^2} + \hat{h}_{\text{rel}}^{(0)} + \hat{h}_{\text{rel}}^{(1)} - \frac{q_e q_n}{8\pi \epsilon_0 m_n M c^2} \frac{Z-1}{|\mathbf{r}|^3} (\mathbf{r} \times \hat{P}_Q) \cdot \hat{s}_n + \hat{h}_{\text{IB}}^{(0)} + \hat{h}_{\text{IB}}^{(1)}. \quad (\text{D7})$$

The prime indicates that electric-field contributions that arise from the transformation of the EM Hamiltonian are not yet included. The relative Hamiltonian is identical to Eq. (24) and  $\hat{h}_{\text{IB}}^{(0)}$  contains the magnetic-field contribution of lowest-order light-matter interaction. It is listed in Table III. The additional part, magnetic-field contributions to light-matter interaction at the order of  $c^{-2}$ , are collected in



$$\begin{aligned}
\hat{h}_{\text{IB}}^{(1)} = & - \left( \frac{\hat{\mathbf{P}}_{\text{PZW}}^2 \hat{h}_{\text{rel,PZW}}^{(0)} - \hat{\mathbf{P}}_Q^2 \hat{h}_{\text{rel}}^{(0)}}{4M^2 c^2} + \text{H.c.} \right) - \frac{\hat{\mathbf{P}}_{\text{PZW}}^4 - \hat{\mathbf{P}}_Q^4}{8M^3 c^2} - \frac{m_n^3 + m_e^3}{M^3} \frac{\hat{\mathbf{P}}_{\text{PZW}}^4 - \hat{\mathbf{p}}^4}{8m_i^3 c^2} - \frac{q_e q_n}{8\pi\epsilon_0 m_n M c^2} \frac{Z-1}{|r|^3} (\mathbf{r} \times \hat{\mathbf{F}}^{(\text{cm})}) \cdot \hat{\mathbf{s}}_n \\
& - \frac{\kappa}{|r|} (\hat{\mathbf{p}}_{\text{PZW}}^2 - \hat{\mathbf{p}}^2) + \frac{\kappa}{|r|^3} \mathbf{r} \times \hat{\mathbf{F}}^{(\text{rel})} \cdot (\alpha_{\ell S} \hat{\mathbf{S}} + \alpha_{\ell s} \hat{\mathbf{s}}) + \sum_i \left[ c_S^{(i)} q_i \frac{\left( \frac{m_i}{M} \hat{\mathbf{P}}_{\text{PZW}} - \frac{q_i}{|q_i|} \hat{\mathbf{p}}_{\text{PZW}} \right) \times \hat{\mathbf{E}}}{4m_i^2 c^2} \cdot \hat{\mathbf{s}}_i + \text{H.c.} \right] \\
& + \sum_i c_{\text{W1}}^{(i)} q_i \frac{\left\{ (\hat{\mathbf{P}}_{\text{PZW}} - \frac{q_i}{|q_i|} \frac{m_r}{m_i} \hat{\mathbf{p}}_{\text{PZW}})^2, \hat{\mathbf{s}}_i \cdot \hat{\mathbf{B}}(x_i) \right\}}{4m_i^3 c^2} - \sum_i c_{\text{A1}}^{(i)} q_i^2 \frac{\hbar^2 \hat{\mathbf{B}}^2(x_i)}{8m_i^3 c^2} + \frac{\left\{ \hat{\mathbf{P}}_{\text{PZW}}^{(1)}, \hat{\mathbf{P}}_{\text{PZW}} \right\}}{2M} + \frac{\left\{ \hat{\mathbf{p}}_{\mathbf{B},\text{PZW}}^{(1)}, \hat{\mathbf{p}}_{\text{PZW}} \right\}}{2m_r} \\
& - \sum_i \left( \hat{\boldsymbol{\mu}}_{i,\text{PZW}}^{(1)} \cdot \hat{\mathbf{B}} + \hat{\boldsymbol{\mu}}_i \cdot \hat{\mathbf{B}}_{\text{PZW}}^{(1)} \right) + \frac{\hbar^2}{16m_r M^2 c^2} \left[ \hat{\mathbf{p}}_{\text{PZW}} \cdot \nabla \times q_1 \hat{\mathbf{B}}_{q_1} - \left( \hat{\mathbf{P}}_{\text{PZW}} + 2 \frac{\Delta m}{m_r} \hat{\mathbf{p}}_{\text{PZW}} \right) \cdot \nabla \times q_2 \hat{\mathbf{B}}_{q_2} + \text{H.c.} \right] \\
& + \frac{\hbar^2}{4m_r M^2 c^2} \left[ q_2 \hat{\mathbf{B}}_{q_2} \cdot \left( Q \hat{\mathbf{B}}_Q + \frac{\Delta m}{m_r} q_1 \hat{\mathbf{B}}_{q_1} \right) + q_1 \hat{\mathbf{B}}_{q_1} \cdot \left( q_1 \hat{\mathbf{B}}_{q_1} + \frac{\Delta m}{m_r} q_2 \hat{\mathbf{B}}_{q_2} \right) \right]. \tag{D8}
\end{aligned}$$

Due to the PZW transformation and the fact that we keep light-matter interactions also in the order  $c^{-2}$ , we find for all  $c^{-2}$  terms from the single-coboson Hamiltonian a light-field contribution that are listed in the first three lines of  $\hat{h}_{\text{IB}}^{(1)}$ . Every term that appears with a subscript ‘‘PZW’’ contains PZW-transformed momenta. The relativistic corrections  $\hat{\boldsymbol{\mu}}_{i,\text{PZW}}^{(1)}$ ,  $\hat{\mathbf{B}}_{\text{PZW}}^{(1)}$ ,  $\hat{\mathbf{P}}_{\text{PZW}}^{(1)}$ , and  $\hat{\mathbf{p}}_{\text{PZW}}^{(1)}$  are the ones from Table V, only with PZW-transformed momenta, where  $\hat{\boldsymbol{\mu}}_i^{(1)} = c_F^{(i)} \hat{\mathbf{s}}_i^{(1)}/m_i$ . Moreover, we collect all PZW-transformed terms of  $\hat{\mathbf{p}}_{\text{PZW}}^{(1)}$  directly proportional to  $\hat{\mathbf{B}}$  in  $\hat{\mathbf{p}}_{\mathbf{B},\text{PZW}}^{(1)}$  that includes light-field induced corrections. The last line in Eq. (D8) represents the remainder of combining c.m. and relative parts of the kinetic correction and the relativistic correction  $\hat{\mathbf{p}}^{(1)}$  due to the noncommutativity of c.m. and relative momenta. We see that in  $c^{-2}$  the influence of the magnetic field becomes cumbersome, but the general structure is expressed through  $\mathbf{r} \times \hat{\mathbf{B}}$ -terms,  $\hat{\mathbf{B}}^2$ -terms and  $\nabla \times \hat{\mathbf{B}}$ -type terms in various combinations with other operators.

## 2. Coboson scattering potential

In the following, we determine the transformation of the scattering potential

$$\hat{V}_{\text{Scatt}} = \sum_{i,j} \left( \hat{V}_C^{(ij)} + \hat{V}_{\text{LL}}^{(ij)} + \hat{V}_{\text{LS}}^{(ij)} + \hat{V}_{\text{SS}}^{(ij)} \right). \tag{D9}$$

To our order, only relativistic corrections to the Coulomb potential

$$\hat{V}_C^{(ij)} = \frac{q_i q_j}{8\pi\epsilon_0 |\chi_{ij}|} \tag{D10}$$

between fermion  $i$  of coboson 1 and fermion  $j$  of coboson 2 at a relative distance  $\chi_{ij} = \mathbf{x}_{1,i} - \mathbf{x}_{2,j}$  have to be considered. Here,  $\mathbf{x}_{k,i} = \mathbf{R}_k - \text{sgn}(q_i) m_r \mathbf{r}_k / m_i$  in NR c.m. and relative coordinates. The transformation resolves to

$$\hat{u}_{12}^{(\text{rel})\dagger} \frac{1}{|\chi_{ij}|} \hat{u}_{12}^{(\text{rel})} = \frac{1}{|\chi_{ij}|} + \hat{\delta}_{1,i}^{(ij)} + \hat{\delta}_{2,j}^{(ij)} + \mathcal{O}(c^{-4}) \tag{D11}$$

with corrections  $\hat{\delta}_{k,t}^{(ij)} = -i[\hat{\lambda}_k^{(\text{rel})}, 1/|\chi_{ij}|]/\hbar$  that take the explicit form

$$\begin{aligned}
\hat{\delta}_{k,t}^{(ij)} = & - \frac{(-1)^k}{4M^2 c^2 |\chi_{ij}|^3} \left\{ \mathbf{r}_k \cdot \chi_{ij} \frac{\Delta m q_e q_n}{4\pi\epsilon_0 |\mathbf{r}_k|} + \hat{\boldsymbol{\ell}}_\beta^{(ij)} \cdot \left( \hat{\mathbf{L}}_k + \frac{\Delta m}{M} \hat{\boldsymbol{\ell}}_k \right) + (\chi_{ij} \cdot \hat{\mathbf{p}}_k) \mathbf{r}_k \cdot \left( \hat{\mathbf{p}}_k - \frac{q_t}{|q_t|} \frac{m_r}{m_t} \hat{\mathbf{p}}_k \right) \right. \\
& \left. + (\chi_{ij} \cdot \hat{\mathbf{p}}_k) \mathbf{r}_k \cdot \left( \frac{\Delta m}{M} \hat{\mathbf{p}}_k + \left( 1 - 2 \frac{\Delta m}{M} \frac{q_t}{|q_t|} \frac{m_r}{m_t} \right) \hat{\mathbf{P}}_k \right) + \frac{M}{m_r} \left( \hat{\boldsymbol{\ell}}^{(ij)} + \frac{q_t}{|q_t|} \frac{m_r}{m_t} \hat{\mathbf{L}} \right) \cdot \hat{\mathbf{s}}_k + \text{H.c.} \right\}. \tag{D12}
\end{aligned}$$

These relativistic corrections can be identified with a scalar correction to the Coulomb potential, orbit-orbit-like and spin-

orbit-like potentials. For instance, the orbit-orbit scattering potential  $\hat{V}_{\text{LL}}^{(ij)}$  describes orbit-orbit coupling between fermions

of two different cobosons due to their respective angular momentum  $\chi_{ij} \times \hat{\mathbf{p}}_i$ . Similar terms appear also in  $\hat{\delta}_{k,t}^{(ij)}$  that depend on the angular momentum  $\hat{\ell}_k^{(ij)} = \chi_{ij} \times \hat{\mathbf{p}}_k$ , which is the outer product of the distance between two fermions of different cobosons and the relative momentum of coboson  $k$ , where the bar indicates again minimally-coupled momenta. These angular momenta between cobosons couple in this case to the *internal* total  $\hat{\mathbf{L}}_k = \mathbf{r}_k \times \hat{\mathbf{p}}_k$  and relative  $\hat{\ell}_k = \mathbf{r}_k \times \hat{\mathbf{p}}_k$  angular momentum of coboson  $k$ . Next, we find a spin-orbit coupling between angular momenta  $\hat{\mathbf{L}}^{(ij)}$  and  $\hat{\ell}^{(ij)}$  to the relative spin  $\hat{\mathbf{s}}_k$ .

Applying the PZW transformation as well changes all momenta in the scattering potentials to the PZW-transformed ones, also in the correction term given in Eq. (D12). Consequently, the transformed scattering potential reads

$$\hat{\mathcal{V}}_{\text{Scatt}} = \sum_{i,j} \frac{q_i q_j}{8\pi\epsilon_0} \left( \frac{1}{|\chi_{ij}|} + \hat{\delta}_{1,i}^{(ij,\text{PZW})} + \hat{\delta}_{2,j}^{(ij,\text{PZW})} \right) + \hat{\mathcal{V}}_{\text{LL}}^{(ij)} + \hat{\mathcal{V}}_{\text{LS}}^{(ij)} + \hat{\mathcal{V}}_{\text{SS}}^{(ij)}. \quad (\text{D13})$$

The potentials  $\hat{\mathcal{V}}_v^{(ij)}$  are the ones from Fig. 3 where we replace  $\mathbf{r}$  by  $\chi_{ij}$  as well as  $\hat{\mathbf{p}}_i \rightarrow m_i \hat{\mathbf{P}}_{1,\text{PZW}}/M - \text{sgn}(q_i) \hat{\mathbf{p}}_{1,\text{PZW}}$  and  $\hat{\mathbf{p}}'_j \rightarrow m_j \hat{\mathbf{P}}_{2,\text{PZW}}/M - \text{sgn}(q_j) \hat{\mathbf{p}}_{2,\text{PZW}}$  for the momenta.

Scattering between two cobosons reduces to interactions between fermion  $i$  and  $j$  of two different cobosons via the Coulomb potential in lowest order together with magnetic moments associated with both spin and orbital motion. By that, all magnetic moments couple, *i. e.*, spin to spin, spin to orbit, and orbit to orbit where the latter has an additional retardation correction. In addition, corrections to NR c.m. and relative coordinates arise from the Coulomb term and modify the Coulomb potential, the LL-coupling, as well as the LS-coupling.

### 3. EM Hamiltonian

Finally, the transformation of the EM Hamiltonian requires the direct computation of the second-quantized unitary  $\hat{U}$  as it contains no cobosonic field operators. Hence, we determine

$$\hat{U}_{\text{PZW}}^\dagger \hat{U}_{\text{rel}}^\dagger \hat{H}_{\text{EM}} \hat{U}_{\text{rel}} \hat{U}_{\text{PZW}}. \quad (\text{D14})$$

Note that momentum operators contained in field-theoretical unitaries do not act on the variables of integration in  $\hat{H}_{\text{EM}}$  such that the transformation is solely determined through EM fields. Moreover,  $\hat{U}_{\text{rel}}$  and  $\hat{U}_{\text{PZW}}$  contain only the vector potential  $\hat{\mathbf{A}}$  that commutes with itself and with the magnetic field  $\hat{\mathbf{B}}$  in Coulomb gauge, so only the electric field gives rise to additional terms. The relevant commutator between the vector potential and the electric field

$$\left[ \hat{A}^{(\ell)}(\mathbf{x}), \hat{E}^{(m)}(\mathbf{y}) \right] = -\frac{i\hbar}{\epsilon_0} \delta^{\ell m, \perp}(\mathbf{x} - \mathbf{y}) \quad (\text{D15})$$

is defined through the transverse delta function [267]. The transformation generating the relativistic corrections gives rise

to the form

$$\hat{U}_{\text{rel}}^\dagger \hat{H}_{\text{EM}} \hat{U}_{\text{rel}} = \hat{H}_{\text{EM}} + \int_{C_1} d^6\mathcal{R}_1 \hat{\phi}_1^\dagger \hat{h}_{\text{IE}}^{(1)} \hat{\phi}_1. \quad (\text{D16})$$

The relativistic corrections can be written as  $\hat{h}_{\text{IE}}^{(1)} = \frac{1}{2} \sum_i \left( \hat{\mathbf{E}}_i^\perp \cdot \hat{\mathbf{d}}_i + \hat{\mathbf{d}}_i \cdot \hat{\mathbf{E}}_i^\perp \right)$  and appears with  $\hat{\mathbf{d}}_i$  defined in Eq. (29), but the momenta are still the minimally-coupled ones. Applying the PZW transformation to the first term in Eq. (D16) results in

$$\hat{U}_{\text{PZW}}^\dagger \hat{H}_{\text{EM}} \hat{U}_{\text{PZW}} = \hat{H}_{\text{EM}} + \int_{C_1} d^6\mathcal{R}_1 \hat{\phi}_1^\dagger \hat{h}_{\text{IE}}^{(0)} \hat{\phi}_1 + \int_{C_1} d^6\mathcal{R}_1 \int_{C_2} d^6\mathcal{R}_2 \hat{\phi}_1^\dagger \hat{\phi}_2^\dagger \hat{\mathcal{V}}_{\text{Self}} \hat{\phi}_2 \hat{\phi}_1. \quad (\text{D17})$$

Here,  $\hat{h}_{\text{IE}}^{(0)}$  contains the electric multipole moments and the self-energy from Table III and  $\hat{\mathcal{V}}_{\text{Self}}$  is the scattering self-energy known from Table IV.

The PZW transformation of the second term in Eq. (D16) reduces now, due to the coboson field operators, to the first-quantized PZW transformation of  $\hat{h}_{\text{IE}}^{(1)}$  only, such that the electric field  $\hat{\mathbf{E}}_i$  is again not affected as  $\mathcal{P}(\mathbf{x}_i) = 0$  vanishes. The momenta are exchanged by their PZW-transformed ones, *i. e.*,  $\hat{h}_{\text{IE}}^{(1)} \rightarrow \hat{h}_{\text{IE}}^{(1)}$ . This Hamiltonian is the electric part of  $c^{-2}$  corrections to light-matter interaction from Eq. (29), where we replace canonical momenta with the PZW-transformed ones.

By taking into account the contributions from the EM Hamiltonian, the single-coboson Hamiltonian is modified in the light-matter interaction part to  $\hat{h}_1^{(k)} = \hat{h}_{\text{IB}}^{(k)} + \hat{h}_{\text{IE}}^{(k)}$  with  $k = 0, 1$ . The scattering potential gets an additional self-energy  $\hat{\mathcal{V}}_{\text{Self}}$ .

### Appendix E: First-order energy shift

To determine first-order energy shifts, the actual form of the wave function of relative modes of hydrogen-like cobosons  $\psi_\beta$  is required and is given in terms of quantum numbers  $n, j, m_j, \ell, S$ . In particular, the wave function

$$\psi_\beta = \alpha_{j,S,1} \psi_{n,\ell,m_j-1} \chi_{S,1} + \alpha_{j,S,0} \psi_{n,\ell,m_j} \chi_{S,0} + \alpha_{j,S,-1} \psi_{n,\ell,m_j+1} \chi_{S,-1} \quad (\text{E1})$$

consists of  $\psi_{n,\ell,m}$ , the standard spatial part of the solution to hydrogen-like Schrödinger equation. The spin wave function  $\chi_{S,m_S}$  is the eigenbasis of operators  $\hat{S}^2$  and  $\hat{S}_z$  of the total spin  $\hat{S} = \hat{s}_e + \hat{s}_n$ . By that, the total spin of a coboson formed by two spin-1/2 fermions can either be  $S = 0$  or  $S = 1$ , while its projection onto the  $z$ -axis can take magnetic spin numbers  $m_S = 0$  or  $m_S = -1, 0, 1$ , respectively. In the superposition of Eq. (E1) together with Clebsch-Gordan coefficients [268] (detailed in Table VI), we find the eigenbasis of the operators  $\hat{J}, \hat{J}_z, \hat{\ell}$ , and  $\hat{S}$ , where  $\hat{J} = \hat{\ell} + \hat{S}$  is the total angular momentum. With this

Table VI. Clebsch-Gordan coefficients  $\alpha_{j,S,m_S}$  for the angular-momentum eigenbasis of total angular momentum  $\hat{\mathbf{J}} = \hat{\mathbf{L}} + \hat{\mathbf{S}}$ . Here,  $j$  is the quantum number of the total angular momentum,  $S$  the quantum number of the total spin, and  $m_S$  its magnetic quantum number. Moreover,  $\ell$  is the quantum number of orbital angular momentum and  $m_j$  the magnetic quantum number of the total angular momentum.

$(j, S)$ \ $m_S$	1	0	-1
$(\ell + 1, 1)$	$\sqrt{\frac{(\ell+m_j)(\ell+m_j+1)}{2(\ell+1)(2\ell+1)}}$	$\sqrt{\frac{(\ell-m_j+1)(\ell+m_j+1)}{(\ell+1)(2\ell+1)}}$	$\sqrt{\frac{(\ell-m_j)(\ell-m_j+1)}{2(\ell+1)(2\ell+1)}}$
$(\ell, 1)$	$\sqrt{\frac{(\ell+m_j)(\ell-m_j+1)}{2\ell(\ell+1)}}$	$-\frac{m_j}{\sqrt{\ell(\ell+1)}}$	$-\sqrt{\frac{(\ell-m_j)(\ell+m_j+1)}{2\ell(\ell+1)}}$
$(\ell - 1, 1)$	$\sqrt{\frac{(\ell-m_j)(\ell-m_j+1)}{2\ell(2\ell+1)}}$	$-\sqrt{\frac{(\ell-m_j)(\ell+m_j)}{\ell(2\ell+1)}}$	$\sqrt{\frac{(\ell+m_j)(\ell+m_j+1)}{2\ell(2\ell+1)}}$
$(\ell, 0)$	0	1	0

explicit wave function in angular momentum eigenbasis we

determine the first-order energy shift  $E_\beta^{(1)} = \int d^3r \psi_\beta^* \hat{h}_{\text{rel}}^{(1)} \psi_\beta$  and arrive at

$$E_\beta^{(1)} = \frac{m_r^2 c^2 (Z\alpha)^4}{M} \left\{ \frac{m_e^3 + m_n^3}{8m_r M^2} \left( 3 - \frac{8n}{2\ell+1} \right) \frac{1}{n^4} + \left( 1 - \frac{3n}{2\ell+1} \right) \frac{1}{n^4} + \left( \alpha_D - \frac{3}{4} \alpha_{\text{ss}} + \alpha_{\text{ss}} \delta_{S,1} \right) \frac{\delta_{\ell,0}}{n^3} + \frac{(\delta_{\ell,0} - 1) \delta_{S,1}}{\ell(\ell+1)(2\ell+1)} C_{j,\ell} \right\}. \quad (\text{E2})$$

The individual terms correspond to the kinetic correction (first), orbit-orbit coupling (second), Darwin and contact interaction (third) where  $\hat{\mathbf{s}}_e \cdot \hat{\mathbf{s}}_n = (\hat{\mathbf{S}}^2 - \hat{\mathbf{s}}_e^2 - \hat{\mathbf{s}}_n^2)/2$  was exploited such that  $\hat{s}_i^2$  takes also a Darwin-like spin-independent form. The last term combines both spin-orbit terms and the magnetic dipole-dipole potential in  $\hat{S}_{ne} = -\hat{\mathbf{s}}_n \cdot \hat{\mathbf{s}}'_e + 3(\mathbf{r} \cdot \hat{\mathbf{s}}_n)(\mathbf{r} \cdot \hat{\mathbf{s}}'_e)/|\mathbf{r}|^2$  with

$$C_{j,\ell} = \begin{cases} \frac{\ell}{2\ell+3} \left[ 2(2\ell+3) \left( \alpha_{\ell S} + \frac{\Delta m}{2M} \alpha_{\ell s} \right) - c_{\text{F}}^{(e)} c_{\text{F}}^{(n)} \right], & \text{for } j = \ell + 1 \\ -2 \left( \alpha_{\ell S} + \frac{\Delta m}{2M} \alpha_{\ell s} \right) + c_{\text{F}}^{(e)} c_{\text{F}}^{(n)}, & \text{for } j = \ell \\ -\frac{\ell+1}{2\ell-1} \left[ 2(2\ell-1) \left( \alpha_{\ell S} + \frac{\Delta m}{2M} \alpha_{\ell s} \right) + c_{\text{F}}^{(e)} c_{\text{F}}^{(n)} \right], & \text{for } j = \ell - 1 \end{cases} \quad (\text{E3})$$

and the low-energy Wilson coefficients  $\alpha_v$  are given in Table II. Hence, the first-order energy shift depends on quantum numbers  $n, j, \ell$ , and  $S$ , but not on  $m_j$ .

- |  |   |
|--|---|
| <p>[1] F. Wilczek, Quantum field theory, <i>Rev. Mod. Phys.</i> <b>71</b>, S85 (1999).</p> <p>[2] M. Tanabashi <i>et al.</i> (Particle Data Group), Review of particle physics, <i>Phys. Rev. D</i> <b>98</b>, 030001 (2018).</p> <p>[3] M. E. Peskin and D. V. Schroeder, <i>An introduction to quantum field theory</i>, Frontiers in Physics (Addison-Wesley, Reading, 1995).</p> <p>[4] S. Giorgini, L. P. Pitaevskii, and S. Stringari, Theory of ultracold atomic Fermi gases, <i>Rev. Mod. Phys.</i> <b>80</b>, 1215 (2008).</p> <p>[5] M. A. Baranov, Theoretical progress in many-body physics with ultracold dipolar gases, <i>Phys. Rep.</i> <b>464</b>, 71 (2008).</p> <p>[6] W. E. Caswell and G. P. Lepage, Effective Lagrangians for bound state problems in QED, QCD, and other field theories, <i>Phys. Lett. B</i> <b>167</b>, 437 (1986).</p> | <p>[7] T. Kinoshita and M. Nio, Radiative corrections to the muonium hyperfine structure: The <math>\alpha^2(Z\alpha)</math> correction, <i>Phys. Rev. D</i> <b>53</b>, 4909 (1996).</p> <p>[8] A. V. Manohar, Heavy quark effective theory and nonrelativistic QCD Lagrangian to order <math>\alpha_s/m^3</math>, <i>Phys. Rev. D</i> <b>56</b>, 230 (1997).</p> <p>[9] A. S. Parkins and D. F. Walls, The physics of trapped dilute-gas Bose-Einstein condensates, <i>Phys. Rep.</i> <b>303</b>, 1 (1998).</p> <p>[10] Y. Kawaguchi and M. Ueda, Spinor Bose-Einstein condensates, <i>Phys. Rep.</i> <b>520</b>, 253 (2012).</p> <p>[11] E. H. Wichmann and N. M. Kroll, Vacuum polarization in a strong Coulomb field, <i>Phys. Rev.</i> <b>101</b>, 843 (1956).</p> <p>[12] G. E. Brown and D. F. Mayers, Lamb shift of a tightly bound electron. II. Calculation for the K-electron in mercury, <i>Proc. R. Soc. A</i> <b>251</b>, 105 (1959).</p> |
|--|---|

- [13] P. J. Mohr, Self-energy radiative corrections in hydrogen-like systems, *Ann. Phys.* **88**, 26 (1974).
- [14] U. D. Jentschura, P. J. Mohr, and G. Soff, Calculation of the electron self-energy for low nuclear charge, *Phys. Rev. Lett.* **82**, 53 (1999).
- [15] G. Paz, The charge radius of the proton, *AIP Conf. Proc.* **1441**, 146 (2012).
- [16] M. Sonnleitner and S. M. Barnett, Mass-energy and anomalous friction in quantum optics, *Phys. Rev. A* **98**, 042106 (2018).
- [17] P. K. Schwartz and D. Giulini, Post-Newtonian Hamiltonian description of an atom in a weak gravitational field, *Phys. Rev. A* **100**, 052116 (2019).
- [18] V. Yudin and A. Taichenachev, Mass defect effects in atomic clocks, *Laser Phys. Lett.* **15**, 035703 (2018).
- [19] G. Paz, An introduction to NRQED, *Mod. Phys. Lett. A* **30**, 1550128 (2015).
- [20] N. H. Bings, A. Bogaerts, and J. A. C. Broekaert, Atomic spectroscopy: A review, *Anal. Chem.* **82**, 4653 (2010).
- [21] M. Ueda, *Fundamentals and new frontiers of Bose-Einstein condensation* (World Scientific, Singapore, 2010).
- [22] V. J. Martínez-Lahuerta, S. Eilers, T. E. Mehlstäubler, P. O. Schmidt, and K. Hammerer, Ab initio quantum theory of mass defect and time dilation in trapped-ion optical clocks, *Phys. Rev. A* **106**, 032803 (2022).
- [23] S. Sinha and J. Samuel, Atom interferometry and the gravitational redshift, *Class. Quantum Gravity* **28**, 145018 (2011).
- [24] M. Zych, F. Costa, I. Pikovski, and Č. Brukner, Quantum interferometric visibility as a witness of general relativistic proper time, *Nat. Commun.* **2**, 505 (2011).
- [25] I. Pikovski, M. Zych, F. Costa, and Č. Brukner, Time dilation in quantum systems and decoherence, *New J. Phys.* **19**, 025011 (2017) and references therein.
- [26] S. Loriani, A. Friedrich, C. Ufrecht, F. Di Pumpo, S. Kleintert, S. Abend, N. Gaaloul, C. Meiners, C. Schubert, D. Tell, É. Wodey, M. Zych, W. Ertmer, A. Roura, D. Schlippert, W. P. Schleich, E. M. Rasel, and E. Giese, Interference of clocks: A quantum twin paradox, *Sci. Adv.* **5**, eaax8966 (2019).
- [27] A. Derevianko and M. Pospelov, Hunting for topological dark matter with atomic clocks, *Nat. Phys.* **10**, 933 (2014).
- [28] A. Arvanitaki, J. Huang, and K. Van Tilburg, Searching for dilaton dark matter with atomic clocks, *Phys. Rev. D* **91**, 015015 (2015).
- [29] A. Arvanitaki, P. W. Graham, J. M. Hogan, S. Rajendran, and K. Van Tilburg, Search for light scalar dark matter with atomic gravitational wave detectors, *Phys. Rev. D* **97**, 075020 (2018).
- [30] C. Ufrecht, F. Di Pumpo, A. Friedrich, A. Roura, C. Schubert, D. Schlippert, E. M. Rasel, W. P. Schleich, and E. Giese, Atom-interferometric test of the universality of gravitational redshift and free fall, *Phys. Rev. Research* **2**, 043240 (2020).
- [31] A. Roura, Gravitational redshift in quantum-clock interferometry, *Phys. Rev. X* **10**, 021014 (2020).
- [32] F. Di Pumpo, C. Ufrecht, A. Friedrich, E. Giese, W. P. Schleich, and W. G. Unruh, Gravitational redshift tests with atomic clocks and atom interferometers, *PRX Quantum* **2**, 040333 (2021).
- [33] F. Di Pumpo, A. Friedrich, A. Geyer, C. Ufrecht, and E. Giese, Light propagation and atom interferometry in gravity and dilaton fields, *Phys. Rev. D* **105**, 084065 (2022).
- [34] F. Di Pumpo, A. Friedrich, C. Ufrecht, and E. Giese, Universality-of-clock-rates test using atom interferometry with  $T^3$  scaling, *Phys. Rev. D* **107**, 064007 (2023).
- [35] A. Pineda and J. Soto, The Lamb shift in dimensional regularisation, *Phys. Lett. B* **420**, 391 (1998).
- [36] A. Pineda and J. Soto, Effective field theory for ultrasoft momenta in NRQCD and NRQED, *Nucl. Phys. B, Proc. Suppl.* **64**, 428 (1998).
- [37] A. Pineda and J. Soto, Potential NRQED: The positronium case, *Phys. Rev. D* **59**, 016005 (1998).
- [38] M. Combescot, O. Betbeder-Matibet, and F. Dubin, The many-body physics of composite bosons, *Phys. Rep.* **463**, 215 (2008).
- [39] M. Combescot and O. Betbeder-Matibet, General many-body formalism for composite quantum particles, *Phys. Rev. Lett.* **104**, 206404 (2010).
- [40] E. A. Power and S. Zienau, Coulomb gauge in non-relativistic quantum electro-dynamics and the shape of spectral lines, *Phil. Trans. R. Soc. A* **251**, 424 (1959).
- [41] R. G. Woolley, Molecular quantum electrodynamics, *Proc. R. Soc. A* **321**, 557 (1971).
- [42] E. P. Gross, Structure of a quantized vortex in boson systems, *Nuovo Cimento (1955-1965)* **20**, 454 (1961).
- [43] L. P. Pitaevskii, Vortex lines in an imperfect Bose gas, *Sov. Phys. JETP* **13**, 451 (1961).
- [44] We omit the composite-particle nature of the nucleus in its dynamical description by treating it as a single fermionic field. The composite-particle nature of the nucleus may be taken into account by deriving an effective QFT in the same spirit. However, nondynamical composite-particles effects are included in prefactors, as detailed later.
- [45] M. Nio and T. Kinoshita, Radiative corrections to the muonium hyperfine structure. II. The  $\alpha(Z\alpha)^2$  correction, *Phys. Rev. D* **55**, 7267 (1997).
- [46] M. Haidar, Z.-X. Zhong, V. I. Korobov, and J.-P. Karr, Non-relativistic QED approach to the fine- and hyperfine-structure corrections of order  $m\alpha^6$  and  $m\alpha^6(m/M)$ : Application to the hydrogen atom, *Phys. Rev. A* **101**, 022501 (2020).
- [47] L. L. Foldy and S. A. Wouthuysen, On the Dirac theory of spin 1/2 particles and its non-relativistic limit, *Phys. Rev.* **78**, 29 (1950).
- [48] K. G. Wilson, Model Hamiltonians for local quantum field theory, *Phys. Rev.* **140**, B445 (1965).
- [49] K. G. Wilson and J. Kogut, The renormalization group and the  $\epsilon$  expansion, *Phys. Rep.* **12**, 75 (1974).
- [50] J. Schwinger, On quantum-electrodynamics and the magnetic moment of the electron, *Phys. Rev.* **73**, 416 (1948).
- [51] S. Laporta and E. Remiddi, The analytical value of the electron  $(g - 2)$  at order  $\alpha^3$  in QED, *Phys. Lett. B* **379**, 283 (1996).
- [52] T. Aoyama, M. Hayakawa, T. Kinoshita, and M. Nio, Tenth-order QED contribution to the electron  $g-2$  and an improved value of the fine structure constant, *Phys. Rev. Lett.* **109**, 111807 (2012).
- [53] R. J. Hill, G. Lee, G. Paz, and M. P. Solon, NRQED Lagrangian at order  $1/M^4$ , *Phys. Rev. D* **87**, 053017 (2013).
- [54] The following form of the Hamiltonian density follows from the flat spacetime Minkowski metric  $\eta_{\mu,\nu} = \text{diag}(+1, -1, -1, -1)$ .
- [55] C. Peset, A. Pineda, and O. Tomalak, The proton radius (puzzle?) and its relatives, *Prog. Part. Nucl. Phys.* **121**, 103901 (2021).
- [56] A. Pineda and J. Soto, Matching at one loop for the four-quark operators in NRQCD, *Phys. Rev. D* **58**, 114011 (1998).
- [57] We use for convenience  $c$  to specify the order, but since  $c$  is connected to other fundamental constants, it is more precise to fix it to  $\alpha/c$  or equivalently  $1/(\epsilon_0 c^2)$ .
- [58] N. Brambilla, A. Pineda, J. Soto, and A. Vairo, Potential NRQCD: An effective theory for heavy quarkonium, *Nucl. Phys. B* **566**, 275 (2000).
- [59] G. S. Adkins, Higher order corrections to positronium energy levels, *J. Phys. Conf. Ser.* **1138**, 012005 (2018).
- [60] G. Breit, The effect of retardation on the interaction of two electrons, *Phys. Rev.* **34**, 553 (1929).
- [61] G. Breit, The fine structure of HE as a test of the spin interactions

- of two electrons, *Phys. Rev.* **36**, 383 (1930).
- [62] G. Breit, Dirac's equation and the spin-spin interactions of two electrons, *Phys. Rev.* **39**, 616 (1932).
- [63] In Lorenz gauge the EM four potential may be quantized with respect to a weaker Lorenz-gauge condition in the spirit of Gupta and Bleuler [269, 270] or with the help of BRST quantization [271, 272].
- [64] H. A. Bethe, The electromagnetic shift of energy levels, *Phys. Rev.* **72**, 339 (1947).
- [65] W. E. Lamb and R. C. Retherford, Fine structure of the hydrogen atom by a microwave method, *Phys. Rev.* **72**, 241 (1947).
- [66] Dropping the scalar potential implies that higher order scalar photons become inaccessible. But when moving to the next order,  $\hat{H}_{f-f}$  has to be redetermined anyway for a consistent treatment.
- [67] T. D. Lee, K. Huang, and C. N. Yang, Eigenvalues and eigenfunctions of a Bose system of hard spheres and its low-temperature properties, *Phys. Rev.* **106**, 1135 (1957).
- [68] T. D. Lee and C. N. Yang, Low-temperature behavior of a dilute Bose system of hard spheres. I. Equilibrium properties, *Phys. Rev.* **112**, 1419 (1958).
- [69] T. T. Wu, Ground state of a Bose system of hard spheres, *Phys. Rev.* **115**, 1390 (1959).
- [70] For simplicity we defined the distance between cobosons with respect to the nucleus coordinate, even though center-of-mass distances are physically more precise. However, both are equivalent by replacing  $b$  by  $b' = b + a$ .
- [71] A. Rivas and S. F. Huelga, *Open quantum systems* (Springer, Berlin, 2012).
- [72] J. Wurtz, P. W. Claeys, and A. Polkovnikov, Variational Schrieffer-Wolff transformations for quantum many-body dynamics, *Phys. Rev. B* **101**, 014302 (2020).
- [73] M. Lewenstein, L. You, J. Cooper, and K. Burnett, Quantum field theory of atoms interacting with photons: Foundations, *Phys. Rev. A* **50**, 2207 (1994).
- [74] R. A. Krajcik and L. L. Foldy, Relativistic center-of-mass variables for composite systems with arbitrary internal interactions, *Phys. Rev. D* **10**, 1777 (1974).
- [75] M. K. Liou, Relativistic center-of-mass variables and relativistic corrections to phenomenological Hamiltonians, *Phys. Rev. D* **9**, 1091 (1974).
- [76] R. G. Woolley, Power-Zienau-Woolley representations of non-relativistic QED for atoms and molecules, *Phys. Rev. Research* **2**, 013206 (2020).
- [77] R. A. Krajcik and L. L. Foldy, Electromagnetic interactions with an arbitrary loosely bound system, *Phys. Rev. Lett.* **24**, 545 (1970).
- [78] F. E. Close and H. Osborn, Relativistic center-of-mass motion and the electromagnetic interaction of systems of charged particles, *Phys. Rev. D* **2**, 2127 (1970).
- [79] C. Baxter, M. Babiker, and R. Loudon, Canonical approach to photon pressure, *Phys. Rev. A* **47**, 1278 (1993).
- [80] C. Cohen-Tanoudji, B. Diu, and F. Laloë, *Quantum Mechanics*, Vol. 1 (Wiley & Sons, New York, 1965).
- [81] M. Wilkens, Spurious velocity dependence of free-space spontaneous emission, *Phys. Rev. A* **47**, 671 (1993).
- [82] M. Wilkens, Significance of Röntgen current in quantum optics: Spontaneous emission of moving atoms, *Phys. Rev. A* **49**, 570 (1994).
- [83] L. G. Boussiakou, C. R. Bennett, and M. Babiker, Quantum theory of spontaneous emission by real moving atoms, *Phys. Rev. Lett.* **89**, 123001 (2002).
- [84] M. Sonnleitner and S. M. Barnett, The Röntgen interaction and forces on dipoles in time-modulated optical fields, *Eur. Phys. J. D* **71**, 336 (2017).
- [85] R. Lopp and E. Martín-Martínez, Quantum delocalization, gauge, and quantum optics: Light-matter interaction in relativistic quantum information, *Phys. Rev. A* **103**, 013703 (2021).
- [86] L. I. Schiff and H. Snyder, Theory of the quadratic Zeeman Effect, *Phys. Rev.* **55**, 59 (1939).
- [87] A. Vukics, T. Griebner, and P. Domokos, Fundamental limitation of ultrastrong coupling between light and atoms, *Phys. Rev. A* **92**, 043835 (2015).
- [88] K. Góral, K. Rzażewski, and T. Pfau, Bose-Einstein condensation with magnetic dipole-dipole forces, *Phys. Rev. A* **61**, 051601 (2000).
- [89] A. J. Olson, D. L. Whitenack, and Y. P. Chen, Effects of magnetic dipole-dipole interactions in atomic Bose-Einstein condensates with tunable  $s$ -wave interactions, *Phys. Rev. A* **88**, 043609 (2013).
- [90] R. Friedberg, S. R. Hartmann, and J. T. Manassah, Frequency shifts in emission and absorption by resonant systems of two-level atoms, *Phys. Rep.* **7**, 101 (1973).
- [91] M. O. Scully, Collective Lamb shift in single photon Dicke superradiance, *Phys. Rev. Lett.* **102**, 143601 (2009).
- [92] A. O. Barut and W. Rasmussen, The hydrogen atom as a relativistic elementary particle. I. The wave equation and mass formulae, *J. Phys. B* **6**, 1695 (1973).
- [93] A. O. Barut and G. L. Strobil, Center-of-mass motion of a system of relativistic Dirac particles, *Few-Body Syst.* **1**, 167 (1986).
- [94] S. R. De Groot and C. A. Ten Seldam, On the energy levels of a model of the compressed hydrogen atom, *Physica* **12**, 669 (1946).
- [95] D. Suryanarayana and J. A. Weil, On the hyperfine splitting of the hydrogen atom in a spherical box, *J. Chem. Phys.* **64**, 510 (1976).
- [96] E. Ley-Koo and S. Rubinstein, The hydrogen atom within spherical boxes with penetrable walls, *J. Chem. Phys.* **71**, 351 (1979).
- [97] J. L. Marín and S. A. Cruz, Enclosed quantum systems: Use of the direct variational method, *J. Phys. B* **24**, 2899 (1991).
- [98] N. Aquino, Accurate energy eigenvalues for enclosed hydrogen atom within spherical impenetrable boxes, *Int. J. Quantum Chem.* **54**, 107 (1995).
- [99] J. L. Marín, R. Rosas, and A. Uribe, Analysis of asymmetric confined quantum systems by the direct variational method, *Am. J. Phys.* **63**, 460 (1995).
- [100] Y. P. Varshni, Accurate wavefunctions for the confined hydrogen atom at high pressures, *J. Phys. B* **30**, L589 (1997).
- [101] N. Aquino, G. Campoy, and H. E. Montgomery Jr., Highly accurate solutions for the confined hydrogen atom, *Int. J. Quantum Chem.* **107**, 1548 (2007).
- [102] F. M. Fernández, The confined hydrogen atom with a moving nucleus, *Eur. J. Phys.* **31**, 285 (2009).
- [103] N. Aquino and R. A. Rojas, The confined hydrogen atom: A linear variational approach, *Eur. J. Phys.* **37**, 015401 (2015).
- [104] C. Laughlin, B. L. Burrows, and M. Cohen, A hydrogen-like atom confined within an impenetrable spherical box, *J. Phys. B* **35**, 701 (2002).
- [105] C. A. Ten Seldam and S. R. De Groot, On the ground state of a model for compressed helium, *Physica* **18**, 891 (1952).
- [106] W. Jaskólski, Confined many-electron systems, *Phys. Rep.* **271**, 1 (1996).
- [107] J. Garza, R. Vargas, and A. Vela, Numerical self-consistent-field method to solve the Kohn-Sham equations in confined many-electron atoms, *Phys. Rev. E* **58**, 3949 (1998).
- [108] J. Garza, R. Vargas, N. Aquino, and K. D. Sen, DFT reactivity

- indices in confined many-electron atoms, *J. Chem. Sci.* **117**, 379 (2005).
- [109] L. G. Boussiakou, C. R. Bennett, and M. Babiker, Electrodynamics of Bose-Einstein condensates in angular motion, *J. Opt. B* **4**, S25 (2002).
- [110] E. L. Raab, M. Prentiss, A. Cable, S. Chu, and D. E. Pritchard, Trapping of neutral sodium atoms with radiation pressure, *Phys. Rev. Lett.* **59**, 2631 (1987).
- [111] A. M. Steane and C. J. Foot, Laser cooling below the Doppler limit in a magneto-optical trap, *Europhys. Lett.* **14**, 231 (1991).
- [112] A. M. Steane, M. Chowdhury, and C. J. Foot, Radiation force in the magneto-optical trap, *J. Opt. Soc. Am. B* **9**, 2142 (1992).
- [113] M. Gajda and J. Mostowski, Three-dimensional theory of the magneto-optical trap: Doppler cooling in the low-intensity limit, *Phys. Rev. A* **49**, 4864 (1994).
- [114] W. Paul, Electromagnetic traps for charged and neutral particles, *Rev. Mod. Phys.* **62**, 531 (1990).
- [115] L. S. Brown, Quantum motion in a Paul trap, *Phys. Rev. Lett.* **66**, 527 (1991).
- [116] G. Baumann, The Paul trap: A completely integrable model?, *Phys. Lett. A* **162**, 464 (1992).
- [117] I. A. Pedrosa, A. Rosas, and I. Guedes, Exact quantum motion of a particle trapped by oscillating fields, *J. Phys. A: Math. and Gen.* **38**, 7757 (2005).
- [118] F. M. Penning, Die glimmentladung bei niedrigem druck zwischen koaxialen zylindern in einem axialen magnetfeld, *Physica* **3**, 873 (1936).
- [119] M. Kretzschmar, Particle motion in a Penning trap, *Eur. J. Phys.* **12**, 240 (1991).
- [120] K. Blaum, Y. N. Novikov, and G. Werth, Penning traps as a versatile tool for precise experiments in fundamental physics, *Contemp. Phys.* **51**, 149 (2010).
- [121] M. Vogel, *Particle Confinement in Penning Traps*, Springer Series on Atomic, Optical, and Plasma Physics (Springer, Cham, 2018).
- [122] D. M. Giltner, R. W. McGowan, and S. A. Lee, Atom interferometer based on Bragg scattering from standing light waves, *Phys. Rev. Lett.* **75**, 2638 (1995).
- [123] H. Müller, S.-W. Chiow, Q. Long, S. Herrmann, and S. Chu, Atom interferometry with up to 24-photon-momentum-transfer beam splitters, *Phys. Rev. Lett.* **100**, 180405 (2008).
- [124] P. A. Altin, M. T. Johnsson, V. Negnevitsky, G. R. Dennis, R. P. Anderson, J. E. Debs, S. S. Szigeti, K. S. Hardman, S. Bennetts, G. D. McDonald, L. D. Turner, J. D. Close, and N. P. Robins, Precision atomic gravimeter based on Bragg diffraction, *New J. Phys.* **15**, 023009 (2013).
- [125] F. Bloch, Über die Quantenmechanik der Elektronen in Kristallgittern, *Z. Phys.* **52**, 555 (1929).
- [126] G. H. Wannier, Wave functions and effective Hamiltonian for Bloch electrons in an electric field, *Phys. Rev.* **117**, 432 (1960).
- [127] M. Ben Dahan, E. Peik, J. Reichel, Y. Castin, and C. Salomon, Bloch oscillations of atoms in an optical potential, *Phys. Rev. Lett.* **76**, 4508 (1996).
- [128] S. R. Wilkinson, C. F. Bharucha, K. W. Madison, Q. Niu, and M. G. Raizen, Observation of atomic Wannier-Stark ladders in an accelerating optical potential, *Phys. Rev. Lett.* **76**, 4512 (1996).
- [129] P. Cladé, S. Guellati-Khélifa, F. Nez, and F. Biraben, Large momentum beam splitter using Bloch oscillations, *Phys. Rev. Lett.* **102**, 240402 (2009).
- [130] Z. Pagel, W. Zhong, R. H. Parker, C. T. Olund, N. Y. Yao, and H. Müller, Symmetric Bloch oscillations of matter waves, *Phys. Rev. A* **102**, 053312 (2020).
- [131] L. Hu, N. Poli, L. Salvi, and G. M. Tino, Atom interferometry with the Sr optical clock transition, *Phys. Rev. Lett.* **119**, 263601 (2017).
- [132] J. Rudolph, T. Wilkason, M. Nantel, H. Swan, C. M. Holland, Y. Jiang, B. E. Garber, S. P. Carman, and J. M. Hogan, Large momentum transfer clock atom interferometry on the 689 nm intercombination line of strontium, *Phys. Rev. Lett.* **124**, 083604 (2020).
- [133] H. Feshbach, Unified theory of nuclear reactions, *Ann. Phys.* **5**, 357 (1958).
- [134] H. Feshbach, A unified theory of nuclear reactions. II, *Ann. Phys.* **19**, 287 (1962).
- [135] U. Fano, Effects of configuration interaction on intensities and phase shifts, *Phys. Rev.* **124**, 1866 (1961).
- [136] A. J. Moerdijk, B. J. Verhaar, and A. Axelsson, Resonances in ultracold collisions of  ${}^6\text{Li}$ ,  ${}^7\text{Li}$ , and  ${}^{23}\text{Na}$ , *Phys. Rev. A* **51**, 4852 (1995).
- [137] C. Chin, R. Grimm, P. Julienne, and E. Tiesinga, Feshbach resonances in ultracold gases, *Rev. Mod. Phys.* **82**, 1225 (2010).
- [138] L. N. Labzowsky, A. V. Shonin, and D. A. Solov'yev, QED calculation of E1M1 and E1E2 transition probabilities in one-electron ions with arbitrary nuclear charge, *J. Phys. B* **38**, 265 (2005).
- [139] L. Labzowsky, D. Solov'yev, G. Plunien, and G. Soff, Two-photon E1M1 and E1E2 transitions between 2p and 1s levels in hydrogen, *Eur. Phys. J. D* **37**, 335 (2006).
- [140] G. Janson, *Doppler-free two-photon transitions in atom interferometry*, Master's thesis, Ulm university (2021).
- [141] E. Jaynes and F. Cummings, Comparison of quantum and semiclassical radiation theories with application to the beam maser, *Proc. IEEE* **51**, 89 (1963).
- [142] W. P. Schleich, D. M. Greenberger, and E. M. Rasel, A representation-free description of the Kasevich-Chu interferometer: A resolution of the redshift controversy, *New J. Phys.* **15**, 013007 (2013).
- [143] J. Seke, Analytic evaluation of exact transition matrix elements in nonrelativistic hydrogenic atoms, *Physica A* **203**, 269 (1994).
- [144] A. D. Ludlow, M. M. Boyd, J. Ye, E. Peik, and P. O. Schmidt, Optical atomic clocks, *Rev. Mod. Phys.* **87**, 637 (2015).
- [145] D. A. Steck, *Atom and quantum optics notes (course notes)*.
- [146] H. Grotch and R. Kashuba, External electromagnetic interactions of hydrogenic atoms and Galilean invariance, *Phys. Rev. A* **5**, 527 (1972).
- [147] E. Kajari, N. L. Harshman, E. M. Rasel, S. Stenholm, G. Süßmann, and W. P. Schleich, Inertial and gravitational mass in quantum mechanics, *Appl. Phys. B* **100**, 43 (2010).
- [148] C. Lämmerzahl, A Hamilton operator for quantum optics in gravitational fields, *Phys. Lett. A* **203**, 12 (1995).
- [149] T. R. Perche and J. Neuser, A wavefunction description for a localized quantum particle in curved spacetimes, *Class. Quantum Gravity* **38**, 175002 (2021).
- [150] A. R. H. Smith and M. Ahmadi, Quantum clocks observe classical and quantum time dilation, *Nat. Commun.* **11**, 5360 (2020).
- [151] I. Pikovski, M. Zych, C. F., and Č. Brukner, Universal decoherence due to gravitational time dilation, *Nat. Phys.* **11**, 668 (2015).
- [152] M. Zych, I. Pikovski, F. Costa, and Č. Brukner, General relativistic effects in quantum interference of "clocks", *J. Phys. Conf. Ser.* **723**, 012044 (2016).
- [153] P. A. Bushev, J. H. Cole, D. Sholokhov, N. Kukharchyk, and M. Zych, Single electron relativistic clock interferometer, *New J. Phys.* **18**, 093050 (2016).
- [154] R. J. Hill and G. Paz, Model independent analysis of proton structure for hydrogenic bound states, *Phys. Rev. Lett.* **107**,

- 160402 (2011).
- [155] P. Hoyer, *Journey to the bound states* (Springer, Cham, 2021).
- [156] P. Hoyer, Fermion bound states by the method of stationary phase, *Phys. Scr.* **30**, 29 (1984).
- [157] P. Hoyer, Fock expansion for QED bound states, *Int. J. Mod. Phys. A* **04**, 4535 (1989).
- [158] M. Järvinen, Hydrogen atom in relativistic motion, *Phys. Rev. D* **71**, 085006 (2005).
- [159] I. Lindgren, S. Salomonson, and B. Åsén, The covariant-evolution-operator method in bound-state QED, *Phys. Rep.* **389**, 161 (2004).
- [160] E. E. Salpeter, Wave functions in momentum space, *Phys. Rev.* **84**, 1226 (1951).
- [161] E. E. Salpeter and H. A. Bethe, A relativistic equation for bound-state problems, *Phys. Rev.* **84**, 1232 (1951).
- [162] R. E. Cutkosky, Solutions of a Bethe-Salpeter equation, *Phys. Rev.* **96**, 1135 (1954).
- [163] N. Nakanishi, A general survey of the theory of the Bethe-Salpeter equation, *Prog. Theor. Phys. Suppl.* **43**, 1 (1969).
- [164] S. Floerchinger, Exact flow equation for bound states, *Eur. Phys. J. C* **69**, 119 (2010).
- [165] R. Alkofer, A. Maas, W. A. Mian, M. Mitter, J. París-López, J. M. Pawłowski, and N. Wink, Bound state properties from the functional renormalization group, *Phys. Rev. D* **99**, 054029 (2019).
- [166] A. Jakovác and A. Patkós, Bound states in functional renormalization group, *Int. J. Mod. Phys. A* **34**, 1950154 (2019).
- [167] K. Pachucki, Effective Hamiltonian approach to the bound state: Positronium hyperfine structure, *Phys. Rev. A* **56**, 297 (1997).
- [168] P. Labelle, S. M. Zebarjad, and C. P. Burgess, Nonrelativistic QED and next-to-leading hyperfine splitting in positronium, *Phys. Rev. D* **56**, 8053 (1997).
- [169] A. Czarnecki, K. Melnikov, and A. Yelkhovsky, Positronium S-state spectrum: Analytic results at  $O(m\alpha^6)$ , *Phys. Rev. A* **59**, 4316 (1999).
- [170] B. A. Kniehl and A. A. Penin, Order  $\alpha^7 \ln(1/\alpha)$  contribution to positronium hyperfine splitting, *Phys. Rev. Lett.* **85**, 5094 (2000).
- [171] C. Peset, Effective field theories for muonic hydrogen, *EPJ Web Conf.* **137**, 08013 (2017).
- [172] U. D. Jentschura, A. Czarnecki, and K. Pachucki, Nonrelativistic QED approach to the Lamb shift, *Phys. Rev. A* **72**, 062102 (2005).
- [173] C. Peset and A. Pineda, Model-independent determination of the Lamb shift in muonic hydrogen and the proton radius, *Eur. Phys. J. A* **51**, 32 (2015).
- [174] C. Peset and A. Pineda, The Lamb shift in muonic hydrogen and the proton radius from effective field theories, *Eur. Phys. J. A* **51**, 156 (2015).
- [175] R. Lange, N. Huntemann, J. M. Rahm, C. Sanner, H. Shao, B. Lipphardt, C. Tamm, S. Weyers, and E. Peik, Improved limits for violations of local position invariance from atomic clock comparisons, *Phys. Rev. Lett.* **126**, 011102 (2021).
- [176] A. Banerjee, D. Budker, M. Filzinger, N. Huntemann, G. Paz, G. Perez, S. Porsev, and M. Safronova, Oscillating nuclear charge radii as sensors for ultralight dark matter (2023), [arXiv:2301.10784 \[hep-ph\]](https://arxiv.org/abs/2301.10784).
- [177] E. Braaten, M. Kusunoki, and D. Zhang, Scattering models for ultracold atoms, *Ann. Phys.* **323**, 1770 (2008).
- [178] P. F. Bedaque, E. Braaten, and H.-W. Hammer, Three-body recombination in Bose gases with large scattering length, *Phys. Rev. Lett.* **85**, 908 (2000).
- [179] F. London, The general theory of molecular forces, *Trans. Faraday Soc.* **33**, 8b (1937).
- [180] B. R. Holstein, The van der Waals interaction, *Am. J. Phys.* **69**, 441 (2001).
- [181] L. Béguin, A. Vernier, R. Chicireanu, T. Lahaye, and A. Browaeys, Direct measurement of the van der Waals interaction between two Rydberg atoms, *Phys. Rev. Lett.* **110**, 263201 (2013).
- [182] P. Barcellona, R. Passante, L. Rizzuto, and S. Y. Buhmann, van der Waals interactions between excited atoms in generic environments, *Phys. Rev. A* **94**, 012705 (2016).
- [183] K. T. Tang and J. P. Toennies, An improved simple model for the van der Waals potential based on universal damping functions for the dispersion coefficients, *J. Chem. Phys.* **80**, 3726 (1984).
- [184] K. T. Tang and J. P. Toennies, The van der Waals potentials between all the rare gas atoms from He to Rn, *J. Chem. Phys.* **118**, 4976 (2003).
- [185] M. Kamiya, T. Tsuneda, and K. Hirao, A density functional study of van der Waals interactions, *J. Chem. Phys.* **117**, 6010 (2002).
- [186] N. Kurita and H. Sekino, Ab initio and DFT studies for accurate description of van der Waals interaction between He atoms, *Chem. Phys. Lett.* **348**, 139 (2001).
- [187] Y. Y. Sun, Y.-H. Kim, K. Lee, and S. B. Zhang, Accurate and efficient calculation of van der Waals interactions within density functional theory by local atomic potential approach, *J. Chem. Phys.* **129**, 154102 (2008).
- [188] K. Berland, V. R. Cooper, K. Lee, E. Schröder, T. Thonhauser, P. Hyldgaard, and B. I. Lundqvist, van der Waals forces in density functional theory: A review of the vdW-DF method, *Rep. Prog. Phys.* **78**, 066501 (2015).
- [189] J. Tao, J. P. Perdew, and A. Ruzsinszky, Accurate van der Waals coefficients from density functional theory, *Proc. Natl. Acad. Sci. U.S.A.* **109**, 18 (2012).
- [190] T. Koga and S. Matsumoto, An exact solution of the van der Waals interaction between two ground-state hydrogen atoms, *J. Chem. Phys.* **82**, 5127 (1985).
- [191] M. O'Carroll and J. Sucher, Exact computation of the van der Waals constant for two hydrogen atoms, *Phys. Rev. Lett.* **21**, 1143 (1968).
- [192] J. J. Sakurai and J. Napolitano, *Modern quantum mechanics* (Cambridge University Press, Cambridge, 2020).
- [193] G. W. Parker, Derivation of the electric dipole-dipole interaction as an electric hyperfine interaction, *Am. J. Phys.* **54**, 715 (1986).
- [194] A. M. Ishkhanyan and V. P. Krainov, Van der Waals attraction of hydrogen atoms, *J. Exp. Theor. Phys.* **132**, 892 (2021).
- [195] J. E. Lennard-Jones, Cohesion, *Proc. Phys. Soc.* **43**, 461 (1931).
- [196] N. Brambilla, V. Shtabovenko, J. Tarrús Castellà, and A. Vairo, Effective field theories for van der Waals interactions, *Phys. Rev. D* **95**, 116004 (2017).
- [197] D. Odell, A. Deltuva, and L. Platter, van der Waals interaction as the starting point for an effective field theory, *Phys. Rev. A* **104**, 023306 (2021).
- [198] Y. S. Kim and R. G. Gordon, Ion-rare gas interactions on the repulsive part of the potential curves, *J. Chem. Phys.* **60**, 4323 (1974).
- [199] Y. S. Kim and R. G. Gordon, Ion-ion interaction potentials and their application to the theory of alkali halide and alkaline earth dihalide molecules, *J. Chem. Phys.* **60**, 4332 (1974).
- [200] F. Bloch, On the magnetic scattering of neutrons, *Phys. Rev.* **50**, 259 (1936).
- [201] F. Bloch, On the magnetic scattering of neutrons. II, *Phys. Rev.* **51**, 994 (1937).
- [202] J. S. Schwinger, On the magnetic scattering of neutrons, *Phys. Rev.* **51**, 544 (1937).
- [203] G. T. Trammell, Magnetic scattering of neutrons from rare earth

- ions, *Phys. Rev.* **92**, 1387 (1953).
- [204] V. Franco and B. Dodrill, *Magnetic Measurement Techniques for Materials Characterization* (Springer, Cham, 2021).
- [205] D. M. Stamper-Kurn and M. Ueda, Spinor Bose gases: Symmetries, magnetism, and quantum dynamics, *Rev. Mod. Phys.* **85**, 1191 (2013).
- [206] S. N. Bose, Plancks Gesetz und Lichtquantenhypothese, *Z. Phys.* **26**, 178 (1924).
- [207] A. Einstein, Quantentheorie des einatomigen idealen Gases, Sitzber. Kgl. Preuss. Akad. Wiss., 261 (1924).
- [208] A. Einstein, Quantentheorie des einatomigen idealen Gases. zweite abhandlung, Sitzber. Kgl. Preuss. Akad. Wiss., 3 (1924).
- [209] I. V. Lukin, A. G. Sotnikov, and Y. V. Slyusarenko, Aspects of Bose-Einstein condensation in a charged boson system over the dielectric surface, *Phys. Lett. A* **417**, 127695 (2021).
- [210] E. R. Christensen, A. Camacho-Guardian, and G. M. Bruun, Charged polarons and molecules in a Bose-Einstein condensate, *Phys. Rev. Lett.* **126**, 243001 (2021).
- [211] M. F. M. Osborne, The Bose-Einstein condensation for charged particles in a magnetic field, *Phys. Rev.* **76**, 400 (1949).
- [212] L. L. Foldy, Charged boson gas, *Phys. Rev.* **124**, 649 (1961).
- [213] M. Girardeau, Ground state of the charged Bose gas, *Phys. Rev.* **127**, 1809 (1962).
- [214] B. W. Ninham, Charged Bose gas, *Nucl. Phys.* **53**, 685 (1964).
- [215] D. Wright, Ground-state energy of the charged Bose gas, *Phys. Rev.* **143**, 91 (1966).
- [216] K. Huang and C. N. Yang, Quantum-mechanical many-body problem with hard-sphere interaction, *Phys. Rev.* **105**, 767 (1957).
- [217] E. P. Gross, Hydrodynamics of a superfluid condensate, *J. Math. Phys.* **4**, 195 (2004).
- [218] N. P. Proukakis, Beyond Gross-Pitaevskii mean-field theory (Springer Berlin Heidelberg, 2008) Chap. 18, pp. 353–373.
- [219] A. L. Fetter, Nonuniform states of an imperfect Bose gas, *Ann. Phys.* **70**, 67 (1972).
- [220] M. Koashi and M. Ueda, Exact eigenstates and magnetic response of spin-1 and spin-2 Bose-Einstein condensates, *Phys. Rev. Lett.* **84**, 1066 (2000).
- [221] M. Ueda and M. Koashi, Theory of spin-2 Bose-Einstein condensates: Spin correlations, magnetic response, and excitation spectra, *Phys. Rev. A* **65**, 063602 (2002).
- [222] L. Salasnich, Self-consistent derivation of the modified Gross-Pitaevskii equation with Lee-Huang-Yang correction, *Appl. Sci.* **8**, 1998 (2018).
- [223] T.-L. Ho and V. B. Shenoy, Binary mixtures of Bose condensates of alkali atoms, *Phys. Rev. Lett.* **77**, 3276 (1996).
- [224] H. Pu and N. P. Bigelow, Properties of two-species Bose condensates, *Phys. Rev. Lett.* **80**, 1130 (1998).
- [225] L. G. Boussiakou, C. R. Bennett, and M. Babiker, Many-body theory of dilute gas condensates - derivation of a field-modified Gross-Pitaevskii equation from multipolar QED (2000), [arXiv:cond-mat/0007263 \[cond-mat\]](https://arxiv.org/abs/cond-mat/0007263).
- [226] J. Anandan, Gravitational and inertial effects in quantum fluids, *Phys. Rev. Lett.* **47**, 463 (1981).
- [227] T. Matos and A. Suárez, Finite temperature and dissipative corrections to the Gross-Pitaevskii equation from  $\lambda\phi^4$  one-loop contributions, *Europhys. Lett.* **96**, 56005 (2011).
- [228] O. Klein, Quantentheorie und fünfdimensionale Relativitätstheorie, *Z. Phys.* **37**, 895 (1926).
- [229] W. Gordon, Der Comptoneffekt nach der Schrödingerschen Theorie, *Z. Phys.* **40**, 117 (1926).
- [230] O. Gabel, *Bose-Einstein condensates in curved space-time - From concepts of general relativity to tidal corrections for quantum gases in local frames*, Ph.D. thesis, Technische Universität, Darmstadt (2019).
- [231] N. B. Delone and V. P. Krainov, AC Stark shift of atomic energy levels, *Phys.-Usp.* **42**, 669 (1999).
- [232] A. Gauguet, T. E. Mehlstäubler, T. Lévêque, J. Le Gouët, W. Chaibi, B. Canuel, A. Clairon, F. P. Dos Santos, and A. Landragin, Off-resonant Raman transition impact in an atom interferometer, *Phys. Rev. A* **78**, 043615 (2008).
- [233] E. Giese, A. Friedrich, S. Abend, E. M. Rasel, and W. P. Schleich, Light shifts in atomic Bragg diffraction, *Phys. Rev. A* **94**, 063619 (2016).
- [234] D. P. Craig and T. Thirunamachandran, *Molecular quantum electrodynamics: An introduction to radiation-molecule interactions* (Dover, New York, 1998).
- [235] G. Kurizki, I. E. Mazets, D. H. J. O’Dell, and W. P. Schleich, Bose-Einstein condensates with laser-induced dipole-dipole interactions beyond the mean-field approach, *Int. J. Mod. Phys. B* **18**, 961 (2004).
- [236] T. Lahaye, C. Menotti, L. Santos, M. Lewenstein, and T. Pfau, The physics of dipolar bosonic quantum gases, *Rep. Prog. Phys.* **72**, 126401 (2009).
- [237] J. Ma, X. Wang, C. P. Sun, and F. Nori, Quantum spin squeezing, *Phys. Rep.* **509**, 89 (2011).
- [238] L. Pezzè, A. Smerzi, M. K. Oberthaler, R. Schmied, and P. Treutlein, Quantum metrology with nonclassical states of atomic ensembles, *Rev. Mod. Phys.* **90**, 035005 (2018).
- [239] L. Salvi, N. Poli, V. Vuletić, and G. M. Tino, Squeezing on momentum states for atom interferometry, *Phys. Rev. Lett.* **120**, 033601 (2018).
- [240] F. Anders, A. Idel, P. Feldmann, D. Bondarenko, S. Loriani, K. Lange, J. Peise, M. Gersemann, B. Meyer-Hoppe, S. Abend, N. Gaaloul, C. Schubert, D. Schlipper, L. Santos, E. M. Rasel, and C. Klempt, Momentum entanglement for atom interferometry, *Phys. Rev. Lett.* **127**, 140402 (2021).
- [241] N. Bogoliubov, On the theory of superfluidity, *J. Phys. USSR* **11**, 23 (1947).
- [242] F. Malet, A. Mirschink, C. B. Mendl, J. Bjerlin, E. Ö. Karabulut, S. M. Reimann, and P. Gori-Giorgi, Density-functional theory for strongly correlated bosonic and fermionic ultracold dipolar and ionic gases, *Phys. Rev. Lett.* **115**, 033006 (2015).
- [243] The replacement may imply a restriction to quantum numbers  $\beta$  whose angular momentum  $\ell = 0$  vanishes.
- [244] S. T. Beliaev, Energy-spectrum of a non-ideal Bose gas, *Sov. Phys. JETP* **7**, 299 (1958).
- [245] V. N. Popov, *Functional integrals and collective excitations* (Cambridge University Press, Cambridge, 1988).
- [246] As a consequence the effective scattering length is not only the width of a narrow dipole-dipole potential but contains numerical contributions as well.
- [247] C. J. Pethick and H. Smith, *Bose-Einstein condensation in dilute gases* (Cambridge University Press, Cambridge, 2008).
- [248] H. Fu, Y. Wang, and B. Gao, Beyond the Fermi pseudopotential: A modified Gross-Pitaevskii equation, *Phys. Rev. A* **67**, 053612 (2003).
- [249] H. Veksler, S. Fishman, and W. Ketterle, Simple model for interactions and corrections to the Gross-Pitaevskii equation, *Phys. Rev. A* **90**, 023620 (2014).
- [250] G. Nandi, R. Walser, E. Kajari, and W. P. Schleich, Dropping cold quantum gases on earth over long times and large distances, *Phys. Rev. A* **76**, 063617 (2007).
- [251] C. Ufrecht, Theoretical approach to high-precision atom interferometry, Ph.D. thesis, Universität Ulm (2019).
- [252] E. Braaten and A. Nieto, Quantum corrections to the ground state of a trapped Bose-Einstein condensate, *Phys. Rev. B* **56**, 14745 (1997).



- [253] J. R. Anglin and A. Vardi, Dynamics of a two-mode Bose-Einstein condensate beyond mean-field theory, *Phys. Rev. A* **64**, 013605 (2001).
- [254] A. R. P. Lima and A. Pelster, Quantum fluctuations in dipolar Bose gases, *Phys. Rev. A* **84**, 041604 (2011).
- [255] A. R. P. Lima and A. Pelster, Beyond mean-field low-lying excitations of dipolar Bose gases, *Phys. Rev. A* **86**, 063609 (2012).
- [256] M. Gupta and K. R. Dastidar, Control of the dynamics of coupled atomic-molecular Bose-Einstein condensates: Modified Gross-Pitaevskii approach, *Phys. Rev. A* **80**, 043618 (2009).
- [257] J. R. Taylor, *Scattering theory: The quantum theory of nonrelativistic collisions* (Dover, New York, 2006).
- [258] N. Brambilla, G. Krein, J. Tarrús C., and A. Vairo, Born-oppenheimer approximation in an effective field theory language, *Phys. Rev. D* **97**, 016016 (2018).
- [259] M. Born and R. Oppenheimer, Zur Quantentheorie der Molekeln, *Ann. Phys.* **389**, 457 (1927).
- [260] R. G. Parr and W. Yang, Density-functional theory of the electronic structure of molecules, *Annu. Rev. Phys. Chem.* **46**, 701 (1995).
- [261] M. Köhl, M. J. Davis, C. W. Gardiner, T. W. Hänsch, and T. Esslinger, Growth of Bose-Einstein condensates from thermal vapor, *Phys. Rev. Lett.* **88**, 080402 (2002).
- [262] D. E. Miller, J. R. Anglin, J. R. Abo-Shaer, K. Xu, J. K. Chin, and W. Ketterle, High-contrast interference in a thermal cloud of atoms, *Phys. Rev. A* **71**, 043615 (2005).
- [263] A. L. Fetter, Rotating trapped Bose-Einstein condensates, *Rev. Mod. Phys.* **81**, 647 (2009).
- [264] G. C. Wick, The evaluation of the collision matrix, *Phys. Rev.* **80**, 268 (1950).
- [265] V. B. Berestetskii, E. M. Lifshitz, and L. P. Pitaevskii, *Quantum Electrodynamics* (Pergamon Press, Oxford, 1982).
- [266] We drop the subscript “1” for operators in the single-coboson sector.
- [267] F. J. Belinfante, On the longitudinal and the transversal delta-function, with some applications, *Physica* **12**, 1 (1946).
- [268] V. P. Krainov, H. R. Reiss, and B. M. Smirnov, *Radiative processes in atomic physics* (John Wiley & Sons, Hoboken, 1997).
- [269] S. N. Gupta, Theory of longitudinal photons in quantum electrodynamics, *Proc. Phys. Soc. A* **63**, 681 (1950).
- [270] K. Bleuler, Eine neue Methode zur Behandlung der longitudinalen und skalaren Photonen, *Helv. Phys. Acta* **23**, 567 (1950).
- [271] C. Becchi, A. Rouet, and R. Stora, Renormalization of the abelian Higgs-Kibble model, *Commun. Math. Phys.* **42**, 127 (1975).
- [272] I. V. Tyutin, Gauge invariance in field theory and statistical physics in operator formalism, Lebedev preprint FIAN, No. 39 (1975), [arXiv:0812.0580](https://arxiv.org/abs/0812.0580) [hep-th].